Accepted Manuscript

Scaffold-hopping of bioactive flavonoids: Discovery of aryl-pyridopyrimidinones as potent anticancer agents that inhibit catalytic role of topoisomerase IIα

Garima Priyadarshani, Suyog Amrutkar, Anmada Nayak, Uttam C. Banerjee, Chanakya N. Kundu, Sankar K. Guchhait

PII: S0223-5234(16)30502-5

DOI: 10.1016/j.ejmech.2016.06.024

Reference: EJMECH 8685

To appear in: *European Journal of Medicinal Chemistry*

Received Date: 9 March 2016

Revised Date: 13 June 2016

Accepted Date: 14 June 2016

Please cite this article as: G. Priyadarshani, S. Amrutkar, A. Nayak, U.C. Banerjee, C.N. Kundu, S.K. Guchhait, Scaffold-hopping of bioactive flavonoids: Discovery of aryl-pyridopyrimidinones as potent anticancer agents that inhibit catalytic role of topoisomerase IIα, *European Journal of Medicinal Chemistry* (2016), doi: 10.1016/j.ejmech.2016.06.024.

Scaffold-hopping of bioactive flavonoids: Discovery of aryl-pyridopyrimidinones as potent anticancer agents that inhibit catalytic role of topoisomerase-IIα

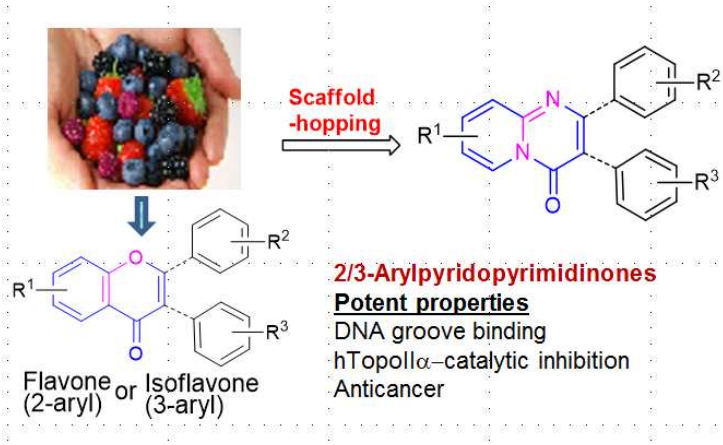

Scaffold-hopping of bioactive flavonoids: Discovery of aryl-pyridopyrimidinones as potent anticancer agents that inhibit catalytic role of topoisomerase IIα

Garima Priyadarshani[a,1], Suyog Amrutkar[b,1], Anmada Nayak[c], Uttam C. Banerjee[b], Chanakya N. Kundu[c], Sankar K. Guchhait*[,a]

[a] Department of Medicinal Chemistry, National Institute of Pharmaceutical Education and Research (NIPER), Sector 67, SAS Nagar, Mohali, Punjab 160062, India

[b] Department of Pharmaceutical Technology (Biotechnology), National Institute of Pharmaceutical Education and Research (NIPER), Sector 67, SAS Nagar, Mohali, Punjab 160062, India

[c] School of Biotechnology, KIIT University, Campus-11, Patia, Bhubaneswar, Orissa 751024, India

[1] Those authors contributed equally.

[*] S.K. Guchhait: Tel.: +91 (0)172 2214683; fax: +91 (0)172 2214692; E-mail addresses: skguchhait@niper.ac.in

KEYWORDS: *Flavonoids, Pyrido[1,2-a]pyrimidin-4-ones, Scaffold-hopping, Human topoisomerase IIα, Anticancer Agent, Drug Discovery.*

ABSTRACT: A strategy of scaffold-hopping of bioactive natural products, flavones and isoflavones, leading to target-based discovery of potent anticancer agents has been reported for the first time. Scaffold-hopped flavones, 2-aryl-4*H*-pyrido[1,2-*a*]pyrimidin-4-ones and the scaffold-hopped isoflavones, 3-aryl-pyrido[1,2-*a*]pyrimidin-4-ones were synthesized *via* Pd-catalyzed activation–arylation methods. Most of the compounds were found to exhibit pronounced human topoisomerase IIα (hTopoIIα) inhibitory activities and several compounds were found to be more potent than etoposide (a hTopoII*α*-inhibiting anticancer drug). These classes of compounds were found to be hTopoII*α*-selective catalytic inhibitors while not interfering with topoisomerase I and interacted with DNA plausibly in groove domain. Cytotoxicities against various cancer cells, low toxicity in normal cells, and apoptotic effects were observed. Interestingly, compared to parent flavones/isoflavones, their scaffold-hopped analogs bearing alike functionalities showed significant/enhanced hTopoII*α*-inhibitory and cytotoxic properties, indicating the importance of a natural product-based scaffold-hopping strategy in the drug discovery.

1. Introduction

Scaffold-hopping [1,2] of bioactive template/drug for drug-design to develop novel molecules with desired properties is an important strategy. Moreover, the new molecule with changed core becomes patentable. Several examples of drug development by scaffold-hopping are known, development of tramadol from morphine being one of the earliest

[2].The discovery of vardenafil from sildenafil [3], and celecoxib and rofecoxib from Dup 697 [4] are certainly amazing. Imigliptin [5], a DPP IV inhibitor, developed by such strategy is currently under clinical trials of type-2 diabetes mellitus.

Natural products (NPs) have played a valuable role in the drug discovery and development [6–8]. Newman and Cragg [9] reported that in the case of cancer around 79% of FDA-approved drugs during a period of 1981-2010 are either natural products or their based/mimicked-compounds. NPs are chosen through evolutionary process via lead optimization to interact with various enzymes/proteins and thus represent biologically relevant regions of the vast chemical space [10]. Despite the immense importance, to the best of our knowledge, there is no precedence for application of scaffold-hopping in the anti-cancer drug discovery utilizing natural product as a lead.

In our anticancer research program for drug discovery [11–13] we considered flavones and isoflavones as valuable templates. They display anticancer activities by various mechanisms [14]. Flavopiridol, a semisynthetic flavones analog, acts as CDK9 inhibitor, is FDA-approved orphan drug for acute myeloid leukemia. Aminoflavone as a prodrug is in phase I clinical trials for solid tumours. Flavones/isoflavones that inhibit topoisomerase II among other mode of anticancer activities are quercetin, fisetin, genistein, orobol, kaempferol, myricetin and morin [15,16]. To our surprise, literature survey revealed that there is no report of scaffold–hopping/modulation of flavones and isoflavones in the discovery of anticancer agents.

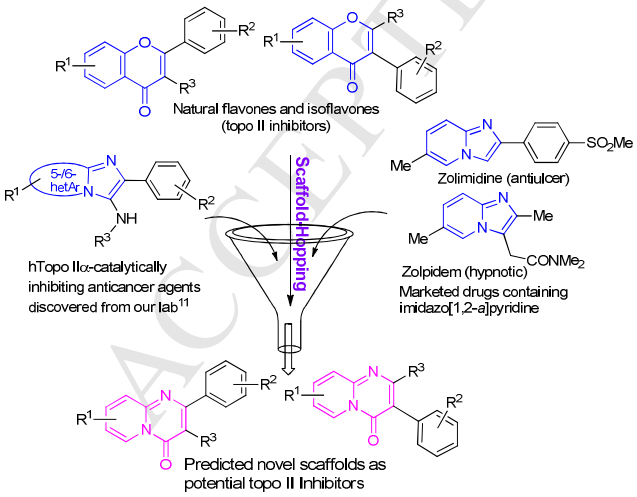

Figure 1: Design of new compounds

We were interested on scaffold-hopping of flavones and isoflavones with consideration of incorporating the structural features of imidazopyridines that we have previously explored as potent human DNA topoisomerase IIα (hTopoIIα)-catalytically inhibiting anticancer agents

[11]. In addition, the imidazopyridine motif is present in the marketed drugs, such as zolpidem and zolimidine [17]. We speculated 2-aryl- and 3-aryl-4*H*-pyrido[1,2-*a*]pyrimidin-4-ones as potential hTopoIIα–inhibiting anticancer agents (Figure 1).

2. Results and Discussion

2.1. Chemistry

In transition-metal-catalyzed cross couplings, the exploration of drug/privileged scaffolds as feasible substrates [18] and the catalyzed arylations via C-O bond cleavage using phenol derivatives [19,20] as electrophiles alternatives to aryl halides have gained importance. Recently, we have developed a new approach for the synthesis of 2-aryl-4*H*-pyrido[1,2-*a*]pyrimidin-4-ones from pyridopyrimidin-2,4-diones via Pd-catalyzed enolic C−O bond activation–arylation [21] (Figure 2a). Keeping in view, the structural features of Topo II-inhibiting flavonoids, a series of investigational compounds with relevantly substituted aryl moieties at C2-position of 4*H*-pyrido[1,2-*a*]pyrimidin-4-ones were synthesized.

In the direction of direct arylation via C-H bond activation of biologically-important scaffold, recently, we have developed a regioselective Pd-catalyzed Ag(I)-assisted direct C3-H activation-arylation of pyrido[1,2-*a*]pyrimidin-4-ones with bromo/iodo-(hetero)arenes to prepare relevantly substituted 3-aryl-pyrido[1,2-*a*]pyrimidin-4-ones (Figure 2b) [22]. Following this method, relevant C3-aryl-substituted 4*H*-pyrido[1,2-*a*]pyrimidin-4-ones were synthesized.

To have closer structural resemblance of investigational compounds to naturally-occurring topo II-inhibiting flavones and isoflavones, (poly)hydroxylated 2- or 3-aryl substituted 4*H*-pyrido[1,2-*a*]pyrimidin-4-ones were prepared via HBr (48% aqueous solution)-mediated ether cleavage [23] of corresponding methoxy derivatives (Figure 2c).

To evaluate the effectiveness of *scaffold-hopping concept* on the topoisomerase II inhibitory activities of flavonoids, several flavones and isoflavones were prepared. These compounds with alike substitutions completely mimic the structures of investigated potent topo II-inhibiting 2-arylpyridopyrimidiones and 3-arylpyridopyrimidinones, such that a comparison in their activities can be made. Three flavones (**C1**-**3**) matching with 2-arylpyridopyrimidinones (**3c**-**e**), and four isoflavones (**C1**-**7**) matching with 3-arylpyridopyrimidinones (**6d**, **6e**, **6n**, **6o**), were prepared following literature reported [24,25] synthetic routes (Figure 2d).

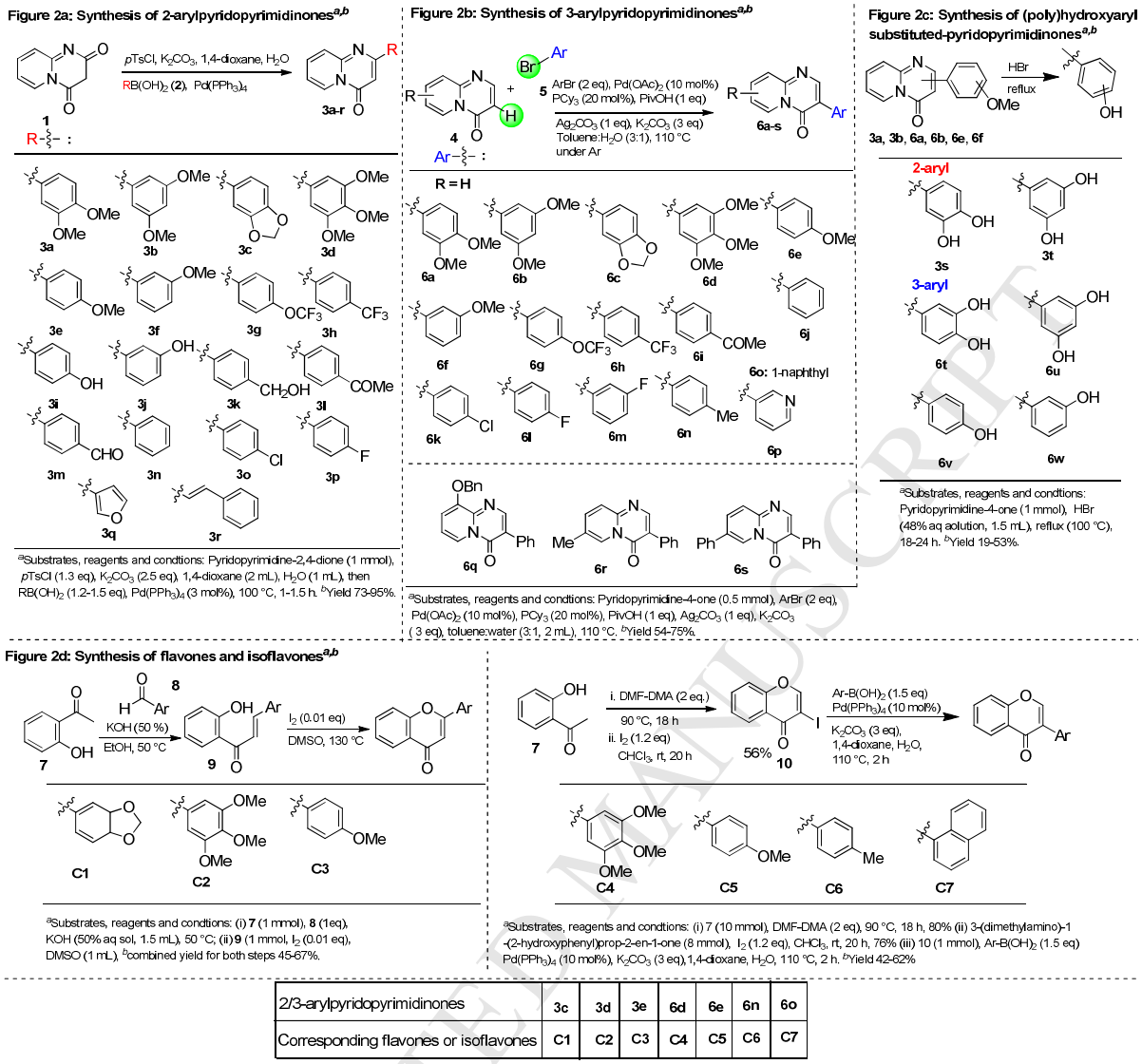

2/3-arylpyridopyrimidinones	3c	3d	3e	6d	6e	6n	6o
Corresponding flavones or isoflavones	C1	C2	C3	C4	C5	C6	C7

Figure 2: Synthetic route for the 2/3- arylpyridopyrimidinones and parent compounds (flavones and isoflavones)

2.2. Biological Studies

Synthesized compounds were investigated for their ability to inhibit hTopoIIα and for the mode of action. A screening kit purchased from TopoGEN, Inc. (Columbus, OH) was used. The screening protocols as provided by the supplier and reported in literature [11–13,26,27] with changed concentration as per our requirement were followed.

2.2.1. Inhibition of hTopoIIα-mediated kDNA decatenation

The compounds (series 3 and series 6) as well as their parent compounds (**C1-7**) were screened for the inhibitory activities of hTopoIIα-mediated decatenation of kinetoplast DNA (kDNA). The decatenation of kDNA by hTopoIIα results in the formation of small minicircles. The extent of hTopoIIα inhibition was measured by comparing the amount of decatenated products formed in the presence and absence of inhibitor (Figure 3). Many of the

synthesized compounds **3a, 3c-e, 3m, 3o, 3s, 6c-f, 6n, 6o, 6q, 6t, 6u, 6w** and **C1-7** were found to be relatively more potent than Etoposide (a hTopoII*α*-inhibiting anticancer drug) against hTopoIIα.

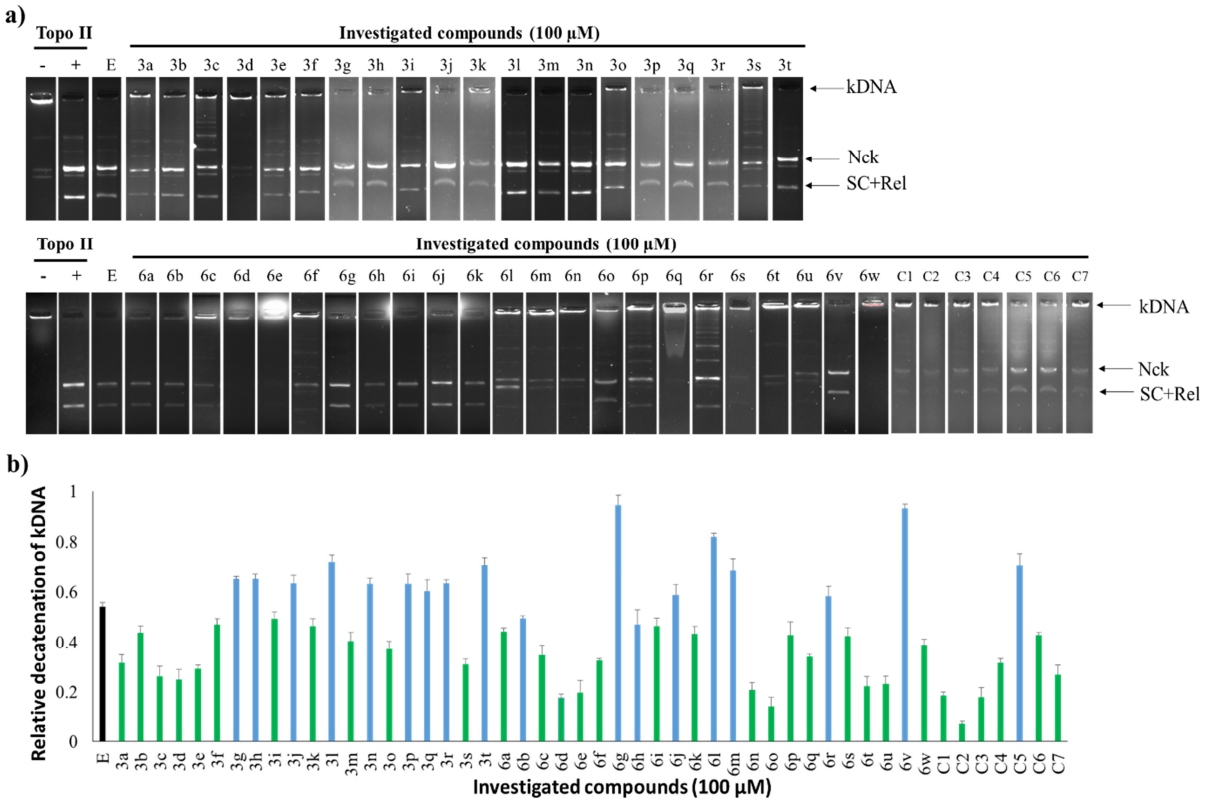

Figure 3: a) Inhibition of hTopoIIα-mediated kDNA decatenation: kDNA was treated with hTopoIIα in the absence or presence of 100 µM etoposide (E) or investigated compounds; b) Quantification of decatenation products.

2.2.2. Cytotoxic potential of selected compounds in cancer cells

The cytotoxic potential of selected compounds (**3a, 3c-e, 3m, 3o, 3s, 6c-f, 6n, 6o, 6q, 6t, 6u, 6w**) as well as the parent compounds (**C1-7**) were investigated by a MTT assay using kidney cancer cells (HEK-293) and normal monkey kidney epithelial cells (Vero). Etoposide was used as positive control. The cells were treated with compounds in increasing concentrations for 48 h and then MTT assay was performed. All the compounds showed a characteristic cytotoxic profile in both the cells (Table 1). A dose dependent decrease of cell viability was noted in cells and more growth inhibition was noted in HEK-293 compared to Vero cells at the same concentration (Figure 4).

Table 1: IC50 values in HEK-293 and Vero cells

Compounds	**LC_{50} (μM) HEK-293**	**LC_{50} (μM) Vero**	Compounds	LC_{50} (μM) HEK-293	LC_{50} (μM) Vero
3a	17 ±2.4	50±1.5	**6o**	7 ± 2.6	60 ± 2.7
3c	15.5±2.3	52±1.4	**6q**	3 ± 2.1	60 ± 2.5
3d	9 ± 1.8	46±2.5	**6t**	9 ± 1.6	38 ± 2.0
3e	8 ± 1.2	60±2.1	**6u**	2 ± 1.3	50 ± 1.9
3m	3 ± 2.0	48 ±1.8	**6w**	6 ± 2.4	52 ± 2.6
3o	2.4 ± 1.5	47.5±2.1	**C1**	8 ± 1.6	48 ± 1.3
3s	13 ± 1.6	32±1.4	**C2**	12 ± 1.6	52 ± 1.3
6c	15 ±2.3	48 ± 2.3	**C3**	8.5 ± 1.6	45 ± 1.3
6d	3 ± 0.3	40 ± 2.1	**C4**	10 ± 1.3	50 ± 1.3
6e	19 ± 2.5	38 ± 1.4	**C5**	12 ± 1.2	52 ± 1.5
6f	9 ± 2.1	46 ± 1.3	**C6**	8 ± 1.2	48 ± 1.3
6n	3.5 ± 1.2	44 ± 1.9	**C7**	12 ± 1.6	42 ± 1.6
Etoposide	22 ± 1.5	55 ± 1.5			

Next, the cytotoxicity of selective potent compounds (**3m, 3o, 6d, 6u, 6n** and **6q**) were tested in other cancer cells, lung (A-549), oral (H-357), colon (HCT-116), cervical (HeLa), and breast (MCF-7) (Table 2a).

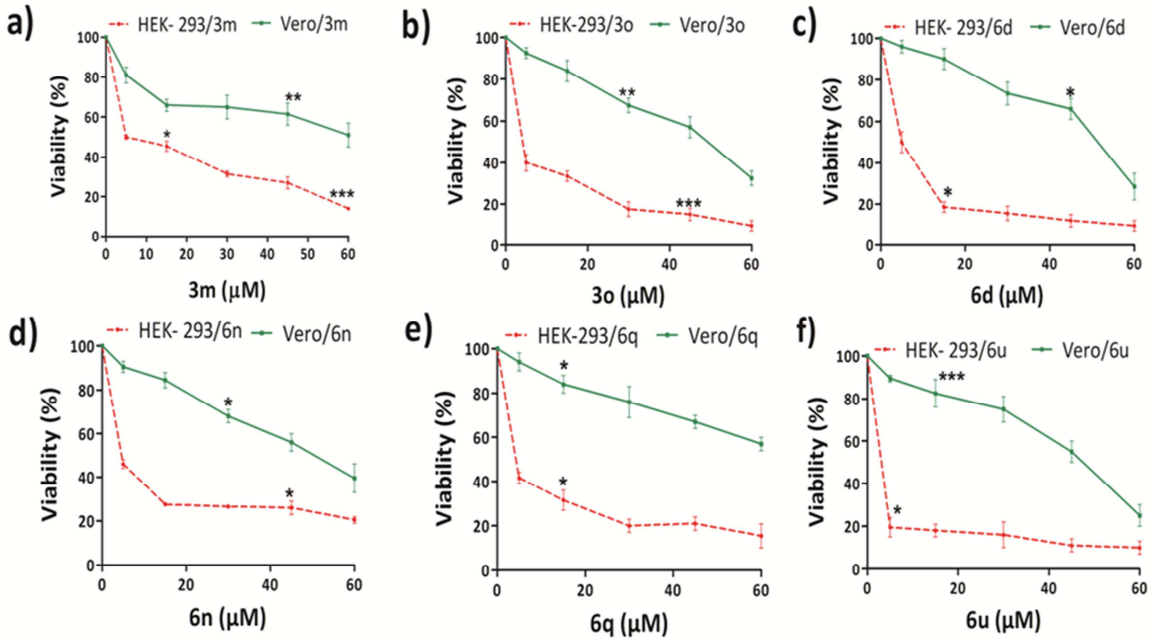

Figure 4: Viability of cells in HEK-293 and Vero cells. Compounds **3m**, **3o**, **6d**, **6u**, **6n** and **6q** were found to be relatively highly cytotoxic to HEK-293 cells compared to Vero cells.

In these cells, significant toxicity with IC_{50} (concentration at which 50% cell death in culture was observed) ranging from 1.5 to 4 µM were observed. To determine the potential of

the compounds in long term cytotoxic effect even after end of treatment, a clonogenic cell survival assay using HEK-293 cells was performed (Table 2b). A dose dependent decrease in colony formation was observed in investigated compounds. The LC_{50} values (concentration at which fifty percent cell death in culture was observed) indicated that they were more potent than etoposide with 5-10 fold higher activities.

Table 2:

	a) IC50 (µM) of compounds in MTT assay					b) LC50 (µM) in clonogenic assay using HEK-293
Compound	**MCF-7**	**HeLa**	**A-549**	**HCT-116**	**H-357**	
3m	2.5 ± 0.2	3 ± 0.2	2.4 ± 0.3	3.5 ± 0.2	2.5 ± 0.2	2.5 ± 0.1
3o	1.8 ± 0.2	2 ± 0.3	2.1 ± 0.2	2.5 ± 0.2	2.3 ± 0.2	2 ± 0.9
6d	3.0 ± 0.3	2.8 ± 0.2	2.1 ± 0.2	3.2 ± 0.2	3 ± 0.2	1.8 ± 0.1
6u	2 ± 0.2	1.5 ± 0.2	2.8 ± 0.2	3 ± 0.2	3 ± 0.3	2.4 ± 0.3
6n	4 ± 0.2	3 ± 0.3	2.5 ± 0.3	2.5 ± 0.3	2.8 ± 0.3	2.5 ± 0.1
6q	2 ± 0.2	1.5± 0.2	2 ± 0.2	3 ± 0.2	3 ± 0.2	3.8 ± 0.7
Etoposide						20 ± 0.1

For further studies of properties and mode of action, the compounds **3o** and **6d** were then selected as representative examples, one from each series, based on their overall superior effects of hTopoIIα-inhibitory activities, cytotoxicities and anti-clonogenic potential.

2.2.3. Inhibition of hTopoI-mediated DNA relaxation

The compounds **3o** and **6d** were screened for inhibition of hTopoI-mediated relaxation of negatively supercoiled DNA. In the presence of compounds almost no inhibition of DNA-relaxation was observed as compared to camptothecin (Figure 5a). Hence, investigated compounds of 100 µM concentration did not act as hTopoI inhibitors.

Next, mode of action for hTopoIIα inhibition was studied.

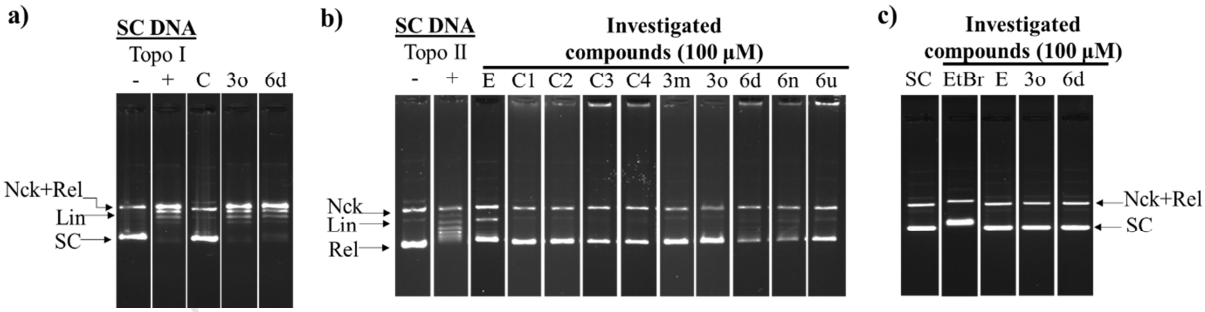

Figure 5: a) hTopoI-mediated DNA relaxation assay (Negatively supercoiled DNA was treated with hTopoI in the absence/presence of 100 µM camptothecin (C) or investigated compounds). b) hTopoIIα DNA cleavage complex assay (Negatively supercoiled DNA (pUC19) was treated with hTopoIIα and immediately incubated with 100 µM etoposide or investigated compounds). c) DNA intercalation assay using SC DNA (pUC19)

2.2.4. hTopoIIα-DNA cleavage complex formation

A hTopoIIα poisons e.g. etoposide stabilizes a TopoII-cleaved DNA complex (cleavage complex) which generally appears as linear band (Lin)[11]. In the presence of

selected active compounds **C1-4**, **3m**, **3o**, **6d**, **6n** and **6u** (100 µM) no such linear band was observed (Figure 5b). It indicates that the investigated compounds with upto 100 µM did not act as hTopoIIα poisons.

2.2.5. DNA-binding

The binding of ligand with DNA takes place either by DNA intercalation or by groove binding[28].

DNA intercalation

DNA intercalators like ethidium bromide (EtBr) retards the movement of SC DNA in the gel electrophoresis. In the presence of etoposide, compound **3o** or compound **6d**, no such retardation of DNA movement was observed (Figure 5c), suggesting the non-intercalating nature of the investigated compounds.

Mode of DNA-binding

In order to check the specificity of the compounds (**3m**, **3o** and **6d**) towards the DNA, an *in vitro* DNA-ligand binding assay was carried out (Figure 6a-e). In principle, pure DNA provides maximum absorbance at 260 nm, however, when a ligand binds to the DNA, the absorbance decreases. In our experiment, it was observed that pure DNA, which gave an exact spectrum with λ_{max} 260 nm, on treatment with investigated compounds of increasing concentrations showed hypochromism in the absorption. This indicates possible binding of the compounds to the DNA. The results were validated by taking EtBr (a known DNA intercalator) as a positive control [29].

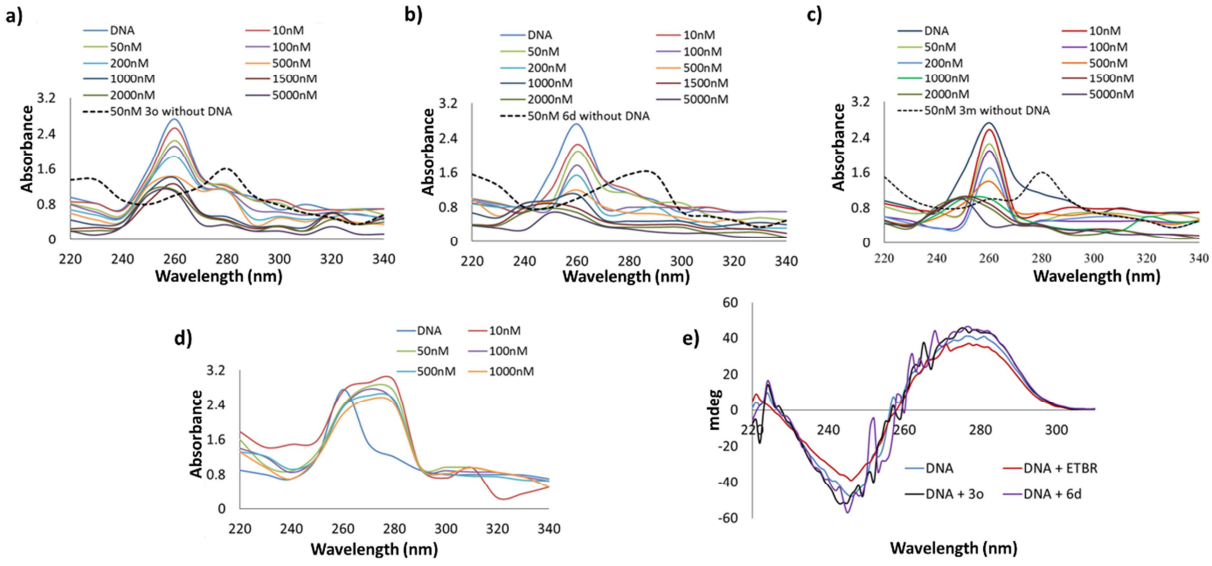

Figure 6: a) DNA-binding of compound **3m**; b) compound **3o**; c) compound **6d**; d) EtBr; e) CD based ligand-DNA binding of compounds EtBr, **3o** and **6d**.

The absorption spectrum of individual compound was found to be different from EtBr-DNA absorption spectra, indicating the occurrence of hypochromism due to interaction of compound with the DNA, not due to property of the compound itself. The binding constant (Kd) were were found to be 2.43 x 10-^{6} M^{-1}, 3.4 x 10^{-6} M^{-1} and 2.5 x 10^{-6}M^{-1} for compounds **3m**, **3o** and **6d** respectively (Figure 7).

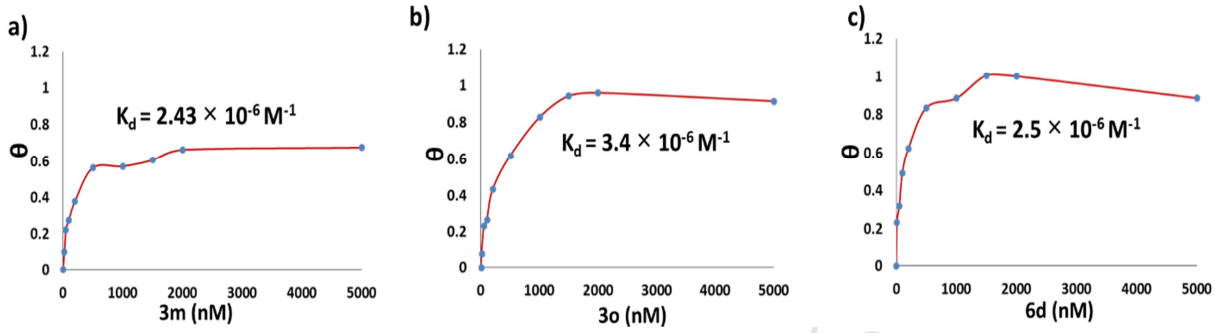

Figure 7: a) Graph showing the binding constant (K_d) of compound **3m**. b) Graph showing the binding constant of compound **3o**. c) Graph showing the binding constant of compound **6d**.

In addition, circular dichroism (CD) spectral analysis was performed to measure the conformational changes in the DNA duplex structure due to binding with compounds **3o** and **6d** (Figure 4e). The CD spectra showed that bands at 275 nm (due to base stacking) and at 245 nm (due to the B-conformation of DNA) did not change significantly in the presence of the tested compounds (**3o** and **6d**), while EtBr (a well-known DNA intercalator) used as a positive control showed changes in the absorption spectra (shape and absorbance) [29]. The DNA-ligand interaction studies all together signify that the investigated compounds may interact with DNA through groove binding and not by DNA intercalation.

2.2.6. Apoptosis measured by DAPI-nuclear staining

To study the cytotoxicity of investigated compounds caused due to possible apoptosis, a fluorescence assay was performed using DAPI which binds only to the nucleus of the cells and not to the cytoplasm. HEK-293 cells were treated with compound **3o** of various concentrations and then stained with DAPI prior to observe under microscope. A dose dependent increase of deformation, shrinkage and bubble shaped nuclei in comparison with untreated cells was noted. More than 5 fold increased apoptotic nuclei were noted at 5 µM of compound **3o** (Figure 8a and 8b).

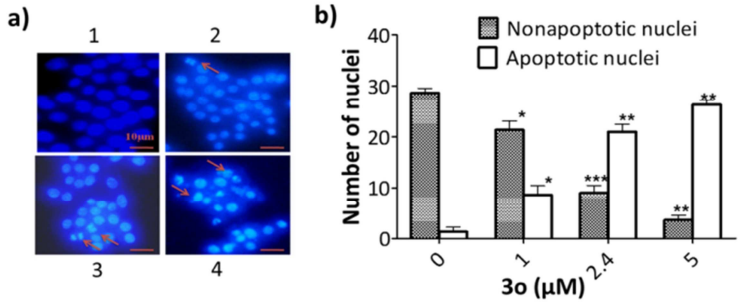

Figure 8: DAPI-stained nuclei of HEK-293 cells after treatment with compound **3o**: a) Images were taken under a fluorescence microscope at 40X magnification (scale bar 10 μM). Images 1, 2, 3, and 4 represent cells treated with compound **3o** of 0, 1, 2.4 and 5 μM, respectively; b) Bar diagram showing the number of apoptotic and non-apoptotic nuclei.

2.2.7. Apoptosis measured by annexin V-FITC/PI dual staining in HEK 293 cells

To further confirm the apoptosis and different phases of apoptosis a more sensitive and reliable assay was carried out by sorting the cells after annexinV-FITC/PI dual stain. Annexin-V/FITC binds to living cells, whereas PI stains apoptotic cells. The distribution of cells in Q1, Q2, Q3 and Q4 represent the normal, early apoptotic, apoptotic and late apoptotic cells, respectively (Figure 9). In treating the cells with compound **3o**, a dose dependent increase in total apoptotic cells (early apoptotic + apoptotic + late apoptotic cells) was noted. More than 22 percent total apoptotic cells were noted at 5μM of compound **3o,** which was significantly higher compared to untreated cells (1%).

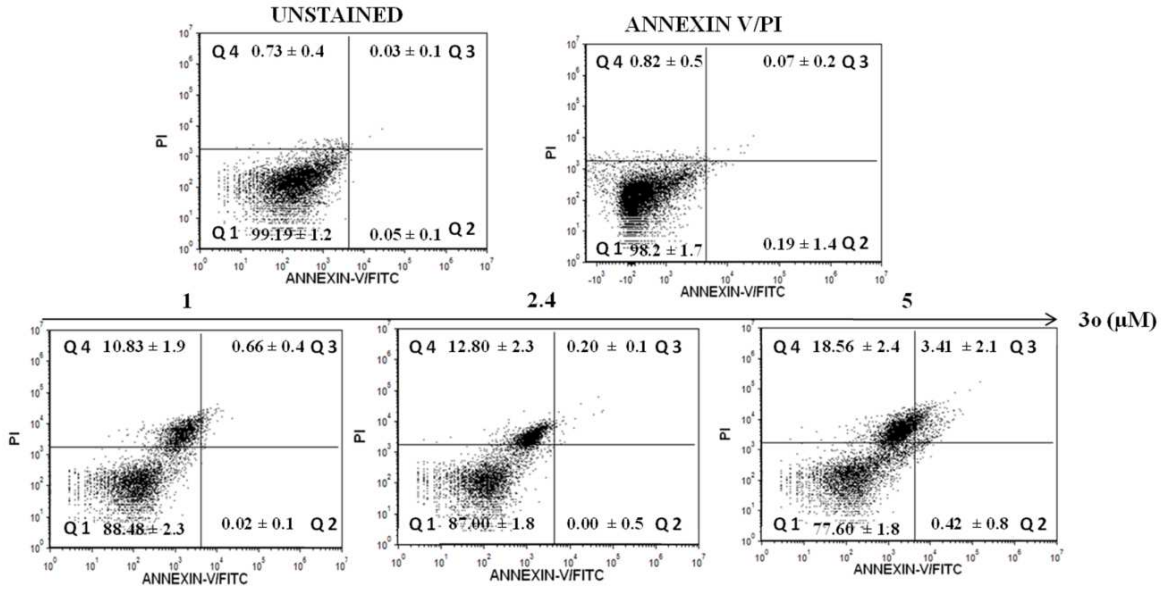

Figure 9: Analysis of Annexin V –FITC/PI stained cells after treatment with compound **3o** in HEK-293 cells

2.2.8. Inhibition of invasiveness of cancer cells

Cancer cells invade easily into the matrix of basement membrane. The effect of compound **3o** in the invasive property was measured by matrigel cell invasion assay. It was noted that with increase in concentration of compound **3o** the percentage of cell invaded into

the matrix decreased in comparison with untreated cells. A 5 fold decrease in the invasiveness was observed in 5 µM of compound **3o** with respect to untreated cells (Figure 10).

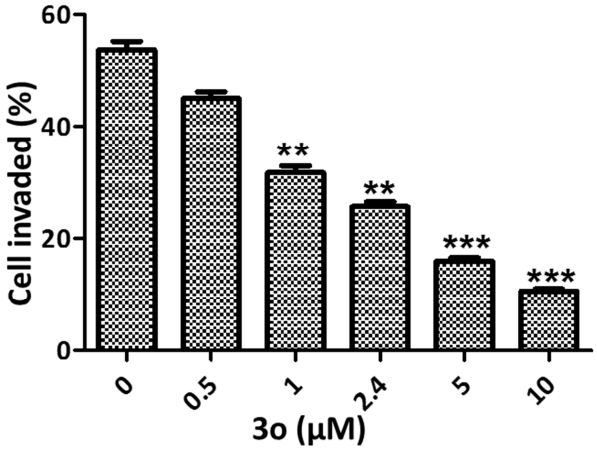

Figure 10: Assay for matrigel invasion in HEK- 293 cell for compound 3o: Histogram showing the number of cell invaded into the matrix.

The comparison of topoisomerase II inhibitory and antiproliferative activities of investigated potent scaffold-hopped analogs with the parent flavones and isoflavones led to the interesting findings. To our glad, the scaffold-hopped analogs of isoflavones (**6d-e**, **6n**, **6o**) were found to be superior compared to parent isoflavones (**C4-7**) in both of topo II inhibitory and antiproliferative activities, and more potent than etoposide. Although less active than their parent compounds (**C1-3**), the scaffold-hopped analogs of flavones (**3c-e**) were found to be significantly potent in topo II inhibitory and antiproliferative activities and higher efficacious compared to etoposide. In addition, these scaffold-hopped analogs belong to the new molecular motifs (2/3-arylpyrido[1,2-*a*]pyrimidinone) that are outside the patent issues.

3. Conclusion

The present study represents for the first time a scaffold-hopping strategy of bioactive natural product in the anticancer drug discovery. Based on scaffold-hopping of flavones and isoflavones with consideration of the structure of marketed relevant drugs and the anticancer agents previously explored by us, 2-aryl-4*H*-pyrido[1,2-*a*]pyrimidin-4-ones and 3-aryl-4*H*-pyrido[1,2-*a*]pyrimidin-4-ones were considered as potential hTopoIIα inhibitors. They were synthesized by Pd-catalyzed C-O activation–arylation and arene C–H bond arylation approaches, respectively. These compounds found to exhibit significant topoisomerase II inhibitory and anticancer activities. Compounds **3a, 3c-e, 3m, 3o, 3s, 6c-f, 6n, 6o, 6q, 6t, 6u, 6w** showed higher topo II inhibition and cytotoxicities than etoposide (a topo II–inhibiting

anticancer drug), while they are relatively less toxic to normal cells. These compounds inhibited the topo II-activity by blocking the catalytic role of hTopoIIα in DNA-process while not interfering with topoisomerase I and interacted with DNA plausibly in groove domain. Compounds (**3m, 3o, 6d, 6u, 6n** and **6q**) were found to be cytotoxic in other cancer cells, lung, oral, colon, cervical, and breast cancer cells as well. These compounds inhibited the invasiveness as well as clonogenic properties of cancer cells. They showed their cytotoxicities by apoptosis.

An appealing attribute of this scaffold-hopping strategy is that the analogs compared to the parent flavones and isoflavones, bearing alike functionalities showed significant/superior hTopoII*α*-inhibitory and cytotoxic properties. Taken all together, these suggest the importance of scaffold-hopping approach in this class of compounds. The present study will certainly encourage for the medicinal chemistry programme of such NPs-based scaffold-hopping strategy in accomplishing rapid drug discovery.

4. Experimental

4.1. Chemistry

4.1.1. General considerations

All reactants and reagents were obtained from commercial source and used without further purification. Bruker Avance III-400 (400 MHz) spectrometer was used for recording ^{1}H NMR and ^{13}C NMR spectra were measured on a Bruker Avance III-400 (100 MHz) spectrometer with complete proton decoupling. Data were reported as follows: chemical shifts in ppm from tetramethylsilane as an internal standard in $CDCl_3$/CD_3OD/DMSO-d_6 integration, multiplicity (s = singlet, d = doublet, t = triplet, q = quartet, m = multiplet, td = triplet of doublet, dt = doublet of triplet, ddd = doublet of doublet of doublet, br = broad), and coupling constants (Hz). The Infrared (IR) spectra were recorded on a Perkin Elmer FTIR with ATR & IR Microscope spectrometer. High-resolution mass spectra (HRMS) were performed on Bruker maxis Q-TOF. Elemental analyses were done on Elementar Vario EL spectrometer. Melting points determined are uncorrected. Analytical HPLC was used to determine the purity of the compounds and the purity was found to be greater than 95%.

4.2.1.Typical experimental procedure for the synthesis of 2-aryl-4H-pyrido[1,2-a]pyrimidin-4-ones (3a-r):[21]

A mixture of the 4*H*-pyrido[1,2-*a*]pyrimidin-4-one (1 mmol), and K_2CO_3 (2.5 eq) in 1,4-dioxane (2 mL) and H_2O (1 mL) taken in a round-bottomed flask and *p*-TsCl (1.3 eq) was added to it. The mixture was stirred under open air for 1h at rt (25-28 °C). The boronic acid

(1.2 eq) and $Pd(PPh_3)_4$ (3 mol %) were subsequently added and the mixture was heated at 100 °C under open air. Upon completion of reaction as indicated by TLC (1-1.5 h), the resultant mixture was cooled to rt and extracted with EtOAc (2x25 mL). The combined organic solution was washed with water (2x5 mL) and brine (1x5 mL), dried with anhyd. Na_2SO_4, and concentrated under reduced pressure. The column chromatographic purification of crude mass was performed on neutral alumina using EtOAc-hexane (30-40%) as eluting solvent afford the arylated products (**3a-r**).

For spectral data and scanned spectra of compounds 3c-e, 3g-r, see: Guchhait, S. K.; Priyadarshani, G. Synthesis of 2-arylpyridopyrimidinones, 6-aryluracils, and tri-and tetrasubstituted conjugated alkenes via pd-catalyzed enolic C–O bond activation–arylation. *J. Org. Chem.* **2015**, *80*, 6342−6349.

Characterization data for 2-aryl-4H-pyrido[1,2-a]pyrimidin-4-ones (3a, 3b, 3f, 3i):

2-(3,4-Dimethoxyphenyl)-4*H*-pyrido[1,2-*a*]pyrimidin-4-one (3a):[30] White solid, 259 mg, 92%, m.p. 168-170 °C; ^{1}H NMR (400 MHz, $CDCl_3$): δ 9.05 (ddd, *J* = 7.0 Hz, *J* = 0.9 Hz, *J* = 0.9 Hz, 1H), 7.75-7.67 (m, 4H), 7.12-7.09 (m, 1H), 6.98 (d, *J* = 8.4 Hz, 1H), 6.87 (s, 1H), 4.01 (s, 3H), 3.95 (s, 3H) ppm; ^{13}C NMR (100 MHz, $CDCl_3$): δ 161.5, 158.6, 151.6, 151.3, 150.9, 149.1, 136.1, 129.8, 127.3, 126.6, 120.6, 114.9, 111.0, 110.1, 98.9, 56.0, 55.9 ppm; IR: ν_{max} 3072, 3004, 1678, 1638, 1486, 1269, 1134, 1022 cm^{-1}; HRMS (ESI) *m/z*: calcd. for $C_{16}H_{15}N_2O_3$ $[M+H]^+$ 283.1082, found: 283.1074.

2-(3,5-Dimethoxyphenyl)-4*H*-pyrido[1,2-*a*]pyrimidin-4-one (3b): White solid, 253 mg, 90%, m.p. 160-162 °C; ^{1}H NMR (400 MHz, $CDCl_3$): δ 9.07 (ddd, *J* = 7.2 Hz, *J* = 1.2 Hz, *J* = 1.2 Hz, 1H), 7.76-7.74 (m, 2H), 7.24 (d, *J* = 2.3 Hz, 2H), 7.16-7.13 (m, 1H), 6.88 (s, 1H), 6.60 (dd, *J* = 2.3 Hz, *J* = 2.3 Hz, 1H), 3.88 (s, 6H) ppm; ^{13}C NMR (100 MHz, $CDCl_3$): δ 161.9, 161.1, 158.6, 150.9, 139.4, 136.1, 127.3,126.8, 115.2, 105.4, 103.0, 100.4, 55.5 ppm; IR: ν_{max} 3110, 2939, 1670, 1632, 1457, 1439, 1152, 1063 cm^{-1}; HRMS (ESI) *m/z*: calcd. for $C_{16}H_{15}N_2O_3$ $[M+H]^+$ 283.1082, found: 283.1073.

2-(3-Methoxyphenyl)-4*H*-pyrido[1,2-*a*]pyrimidin-4-one (3f): White solid, 232 mg, 92%, m.p. 176-178 °C; ^{1}H NMR (400 MHz, $CDCl_3$): δ 9.06 (ddd, *J* = 7.1 Hz, *J* = 1.0 Hz, *J* = 1.0 Hz, 1H), 7.74-7.73 (m, 2H), 7.66-7.63 (m, 2H), 7.40 (dd, *J* = 8 Hz, *J* = 7.8 Hz, 1H), 7.14-7.10 (m, 1H), 7.03 (ddd, *J* = 8.2 Hz, *J* = 2.5 Hz, *J* = 0.9 Hz, 1H), 6.90 (s, 1H), 3.90 (s, 3H) ppm; ^{13}C NMR (100 MHz, $CDCl_3$): δ 161.9, 160.0, 158.6, 150.9, 138.8, 136.1, 129.8, 127.3, 126.8, 119.8, 116.6, 115.2, 112.6, 100.3, 55.4 ppm; IR: ν_{max} 3082, 2995, 1670, 1639, 1442,

1253, 1037 cm^{-1}; HRMS (ESI) *m/z*: calcd. for $C_{15}H_{13}N_2O_2$ $[M+H]^+$ 253.0977, found: 253.0974.

2-(4-Hydroxyphenyl)-4*H*-pyrido[1,2-*a*]pyrimidin-4-one (3i):[30] Off-white solid, 174 mg, 73%, m.p. >200 °C; ^{1}H NMR (400 MHz, DMSO-d_6): δ 10.06 (s, 1*O*H), 8.92 (ddd, *J* = 7.1 Hz, *J* = 0.7 Hz, *J* = 0.7 Hz, 1H), 8.07 (d, *J* = 8.8 Hz, 2H), 7.93 (ddd, *J* = 8.8 Hz, *J* = 6.7 Hz, *J* = 1.6 Hz, 1H), 7.69 (dd, *J* = 8.7 Hz, *J* = 0.8 Hz, 1H), 7.29 (ddd, *J* = 8.2 Hz, *J* = 6.9 Hz, *J* = 1.3 Hz, 1H), 6.89 (d, *J* = 8.8 Hz, 2H), 6.85 (s, 1H) ppm; ^{13}C NMR (100 MHz, DMSO-d_6): δ 160.8, 160.5, 158.1, 151.0, 137.9, 129.5, 127.7, 127.3, 126.5, 116.2, 115.9, 97.2 ppm; IR: ν_{max} 3277, 2832, 1658, 1630, 1450, 1239, 1015 cm^{-1}; HRMS (ESI) *m/z*: calcd. for $C_{14}H_{11}N_2O_2$ $[M+H]^+$ 239.0821, found: 239.0816**.**

4.2.2. Typical experimental procedure for the synthesis of 3-aryl-4H-pyrido[1,2-a]pyrimidin-4-ones (6a-s):[22]

Pyridopyrimidinone (1 mmol), K_2CO_3 (3 mmol, 414 mg, 3 eq), Ag_2CO_3 (1 mmol, 275 mg, 1 eq), PCy_3 (0.2 mmol, 56 mg, 0.2 eq), $Pd(OAc)_2$ (0.1 mmol, 22 mg, 0.1 eq) were weighed in air to a sealed tube equipped with magnetic stirring bar. PivOH (1 mmol, 0.12 mL, 1 eq) and bromoarene (2 mmol, 2 eq) were added to the tube. The tube was back filled with argon and toluene (3 mL) and water (1 mL) were added. The mixture was heated at 110 °C for 18-24 h until complete consumption of the substrate as indicated by TLC. The resultant mixture was cooled to rt and concenterated under reduced pressure. The mixture was extracted with EtOAc (2x50 mL) and washed with 10% aqueous ammonia solution (3x20 mL). The combined organic solution was washed with water (2x5 mL) and brine (1x5 mL), dried with anhyd. Na_2SO_4, and concentrated under reduced pressure. The column chromatographic purification of crude mass was performed on silica gel partially de-acidified by passing triethylamine (1-2 mL) using EtOAc-hexane (25-40%) as eluting solvent to afford the arylated products (**6a-s**).

For spectral data and scanned spectra of compounds 6a-s, see: Guchhait, S. K.; Priyadarshani, G. Pd-Catalyzed Ag (I)-promoted C3-arylation of pyrido [1,2-*a*] pyrimidin-4-ones with bromo/iodo-arenes. *J. Org. Chem.* **2015**, *80*, 8482–8488.

4.2.3.Typical experimental procedure for the synthesis of (poly)hydroxyaryl substituted-pyridopyrimidinones (3s-t, 6t-w):[23]

The methoxy compound (1.5 mmol) was taken into 48% HBr (7 mL) and refluxed at 100 °C. The reaction was continued until complete consumption of the starting material as monitored by TLC (3-5 h). The mixture was cooled to room temperature and neutralized with 0.1 N NaOH. Solids were collected and purified by neutral alumina column chromatography using 5% methanol in dichloromethane.

Characterization data for compounds 3s, 3t, 6t-w:

2-(3,4-Dihydroxyphenyl)-4*H*-pyrido[1,2-*a*]pyrimidin-4-one (3s):[30] Light yellow solid, 129 mg, 34%, m.p. >200 °C; ^{1}H NMR (400 MHz, DMSO-d_6): δ 9.04 (d, J = 6.4 Hz, 1H), 8.23 (dd, J = 7.4 Hz, J = 6.4 Hz, 1H), 7.94 (d, J = 8.3 Hz, 1H), 7.56-7.41 (m, 3H), 6.92 (d, J = 8.1 Hz, 1H), 6.77 (s, 1H) ppm; ^{13}C NMR (100 MHz, DMSO-d_6): δ 157.2, 156.7, 149.8, 149.3, 146.1, 141.8, 128.6, 124.6, 122.5, 120.4, 118.4, 116.4, 115.1, 97.9 ppm; IR: ν_{max} 3544, 3407, 1659, 1615, 1277, 1134 cm^{-1}; HRMS (ESI) *m/z*: calcd. for $C_{14}H_{10}N_2O_3Na$ $[M+Na]^+$ 277.0589, found: 277.0580**.**

2-(3,5-Dihydroxyphenyl)-4*H*-pyrido[1,2-*a*]pyrimidin-4-one (3t): Light brown solid, 110 mg, 29%, m.p. >200 °C; ^{1}H NMR (400 MHz, DMSO-d_6): δ 8.94 (d, J = 6.5 Hz, 1H), 7.96 (ddd, J = 8.6 Hz, J = 6.7 Hz, J = 1.5 Hz, 1H), 7.71 (d, J = 8.7 Hz, 1H),), 7.33 (ddd, J = 8.1 Hz, J = 6.9 Hz, J = 1.3 Hz, 1H), 7.01 (d, J = 2.2 Hz, 2H), 6.72 (s, 1H), 6.40 (dd, J = 2.2 Hz, J = 2.1 Hz, 1H) ppm; ^{13}C NMR (100 MHz, DMSO-d_6): δ 161.4, 159.6, 158.1, 150.9, 138.8, 138.1, 127.4, 126.6, 116.6, 105.7, 105.6, 98.8 ppm; IR: ν_{max} 3286, 3113, 1668, 1634, 1164 cm^{-1}; HRMS (ESI) *m/z*: calcd. for $C_{14}H_{11}N_2O_3$ $[M+H]^+$ 255.0770, found: 255.0763.

3-(3,4-Dihydroxyphenyl)-4*H*-pyrido[1,2-*a*]pyrimidin-4-one (6t): Yellow solid, 87 mg, 23%, m.p. 160-162 °C; ^{1}H NMR (400 MHz, DMSO-d_6): δ 9.08 (ddd, J = 7.2 Hz, J = 1.4 Hz, J = 0.8 Hz, 1H), 9.06 (s, 1*O*H), 9.00 (s, 1*O*H), 8.50 (s, 1H), 7.93 (ddd, J = 8.4 Hz, J = 6.7 Hz, J = 1.6 Hz, 1H), 7.71 (dd, J = 8.7 Hz, J = 1.1 Hz, 1H),), 7.39 (ddd, J = 8.2 Hz, J = 7.0 Hz, J = 1.2 Hz, 1H), 7.34 (d, J = 2.2 Hz, 1H), 7.10 (dd, J = 8.2 Hz, J = 2.2 Hz, 1H), 6.80 (d, J = 8.2 Hz, 1H) ppm; ^{13}C NMR (100 MHz, DMSO-d_6): δ 156.4, 152.0, 150.1, 145.6, 145.3, 136.8, 127.6, 126.5, 125.8, 119.9, 117.0, 116.3, 115.9 (2C) ppm; IR: ν_{max} 3219, 2941, 1682, 1486, 1282, 1016 cm^{-1}; HRMS (ESI) *m/z*: calcd. for $C_{14}H_{11}N_2O_3$ $[M+H]^+$ 255.0770, found: 255.0762.

3-(3,5-Dihydroxyphenyl)-4*H*-pyrido[1,2-*a*]pyrimidin-4-one (6u): Yellow solid, 72 mg, 19%, m.p. >200 °C; ^{1}H NMR (400 MHz, DMSO-d_6): δ 9.13 (d, J = 6.9 Hz, 1H), 8.53 (s, 1H), 8.11 (dd, J = 7.6 Hz, J = 7.5 Hz, 1H), 7.81 (d, J = 8.7 Hz, 1H),), 7.52 (dd, J = 7.0 Hz, J = 6.7 Hz, 1H), 6.68 (d, J = 1.9 Hz, 2H), 6.25 (dd, J = 1.9 Hz, J = 1.9 Hz, 1H) ppm; ^{13}C NMR (100 MHz, DMSO-d_6): δ 158.7 (3C), 155.9, 149.6, 139.4, 135.6, 128.5, 124.4, 118.1, 115.8, 107.0, 102.6 ppm; IR: ν_{max} 3310, 3098, 1675, 1038 cm^{-1}; HRMS (ESI) *m/z*: calcd. for $C_{14}H_{10}N_2O_3Na$ $[M+Na]^+$ 277.0589, found: 277.0584.

3-(4-Hydroxyphenyl)-4*H*-pyrido[1,2-*a*]pyrimidin-4-one (6v): Yellow solid, 189 mg, 53%, m.p. >200 °C; ^{1}H NMR (400 MHz, DMSO-d_6): δ 9.61 (s, 1*O*H), 9.08 (d, J = 6.6 Hz, 1H), 8.53 (s, 1H), 7.93 (dd, J = 7.5 Hz, J = 7.2 Hz, 1H), 7.72-7.66 (m, 3H), 7.39 (dd, J = 6.4 Hz, J = 6.3 Hz, 1H), 6.84 (d, J = 7.9 Hz, 2H) ppm; ^{13}C NMR (100 MHz, DMSO-d_6): δ 157.4, 156.5, 152.0, 150.2, 136.8, 129.9, 127.6, 126.5, 125.4, 117.0, 115.9, 115.6 ppm; IR: ν_{max} 3300, 3068, 1654, 1628, 1444, 1217 cm^{-1}; HRMS (ESI) *m/z*: calcd. for $C_{14}H_{11}N_2O_2$ $[M+H]^+$ 239.0821, found: 239.0805**.**

3-(3-Hydroxyphenyl)-4*H*-pyrido[1,2-*a*]pyrimidin-4-one (6w): Yellow solid, 160 mg, 45%, m.p. >200 °C; ^{1}H NMR (400 MHz, DMSO-d_6): δ 9.50 (s, 1*O*H), 9.10 (dd, J = 7.2 Hz, J = 0.6 Hz, 1H), 8.56 (s, 1H), 7.97 (ddd, J = 8.7 Hz, J = 6.7 Hz, J = 1.5 Hz, 1H), 7.73 (d, J = 8.8 Hz, 1H), 7.42 (ddd, J = 8.2 Hz, J = 7.0 Hz, J = 1.4 Hz, 1H),), 7.31-7.30 (m, 1H), 7.26-7.20 (m, 2H), 6.75 (ddd, J = 7.4 Hz, J = 2.0 Hz, J = 0.6 Hz, 1H) ppm; ^{13}C NMR (100 MHz, DMSO-d_6): δ 157.6, 156.3, 152.9, 150.7, 137.5, 136.1, 129.7, 127.9, 126.5, 119.4, 117.3, 115.7, 115.5, 114.9 ppm; IR: ν_{max} 3300, 3105, 1678, 1632, 1483, 1255 cm^{-1}; HRMS (ESI) *m/z*: calcd. for $C_{14}H_{10}N_2O_2Na$ $[M+Na]^+$ 261.0640, found: 261.0634.

4.2.4. Synthesis and characterization data of flavones (C1-C3):

The control compounds were synthesized following the literature reported method [21].

2-(Benzo[*d*][1,3]dioxol-5-yl)-4*H*-chromen-4-one (C1):[31] White solid, 143 mg, 54%, m.p. 198-200 °C; ^{1}H NMR (400 MHz, $CDCl_3$+DMSO-d_6): δ 8.18 (dd, J = 7.9 Hz, J = 1.6 Hz, 1H), 7.70 (ddd, J = 8.6 Hz, J = 7.2 Hz, J = 1.7 Hz, 1H), 7.55 (d, J = 8.4 Hz, 1H), 7.51 (dd, J = 8.3 Hz, J = 1.8 Hz, 1H), 7.42 (ddd, J = 8.0 Hz, J = 0.9 Hz, J = 0.9 Hz, 1H), 7.37 (d, J = 1.8 Hz, 1H), 6.94 (d, J = 8.2 Hz, 1H), 6.70 (s, 1H), 6.08 (s, 2H) ppm; ^{13}C NMR (100 MHz, $CDCl_3$+DMSO-d_6): δ 178.2, 163.0, 156.0, 150.6, 148.4, 133.7, 125.5, 125.4, 125.1, 123.7, 121.4, 117.9, 108.7, 106.3, 106.2, 101.9 ppm; IR: ν_{max} 2992, 1642, 1446, 1244, 1024 cm^{-1};

MS (ESI) *m/z* 289 (M + Na^+); Anal. Calcd. for $C_{16}H_{10}O_4$: C%, 72.18; H%, 3.79; Found: C%, 72.42; H%, 3.68.

2-(3,4,5-Trimethoxyphenyl)-4*H*-chromen-4-one (C2):[32] White solid, 140 mg, 45%, m.p. 159-161 °C; ^{1}H NMR (400 MHz, $CDCl_3$): δ 8.23 (dd, *J* = 7.9 Hz, *J* = 1.5 Hz, 1H), 7.71 (ddd, *J* = 8.6 Hz, *J* = 1.6 Hz, *J* = 1.3 Hz, 1H), 7.59 (d, *J* = 8.4 Hz, 1H), 7.43 (dd, *J* = 7.9 Hz, *J* = 7.2 Hz, 1H), 7.14 (s, 2H), 6.77 (s, 1H), 3.96 (s, 6H), 3.94 (s, 3H) ppm; ^{13}C NMR (100 MHz, $CDCl_3$): δ 178.3, 163.3, 156.2, 153.6, 141.2, 133.7, 127.0, 125.7, 125.3, 123.9, 118.1, 107.4, 103.8, 61.0, 56.4 ppm; IR: ν_{max} 2936, 1636, 1606, 1243, 1123 cm^{-1}; MS (ESI) *m/z* 335 (M + Na^+); Anal. Calcd. for $C_{18}H_{16}O_5$: C%, 69.22; H%, 5.16; Found: C%, 69.31; H%, 5.37.

2-(4-Methoxyphenyl)-4*H*-chromen-4-one (C3):[33] White solid, 169 mg, 67%, m.p. 158-160 °C; ^{1}H NMR (400 MHz, $CDCl_3$): δ 8.22 (dd, *J* = 7.9 Hz, *J* = 1.6 Hz, 1H), 7.88 (d, *J* = 8.9 Hz, 2H), 7.68 (ddd, *J* = 8.6 Hz, *J* = 7.1 Hz, *J* = 1.7 Hz, 1H), 7.54 (dd, *J* = 8.4 Hz, *J* = 0.6 Hz, 1H), 7.40 (ddd, *J* = 8.0 Hz, *J* = 1.0 Hz, *J* = 1.0 Hz, 1H), 7.02 (d, *J* = 8.9 Hz, 2H), 6.74 (s, 1H), 3.88 (s, 3H) ppm; ^{13}C NMR (100 MHz, $CDCl_3$): δ 178.4, 163.4, 162.4, 156.2, 133.6, 128.0, 125.7, 125.1, 124.0, 123.9, 117.9, 114.5, 106.2, 55.5 ppm; IR: ν_{max} 3050, 2992, 1645, 1265, 1122, 1024 cm^{-1}; MS (ESI) *m/z* 275 (M + Na^+); Anal. Calcd. for $C_{16}H_{12}O_3$: C%, 76.18; H%, 4.79; Found: C%, 76.46; H%, 4.71.

4.2.5. Synthesis and characterization data of isoflavones (C4-C7):

The control compounds were synthesized following the literature reported method[30]. 3-Iodo-4*H*-1-benzopyran-4-one was synthesised following the literature report. 3-Iodo-4*H*-1-benzopyran-4-one (1 mmol, 272 mg), K_2CO_3 (3 mmol, 414 mg, 3 eq), boronic acid (1.2 eq) and $Pd(PPh_3)_4$ (0.1 mmol, 115 mg, 10 mol %) were taken in a round-bottom flask and 1,4-dioxane (3 mL) and H_2O (0.5 mL) were added to the mixture. The mixture was heated at 110 °C for 18-24 h until complete consumption of the substrate as indicated by TLC. It was cooled to rt and concenterated under reduced pressure. The mixture was extracted with EtOAc (2x50 mL) and washed with water (2x5 mL) and brine (1x5 mL), dried with anhyd. Na_2SO_4, and concentrated under reduced pressure. The column chromatographic purification of crude mass was performed on silica gel using EtOAc-hexane (25-40%) as eluting solvent to afford the isoflavones (**C4-C7**).

3-(3,4,5-Trimethoxyphenyl)-4*H*-chromen-4-one (C4): Off-white solid, 193 mg, 62%, m.p. 117-119 °C; ^{1}H NMR (400 MHz, $CDCl_3$): δ 8.32 (dd, *J* = 8.0 Hz, *J* = 1.6 Hz, 1H), 8.05 (s,

1H), 7.70 (ddd, *J* = 8.6 Hz, *J* = 7.1 Hz, *J* = 1.7 Hz, 1H), 7.50 (d, *J* = 7.8 Hz, 1H), 7.45 (ddd, *J* = 8.0 Hz, *J* = 1.0 Hz, *J* = 1.0 Hz, 1H), 6.80 (s, 2H), 3.90 (s, 6H), 3.88 (s, 3H) ppm; ^{13}C NMR (100 MHz, $CDCl_3$): δ 176.3, 156.1, 153.3, 153.0, 138.3, 133.7, 127.3, 126.4, 125.3, 124.5, 118.1, 106.3, 60.8, 56.2 ppm; IR: ν_{max} 3069, 2976, 1644, 1118 cm^{-1}; MS (ESI) *m/z* 335 (M + Na^+); Anal. Calcd. for $C_{18}H_{16}O_5$: C%, 69.22; H%, 5.16; Found: C%, 69.49; H%, 5.17.

3-(4-Methoxyphenyl)-4*H*-chromen-4-one (C5):[25] White solid, 118 mg, 47%, m.p. 140-142 °C; ^{1}H NMR (400 MHz, $CDCl_3$): δ 8.31 (d, *J* = 8.0 Hz, 1H), 7.99 (s, 1H), 7.67 (dd, *J* = 8.2 Hz, *J* = 7.3 Hz, 1H), 7.51 (d, *J* = 8.7 Hz, 2H), 7.45 (d, *J* = 8.4 Hz, 1H), 7.42 (dd, *J* = 7.8 Hz, *J* = 7.3 Hz, 1H), 6.98 (d, *J* = 8.7 Hz, 2H), 3.84 (s, 3H) ppm; ^{13}C NMR (100 MHz, $CDCl_3$): δ 176.4, 159.7, 156.2, 152.5, 133.5, 130.1, 126.4, 125.1, 125.0, 124.5, 124.1, 118.0, 114.0, 55.3 ppm; IR: ν_{max} 3007, 2954, 1626, 1245, 1181 cm^{-1}; MS (ESI) *m/z* 275 (M + Na^+); Anal. Calcd. for $C_{16}H_{12}O_3$: C%, 76.18; H%, 4.79; Found: C%, 76.47; H%, 4.76.

3-(4-Methylphenyl)-4*H*-chromen-4-one (C6):[34] White solid, 118 mg, 50%, m.p. 156-158 °C; ^{1}H NMR (400 MHz, $CDCl_3$): δ 8.31 (dd, *J* = 8.0 Hz, *J* = 1.6 Hz, 1H), 8.00 (s, 1H), 7.67 (ddd, *J* = 8.6 Hz, *J* = 7.1 Hz, *J* = 1.7 Hz, 1H), 7.48-7.45 (m, 3H), 7.41 (ddd, *J* = 8.0 Hz, *J* = 1.0 Hz, *J* = 1.0 Hz, 1H), 7.25 (d, *J* = 7.8 Hz, 2H), 2.39 (s, 3H) ppm; ^{13}C NMR (100 MHz, $CDCl_3$): δ 176.3, 156.2, 152.8, 138.1, 133.5, 129.2, 128.9, 128.8, 126.4, 125.4, 125.2, 124.6, 118.0, 21.3 ppm; IR: ν_{max} 3008, 1633, 1276, 1112 cm^{-1}; MS (ESI) *m/z* 259 (M + Na^+); Anal. Calcd. for $C_{16}H_{12}O_2$: C%, 81.34; H%, 5.12; Found: C%, 81.24; H%, 5.10.

3-(Naphthalen-1-yl)-4*H*-chromen-4-one (C7):[35] White solid, 114 mg, 42%, m.p. 122-124 °C; ^{1}H NMR (400 MHz, $CDCl_3$): δ 8.36 (dd, *J* = 7.9 Hz, *J* = 1.4 Hz, 1H), 8.03 (s, 1H), 7.94-7.89 (m, 2H), 7.76-7.72 (m, 2H), 7.57-7.43 (m, 6H) ppm; ^{13}C NMR (100 MHz, $CDCl_3$): δ 176.5, 156.5, 154.2, 133.8, 133.7, 132.5, 129.8, 129.2, 128.4, 128.3, 126.6, 126.4, 126.0, 125.7, 125.5, 125.40, 125.37, 124.5, 118.2 ppm; IR: ν_{max} 3043, 1637, 1464, 1116 cm^{-1}; MS (ESI) *m/z* 295 (M + Na^+); Anal. Calcd. for $C_{19}H_{12}O_2$: C%, 83.81; H%, 4.44; Found: C%, 83.54; H%, 4.41.

4.3. Biology

Synthesized compounds were investigated for their ability to inhibit human DNA topoisomerase IIα (hTopoIIα) and for the investigation of mode of action. A screening kit purchased from TopoGEN, Inc. (Columbus, OH) was used. The screening protocols as

provided supplier and reported in literature[11,13,36] were followed. The concentrations of the reagents were varied according to need of our experiments.

4.3.1. hTopoIIα-mediated DNA decatenation assay

In hTopoIIα-mediated DNA decatenation assay, kinetoplast DNA (kDNA) was used as a substrate. All the reactions were carried out in micro centrifuge tubes on ice. Reaction mixture contains 4 units of purified hTopoIIα, 150 ng of catenated kDNA, and 100 μM investigated compound or standard drug (dissolved in DMSO) were combined in freshly prepared 5x complete reaction buffer. The final volume of reaction mixture was brought to 20 μL with distilled H_2O. In the standard assay method, the order of addition for assay components was H_2O, 5x complete buffer (buffer A: 0.5 M Tris-HCl (pH 8), 1.5 M sodium chloride, 100 mM magnesium chloride, 5 mM dithiothreitol, 300 μg of bovine serum albumin/mL and buffer B: 20 mM ATP in water), kDNA, followed by either test compound or standard drug and finally hTopoIIα. The reaction mixture was incubated at 37 ºC for 30 min. Further the reaction was stopped with 10% SDS, followed by digestion with proteinase K then incubated at 37 ºC for 15 min. Topological forms of kDNA were determined by running 1% agarose gel electrophoresis in Tris-acetate-EDTA (TAE) buffer containing 0.5 μg/mL ethidium bromide and further de-stained with water for 20 min. The bands of kDNA and decatenated products were visualized by Gel Doc EZ imager (BioRad, U. S. A.) and the products were quantified by using ImageLab (BioRad).

4.3.2. hTopoIIα-mediated DNA relaxation assay

In relaxation assay, a hot spot sequence for hTopoIIα containing supercoiled plasmid (pRYG) was used as a substrate. In the reaction mixture following components were added, freshly prepared 5x complete buffer (A: 0.5M Tris- HCl,pH 8), 1.50 M sodium chloride, 100 mM magnesium chloride, 5 mM dithiothreitol, 300 μg of bovine serum albumin/mL and buffer B: 20 mM ATP in water), 250 ng of supercoiled pHOT, followed by either test compound or etoposide (100 μM) and finally topoisomerase II (4 units). The final volume of reaction mixture was brought to 20 μL with distilled H_2O. Relaxation was carried out at 37 ºC for 30 min. The reaction was stopped with addition of 10% SDS followed by digestion with proteinase K and further incubated at 37 ºC for 15 min. Electrophoresis was performed in a 1% agarose gel in TAE buffer without ethidium bromide. Further the gel was stained with ethidium bromide (0.5 μg/mL) for 15 min, de-stained with water for 20 min, and photographed using Gel Doc EZ imager (BioRad, U. S. A.) of the quantification of products was carried out using ImageLab (BioRad).

4.3.3. Cleavage complex assay

Cleavage complex assay was performed using negatively small circular supercoiled plasmid (pHOT) as a substrate, following above mentioned protocol of the relaxation assay with modification that 8 units of hTopoIIα was added 3-5 min before the addition of the compound. Cleavage complex formation was started by incubating reaction mixture at 37 ºC for 20 min and stopped with 10% SDS, followed by digestion with proteinase K with subsequent incubation at 45 ºC for 30 min. After addition of the loading buffer, the reaction was heated at 70 ºC for 2 min. Electrophoresis was performed in a 1% agarose gel in TAE buffer containing ethidium bromide (0.5 µg/mL). Further the gel was de-stained with water for 20 min and photographed using Gel Doc EZ imager (BioRad, U. S. A.).Quantification of the products was carried out using ImageLab (BioRad).

4.3.4. DNA-intercalation assay

In this assay, 250 ng plasmid (pUC19) was incubated at 37 ºC for 20 min with 1 µg/ mL ethidium bromide, 100 µM standard drug (etoposide) or investigated compounds. Electrophoresis was carried out in a 1% agarose gel in TAE buffer without ethidium bromide. Further the gel was stained with ethidium bromide (0.5 µg/mL) for 15 min, de-stained with water for 20 min, and photographed using Gel Doc EZ imager (BioRad, U. S. A.).

4.3.5. Topo I-mediated relaxation assay

Negatively supercoiled DNA (pRYG) was used as a substrate in TopoI mediated DNA relaxation assay. Reaction mixture contained freshly prepared 5x complete buffer (100 mM Tris–HCl pH 7.9, 10 mM EDTA, 1.5 M NaCl, 1% Bovine Serum Albumin, 1 mM Spermidine and 50% glycerol), 250 ng of pRYG, followed by either test compound or standard drug camptothecin (100 µM) and finally topoisomerase I (4 units). The final volume of reaction mixture was brought to 20 µL with distilled H2O. Reaction mixture was incubated at 37 °C for 30 min and was quenched with the addition of 10% SDS followed by digestion with proteinase K at 37 °C for 15 min. Electrophoresis of the each sample was carried out in 1% agarose gel in TAE buffer without ethidium bromide. Gel was stained with ethidium bromide (0.5 µg/mL) for 15 min. Further, the gel was de-stained with water for 20 min and photographed using Gel Doc EZ imager (BioRad, U. S. A.).

4.3.6. CD based drug-DNA binding study*:*

Reaction mixture for CD spectroscopic study was containing 50 mM Tris-HCl buffer of pH 7.5, compound solution (100 µM) and CT-DNA solution (500 µg/mL), incubated at 25 °C for 2h. The CD spectra of the CT-DNA solution (500 µg/mL) recorded in the presence and

absence of investigated compounds and ethidium bromide (100 µM). EtBr (100 µM) was used as a positive control (known DNA intercalating agent CD spectroscopic measurements were carried out at 25 °C with cuvette having path length 1 mm using CD spectrometer (Jasco J-815) with the sensitivity of 100 millidegree and in continuous scanning mode with a speed of 100 nm/min; band-width was 1 nm and the number of accumulations was three. Scans were taken from 220 to 340 nm[37,38].

4.3.7. Measurement of Drug -DNA interaction using UV-Vis spectrophotometer

To measure the drug –DNA binding interaction a UV-Vis absorption spectrophotometric study was carried out with 1 cm path length quartz cuvette using UV-Vis spectrophotometer; (UV-2450 Shimadzu). The spectra were scanned in the wavelength range 220-340 nm. Stock solutions of the compounds (3m, 30 and 6d) were prepared in DMSO. This stock of each compound was diluted to various concentrations in 50 mM Tris-HCl/NaCl buffer (pH 7.5). For this assay a fixed concentration of DNA was used i.e. 50ng/mL. The drug DNA solutions were incubated for 1 h in 37ºC incubator to allow the formation of drug-DNA complex. Then the absorption spectra for different concentrations were taken within the wave length range 220-340 nm[29].

4.3.8. Calculation of binding constant (K_d)

The binding isotherm (θ) for **3m**, **3o** and **6d** was calculated by following formula:

$\theta = (A_0 - A_i)/ (A_0 - A_\alpha)$,

Here, A_0 is the absorbance of DNA in the absence of compound at 260 nm, A_i is the absorbance of DNA in the presence of any concentration, and A_α is the absorbance of DNA at a concentration for which maximum binding took place. K_M was calculated that is correspond to the half saturation point and the reciprocal of K_M was given by K_d (binding constant).

4.3.9. MTT assay

The anchorage dependant cell viability of the investigational compounds, etoposide and parent compounds were measured using MTT cell viability assay. Briefly, exponentially growing cells (8000-10,000cells/well) were seeded in 96 well flat bottom tissue culture plates. Then cells were treated with increasing concentrations of the compounds for 48 h prior to harvest. Then media was aspirated and washed once with 1XPBS. Then 0.05% MTT solution was added to each well and incubated in 37°C for 5 h to allow formation of formazan crystals. The formazan crystals were dissolved by adding 100 µL of 0.2% NP-40 detergent solution and incubated in dark for 1 h. The colour intensity was measured spectrophotometrically at 570 nm by using microplate reader (Mithras LB 940, Berthold,

Germany). The data obtained were presented graphically as percent viability against concentrations. The fifty percent viability (IC_{50}) was obtained from the graph. Each data point was calculated in triplicate and all the assays were performed at least thrice[11].

4.3.10. Clonogenic assay

The colony forming ability of cells after exposure to the compounds were measured using a well-defined assay known as colony forming assay or clonogenic assay. Briefly, HEK 293 cells (500/well) in 80-90% confluent were seeded and grown for 24 h. Then cells were treated varied concentrations of the compounds for 48 h. Then media was aspirated and replaced with the fresh media and allowed to grow for 6 days. Then plates were washed twice with 1X PBS and followed by stainied with 0.2% crystal violet for 1 h. After washing with water and air drying the plate, the colonies were counted. The data were calculated and graphically represented as percent survival against concentrations. Each data point was calculated in triplicate and all the assays were performed at least three times[39].

4.3.11. Detection of apoptotic nuclei by DAPI stain

Apoptotic nuclei after treatment with compound 3o was determined using DAPI saining method. Briefly ~1 × 10^6 cells were seeded in 40-mm dishes. After reaching 70–80% confluency, cells were treated with increasing concentration of compound 3o (0–10 μM) for 48 h. Cells were washed with ice-cold PBS and fixed with ice-chilled acetone: methanol (1:1) for 10 min at -20°C. Fixed cells were washed with ice cold PBS followed by incubation with the DAPI and 1h in dark. Excess DAPI was removed by repeated washing with chilled 1× PBS, and the samples were observed under fluorescence microscope (Nikon, Tokyo, Japan) at 40× magnification. The data provided here are from one of three independent experiments[39].

4.3.12. Matrigel invasion assay*:*

Matrigel invasion assay was carried out to study the ability of cells invade through the matrix. This assay was carried out with little modification in the protocol described by Mousseau *et al.* 2014. For this assay a matrix was prepared in a 6 well cell culture plate using egg albumin after carefully taking the albumin inside laminar hood and allowed to settle down by heating it in a hotpot at 65ºc temperature. The cells were seeded above the matrix and allowed to grow for next 24 hour. Cells were treated with increasing concentration of compound for 48 hours. After the required time period media were discarded followed by washing with 1X PBS. Cells were stained with 0.2% crystal violet after fixing with 4% para formaldehyde.

Excess stains were washed with 1X PBS and invaded colonies were counted using colony counter. Data were the replica of three independent experiments[40].

4.3.13. Annexin-V/FITC/PI dual staining*:*

Annexin-V/FITC/PI dual staining is used to detect the distribution of cells in early apoptotic, late apoptotic and necrosis phases. For this assay, cells were seeded in a 6 well cell culture plate at a density of 1 $x10^5$ cells per well. 70–80 percent confluent cells were treated with varying concentrations of compound 3o for 48 h. Then, the cells were harvested, washed and stained with Annexin-V/FITC and PI according to manufacturer's protocol (Sigma) and finally sorted by FACS and data were analysed by FCS express 5.0 software. Data given here is representative of one of three independent experiments[39].

4.3.14. Statistical analysis:

- Statistical significance was determined by paired *t* test *(*p<0.05), (**p<0.005), (***p<0.001).*

Abbreviations

hTopoIIα, Human topoisomerase IIα; kDNA, Kinetoplast DNA; Nck, Nicked; Rel, Relaxed; Lin, Linear; SC, Supercoiled; TAE, Tris-acetate-EDTA; MTT, 3-(4,5-Dimethylthiazol-2-yl)-2,5-diphenylte-trazolium bromide.

Acknowledgment

We gratefully acknowledge financial support from DBT, DST, and CSIR, Government of India, New Delhi, for this investigation. GP and SMA are thankful to NIPER for their fellowships. AN is thankful to ICMR for providing fellowship.

Supporting Information

Details of the analytical data of compounds are provided in the supporting information.

References

[1] N. Brown, E. Jacoby, On Scaffolds and Hopping in Medicinal Chemistry, Mini-Reviews Med. Chem. 6 (2006) 1217–1229. doi:10.2174/138955706778742768.

[2] H. Sun, G. Tawa, A. Wallqvist, Classification of scaffold-hopping approaches, Drug Discov. Today. 17 (2012) 310–324. doi:10.1016/j.drudis.2011.10.024.

[3] N.T. Southall, Ajay, Kinase Patent Space Visualization Using Chemical Replacements, J. Med. Chem. 49 (2006) 2103–2109. doi:10.1021/jm051201m.

[4] P. Singh, A. Mittal, Current Status of COX-2 Inhibitors, Mini-Reviews Med. Chem. 8 (2008) 73–90. doi:10.2174/138955708783331577.

[5] C. Shu, H. Ge, M. Song, J.H. Chen, H. Zhou, Q. Qi, et al., Discovery of Imigliptin, a Novel Selective DPP-4 Inhibitor for the Treatment of Type 2 Diabetes, ACS Med Chem Lett. 5 (2014) 921–926. doi:10.1021/ml5001905.

[6] F.E. Koehn, G.T. Carter, The evolving role of natural products in drug discovery, Nat. Rev. Drug Discov. 4 (2005) 206–220. doi:10.1038/nrd1657.

[7] M.S. Butler, The Role of Natural Product Chemistry in Drug Discovery, J. Nat. Prod. 67 (2004) 2141–2153. doi:10.1021/np040106y.

[8] G.M. Cragg, P.G. Grothaus, D.J. Newman, Impact of natural products on developing new anti-cancer agents, Chem. Rev. 109 (2009) 3012–3043. doi:10.1021/cr900019j.

[9] D.J. Newman, G.M. Cragg, Natural Products As Sources of New Drugs over the 30 Years from 1981 to 2010, J. Nat. Prod. 75 (2012) 311–335. doi:10.1021/np200906s.

[10] J. Rosén, J. Gottfries, S. Muresan, A. Backlund, T.I. Oprea, Novel Chemical Space Exploration via Natural Products, J. Med. Chem. 52 (2009) 1953–1962. doi:10.1021/jm801514w.

[11] A.T. Baviskar, C. Madaan, R. Preet, P. Mohapatra, V. Jain, A. Agarwal, et al., N-Fused Imidazoles As Novel Anticancer Agents That Inhibit Catalytic Activity of Topoisomerase IIα and Induce Apoptosis in G1/S Phase, J. Med. Chem. 54 (2011) 5013–5030. doi:10.1021/jm200235u.

[12] M. Kashyap, S. Kandekar, A.T. Baviskar, D. Das, R. Preet, P. Mohapatra, et al., Indenoindolone derivatives as topoisomerase II-inhibiting anticancer agents, Bioorganic Med. Chem. Lett. 23 (2013) 934–938. doi:10.1016/j.bmcl.2012.12.063.

[13] A.T. Baviskar, S.M. Amrutkar, N. Trivedi, V. Chaudhary, A. Nayak, S.K. Guchhait, et al., Switch in Site of Inhibition: A Strategy for Structure-Based Discovery of Human Topoisomerase IIα Catalytic Inhibitors, ACS Med. Chem. Lett. 6 (2015) 481–485. doi:10.1021/acsmedchemlett.5b00040.

[14] Y. Li, H. Fang, Wenfang Xu, Y. Li, H. Fang, W. Xu, Recent Advance in the Research of Flavonoids as Anticancer Agents, Mini-Reviews Med. Chem. 7 (2007) 663–678. doi:10.2174/138955707781024463.

[15] Y. Yoshinori, K. Sho-Zou, N. Hirofumi, Induction of mammalian topoisomerase ii dependent dna cleavage by nonintercalative flavonoids, genistein and orobol, Biochem. Pharmacol. 39 (1990) 737–744. doi:10.1016/0006-2952(90)90153-C.

[16] A. Constantinou, R. Mehta, C. Runyan, K. Rao, A. Vaughan, R. Moon, Flavonoids as DNA Topoisomerase Antagonists and Poisons: Structure-Activity Relationships, J. Nat. Prod. 58 (1995) 217–225. doi:10.1021/np50116a009.

[17] N. Chernyak, V. Gevorgyan, General and efficient copper-catalyzed three-component coupling reaction towards imidazoheterocycles: one-pot synthesis of alpidem and zolpidem., Angew. Chem. Int. Ed. Engl. 49 (2010) 2743–6. doi:10.1002/anie.200907291.

[18] S.K. Guchhait, S. Kandekar, M. Kashyap, N. Taxak, P. V Bharatam, C–H Bond Functionalization Under Metalation–Deprotonation Process: Regioselective Direct Arylation of 3-Aminoimidazo[1,2-a]pyrazine, J. Org. Chem. 77 (2012) 8321–8328. doi:10.1021/jo301065s.

[19] J.W. Dankwardt, Nickel-Catalyzed Cross-Coupling of Aryl Grignard Reagents with Aromatic Alkyl Ethers: An Efficient Synthesis of Unsymmetrical Biaryls, Angew. Chemie. 116 (2004) 2482–2486. doi:10.1002/ange.200453765.

[20] F. Kakiuchi, M. Usui, S. Ueno, N. Chatani, S. Murai, Ruthenium-Catalyzed Functionalization of Aryl Carbon-Oxygen Bonds in Aromatic Ethers with Organoboron Compounds, J. Am. Chem. Soc. 126 (2004) 2706–2707. doi:10.1021/ja0393170.

[21] S.K. Guchhait, G. Priyadarshani, Synthesis of 2-Arylpyridopyrimidinones, 6-Aryluracils, and Tri- and Tetrasubstituted Conjugated Alkenes via Pd-Catalyzed Enolic C–O Bond Activation–Arylation, J. Org. Chem. 80 (2015) 6342–6349. doi:10.1021/acs.joc.5b00771.

[22] S.K. Guchhait, G. Priyadarshani, Pd-Catalyzed Ag(I)-Promoted C3-Arylation of Pyrido[1,2-a]pyrimidin-4-ones with Bromo/Iodo-Arenes, J. Org. Chem. 80 (2015) 8482–8488. doi:10.1021/acs.joc.5b01573.

[23] N.C.W. Johansson, J. O.; Hansen, H. C.; Chiacchia, F. S.; Wong, Pharmaceutical compositions for the prevention and treatment of complex diseases and their delivery by insertable medical devices., PCT/US2006/029827, 2007.

[24] A.-S. Lin, K. Nakagawa-Goto, F.-R. Chang, D. Yu, S.L. Morris-Natschke, C.-C. Wu, et al., First Total Synthesis of Protoapigenone and Its Analogues as Potent Cytotoxic Agents, J. Med. Chem. 50 (2007) 3921–3927. doi:10.1021/jm070363a.

[25] D.A. Vasselin, A.D. Westwell, C.S. Matthews, T.D. Bradshaw, M.F.G. Stevens, Structural Studies on Bioactive Compounds. 40. 1 Synthesis and Biological Properties of Fluoro-, Methoxyl-, and Amino-Substituted 3-Phenyl-4 H -1-benzopyran-4-ones and a Comparison of Their Antitumor Activities with the Activities of Related 2-Phenylbenzo, J. Med. Chem. 49 (2006) 3973–3981. doi:10.1021/jm060359j.

[26] D. Darpan, G. Joshi, S.M. Amrutkar, A.T. Baviskar, H. Kler, S. Singh, et al., Synthesis and biological evaluation of new 2,5-dimethylthiophene/furan based N-acetyl pyrazolines as selective topoisomerase II inhibitors, RSC Adv. 6 (2016) 14880–14892. doi:10.1039/C5RA25705K.

[27] A. Negi, J.M. Alex, S.M. Amrutkar, A.T. Baviskar, G. Joshi, S. Singh, et al., Imine/amide–imidazole conjugates derived from 5-amino-4-cyano-N1-substituted benzyl imidazole: Microwave-assisted synthesis and anticancer activity via selective topoisomerase-II-α inhibition, Bioorg. Med. Chem. 23 (2015) 5654–5661. doi:10.1016/j.bmc.2015.07.020.

[28] R. Palchaudhuri, P.J. Hergenrother, DNA as a target for anticancer compounds: methods to determine the mode of binding and the mechanism of action, Curr. Opin. Biotechnol. 18 (2007) 497–503. doi:10.1016/j.copbio.2007.09.006.

[29] R. Preet, B. Chakraborty, S. Siddharth, P. Mohapatra, D. Das, S.R. Satapathy, et al., Synthesis and biological evaluation of andrographolide analogues as anti-cancer agents, Eur. J. Med. Chem. 85 (2014) 95–106. doi:10.1016/j.ejmech.2014.07.088.

[30] C. La Motta, S. Sartini, L. Mugnaini, F. Simorini, S. Taliani, S. Salerno, et al., Pyrido[1,2- a]pyrimidin-4-one Derivatives as a Novel Class of Selective Aldose Reductase Inhibitors Exhibiting Antioxidant Activity, J. Med. Chem. 50 (2007) 4917–4927. doi:10.1021/jm070398a.

[31] X. Huang, E. Tang, W.-M. Xu, J. Cao, Lewis Acid Catalyzed Solid-Phase Synthesis of Flavonoids Using Selenium-Bound Resin, J. Comb. Chem. 7 (2005) 802–805. doi:10.1021/cc0498231.

[32] Z. Du, H. Ng, K. Zhang, H. Zeng, J. Wang, Ionic liquid mediated Cu-catalyzed cascade oxa-Michael-oxidation: efficient synthesis of flavones under mild reaction conditions, Org. Biomol. Chem. 9 (2011) 6930-6933. doi:10.1039/c1ob06209c.

[33] J. Zhao, Y. Zhao, H. Fu, K 2 CO 3 -Catalyzed Synthesis of Chromones and 4-Quinolones through the Cleavage of Aromatic C–O Bonds, Org. Lett. 14 (2012) 2710–2713. doi:10.1021/ol300908g.

[34] M. Rao, V. Venkatesh, D. Jadhav, Pd-Catalyzed Efficient Cross-Couplings of 3-

Iodochromones with Triaryl-bismuths as Substoichiometric Multicoupling Organometallic Nucleophiles, Synlett. 2009 (2009) 2597–2600. doi:10.1055/s-0029-1217959.

[35] Y. Hoshino, N. Miyaura, A. Suzuki, Novel synthesis of isoflavones by the palladium-catalyzed cross-coupling reaction of 3-bromochromones with arylboronic acids or its esters., Bull. Chem. Soc. Jpn. 61 (1988) 3008–3010. doi:10.1246/bcsj.61.3008.

[36] S. Jiménez-Alonso, H.C. Orellana, A. Estévez-Braun, A.G. Ravelo, E. Pérez-Sacau, F. Machín, Design and synthesis of a novel series of pyranonaphthoquinones as topoisomerase II catalytic inhibitors, J. Med. Chem. 51 (2008) 6761–6772. doi:10.1021/jm800499x.

[37] R. Preet, B. Chakraborty, S. Siddharth, P. Mohapatra, D. Das, S.R. Satapathy, et al., Synthesis and biological evaluation of andrographolide analogues as anti-cancer agents, Eur. J. Med. Chem. 85 (2014) 95–106. doi:10.1016/j.ejmech.2014.07.088.

[38] S.K. Samanta, D. Dutta, S. Roy, K. Bhattacharya, S. Sarkar, A.K. Dasgupta, et al., Mahanine, A DNA Minor Groove Binding Agent Exerts Cellular Cytotoxicity with Involvement of C-7-OH and −NH Functional Groups, J. Med. Chem. 56 (2013) 5709–5721. doi:10.1021/jm400290q.

[39] V. Chaudhary, S. Das, A. Nayak, S.K. Guchhait, C.N. Kundu, Scaffold-hopping and hybridization based design and building block strategic synthesis of pyridine-annulated purines: discovery of novel apoptotic anticancer agents, RSC Adv. 5 (2015) 26051–26060. doi:10.1039/C5RA00052A.

[40] Y. Mousseau, S. Mollard, H. Qiu, L. Richard, R. Cazal, A. Nizou, et al., In vitro 3D angiogenesis assay in egg white matrix: comparison to Matrigel, compatibility to various species, and suitability for drug testing, Lab. Investig. 94 (2014) 340–349. doi:10.1038/labinvest.2013.150.

Supplementary Information

Experimental Section

Scanned NMR spectra

3a: ^{1}H NMR

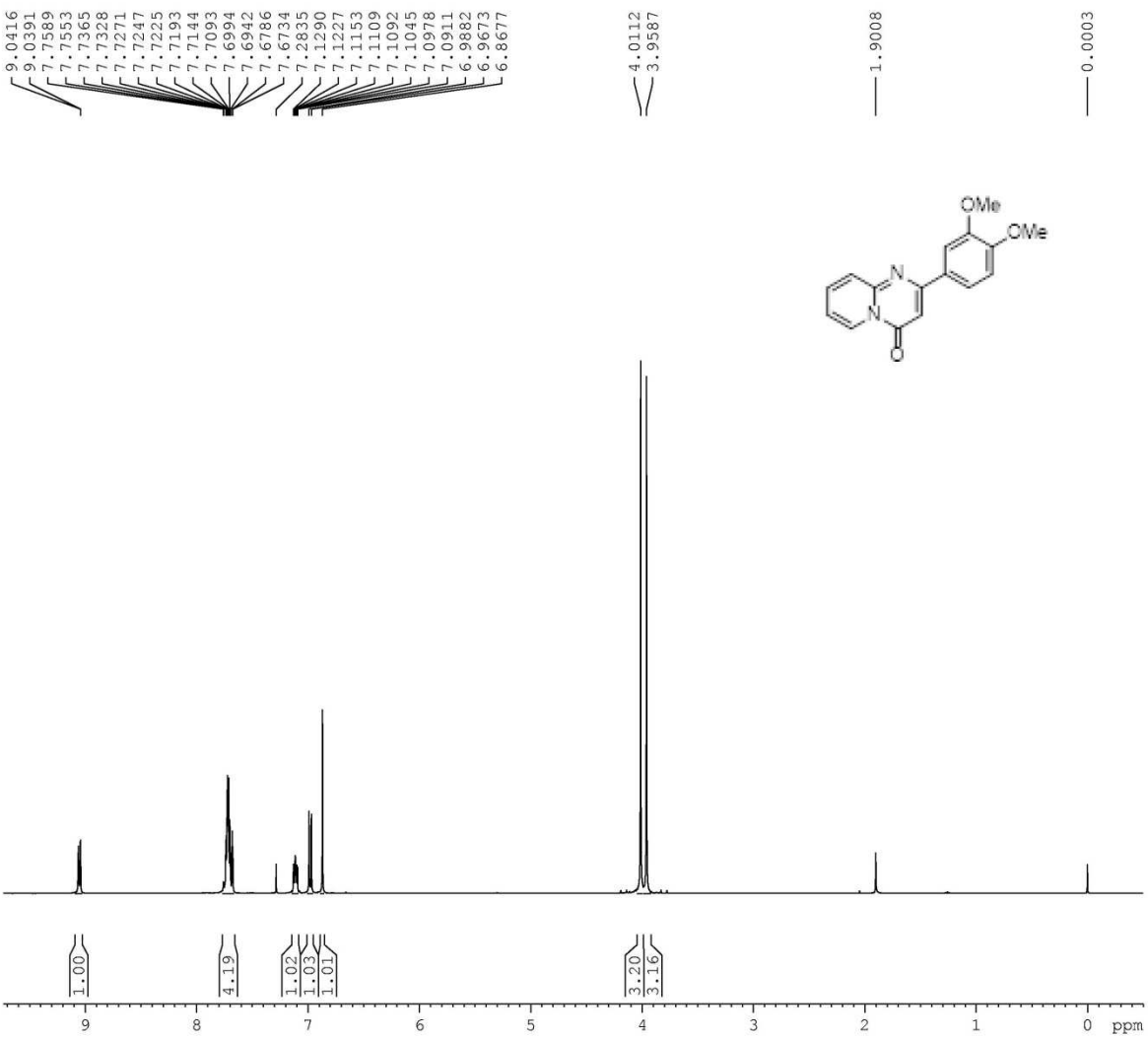

3a: ^{13}C NMR

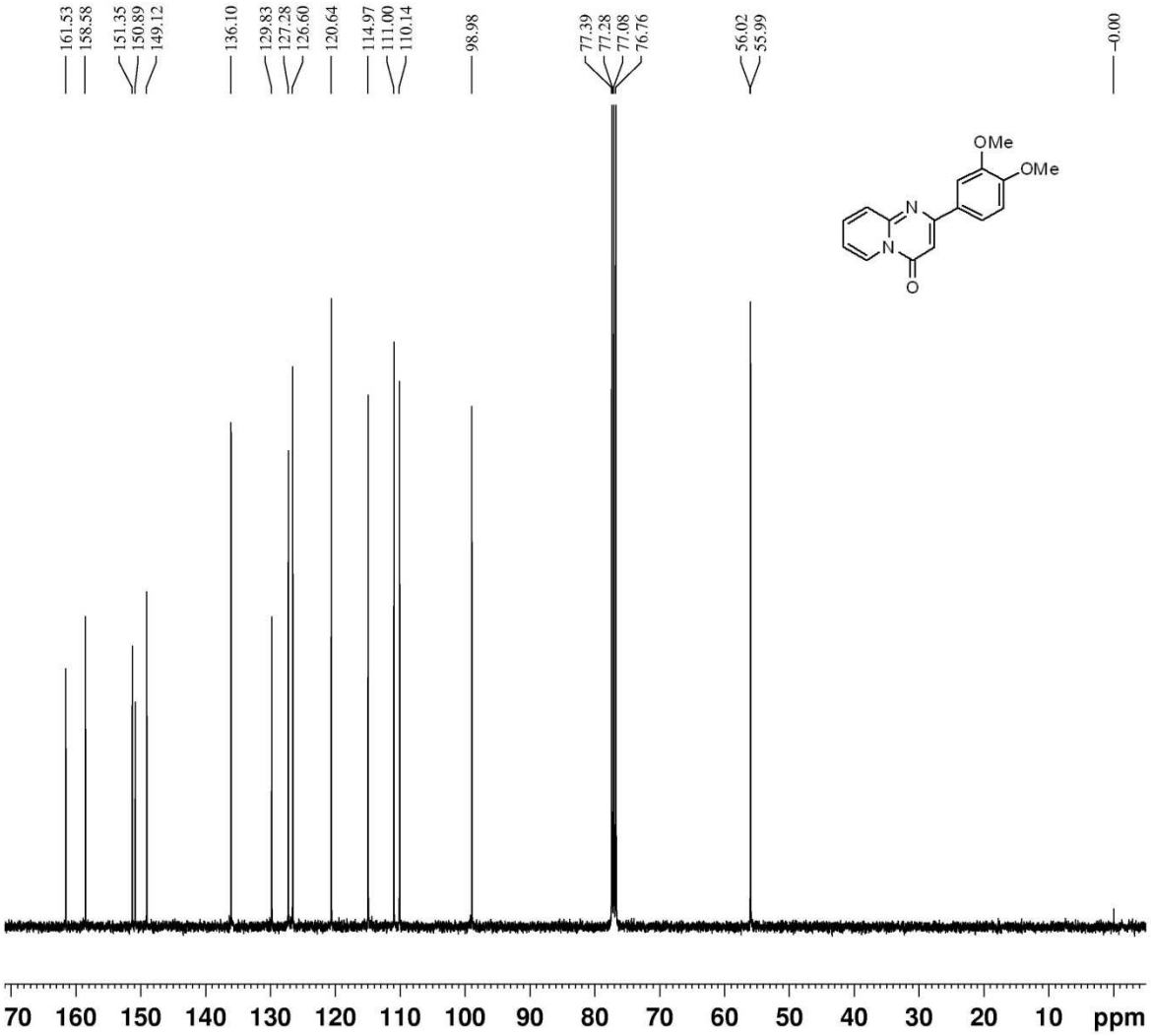

3b: ^{1}H NMR

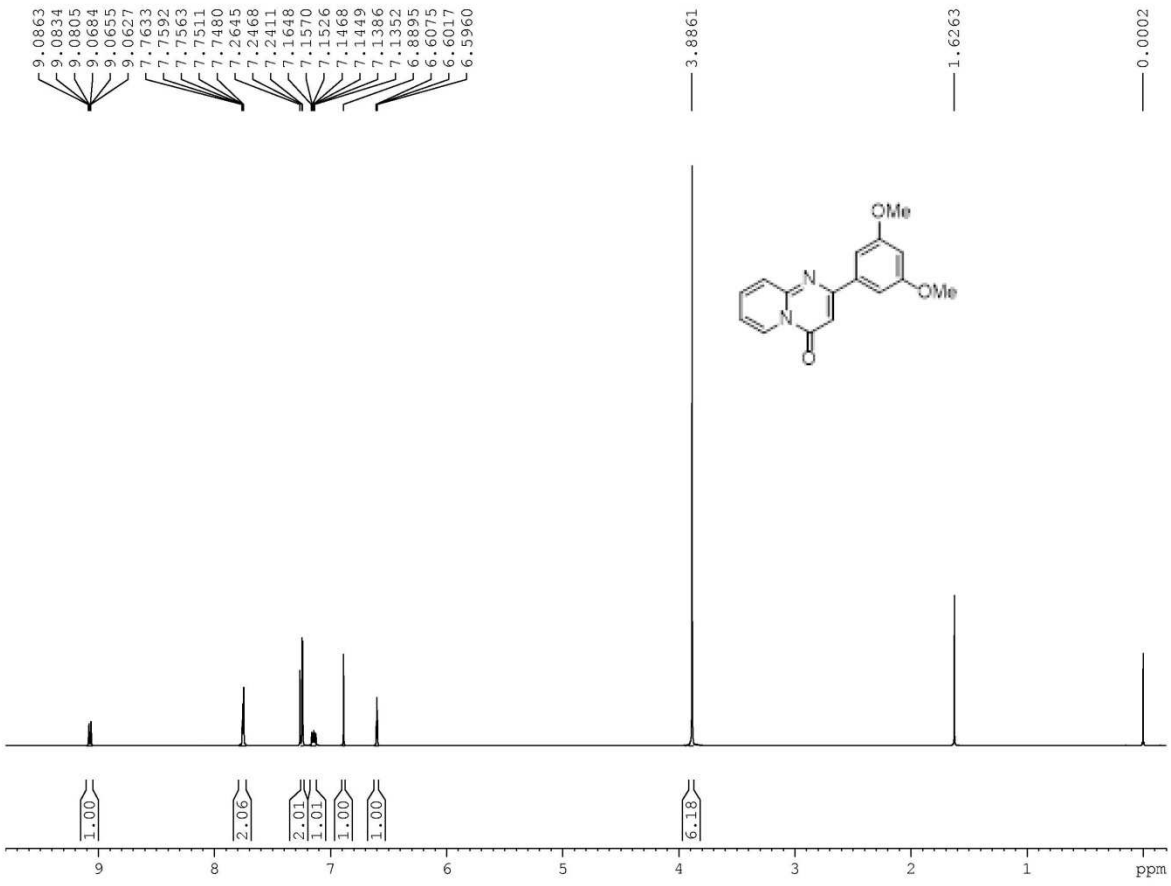

3b: ^{13}C NMR

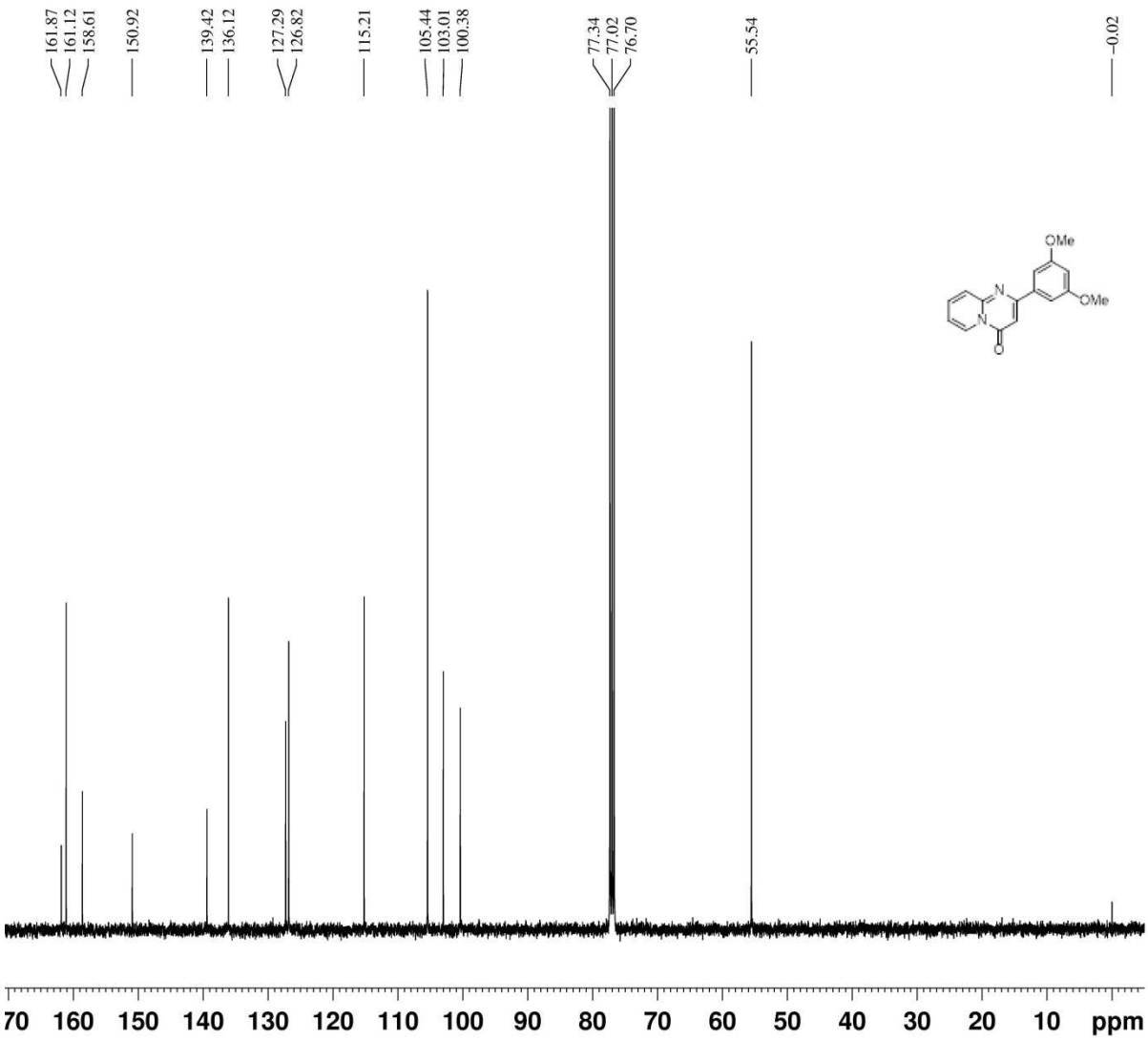

3f: ^{1}H NMR

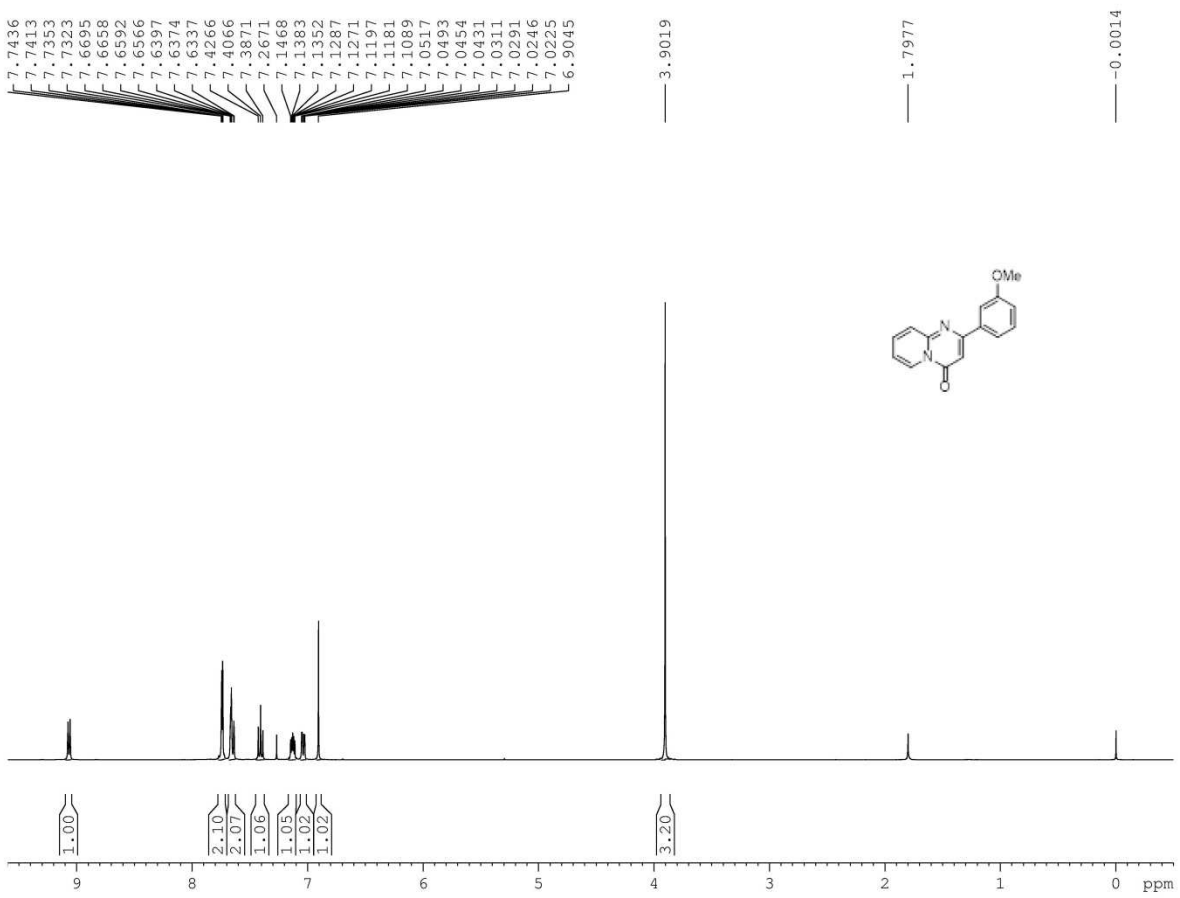

3f: ^{13}C NMR

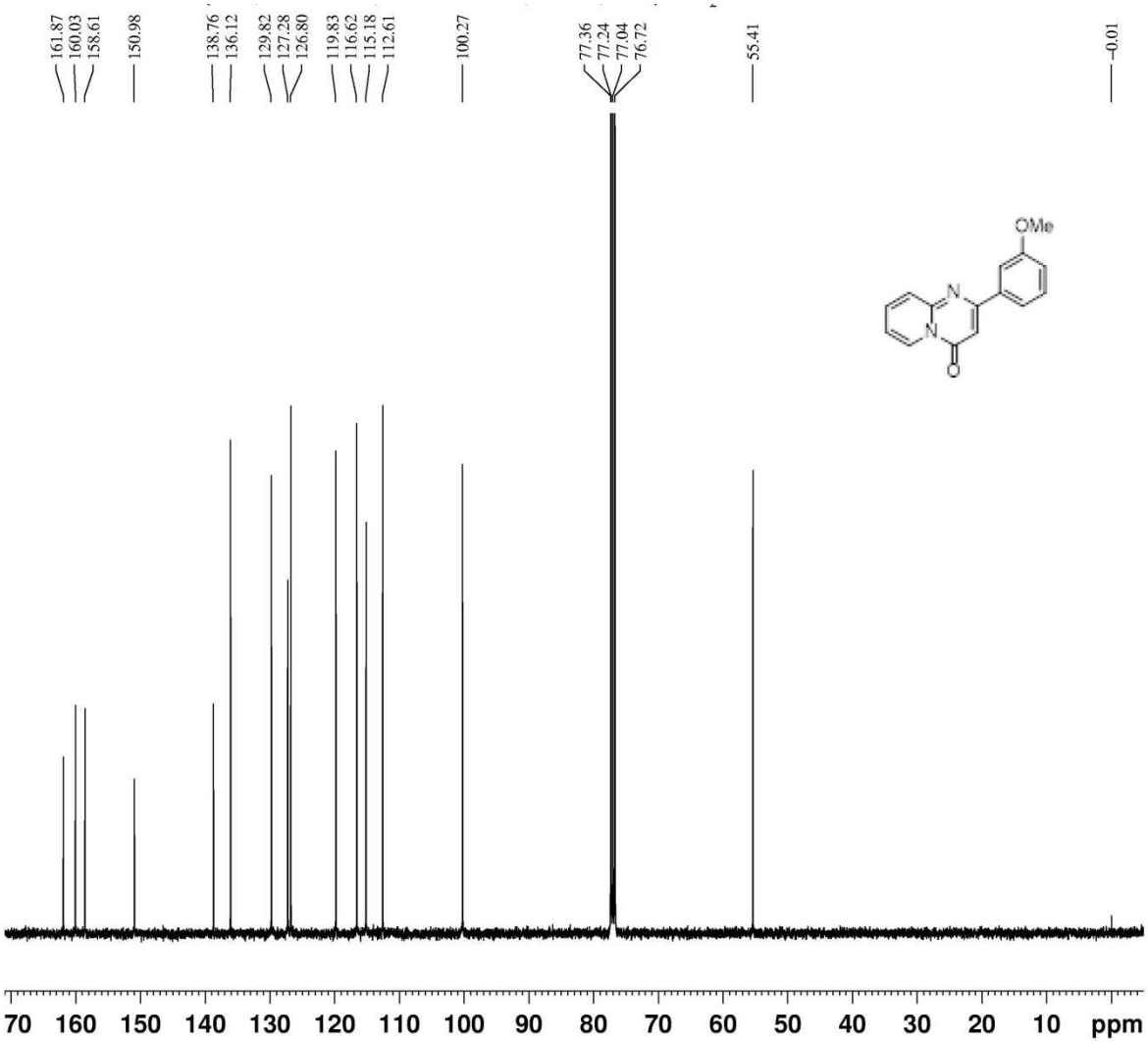

3i: ^{1}H NMR

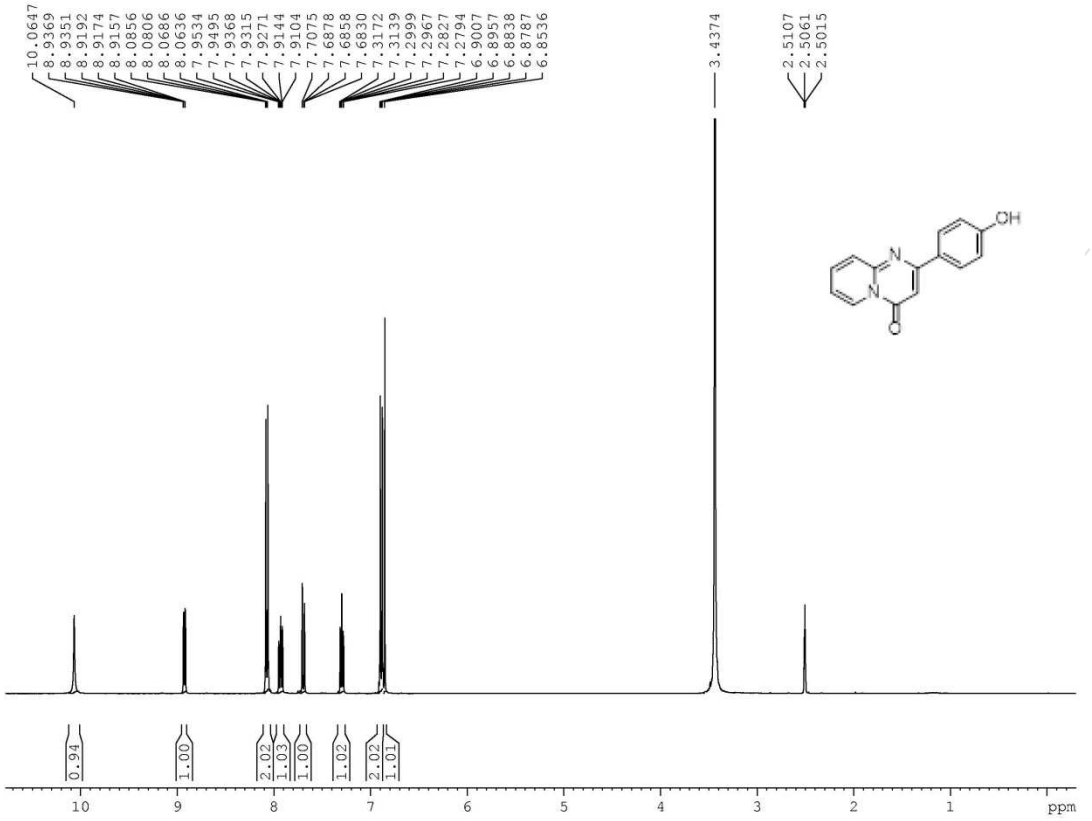

3i: ^{13}C NMR

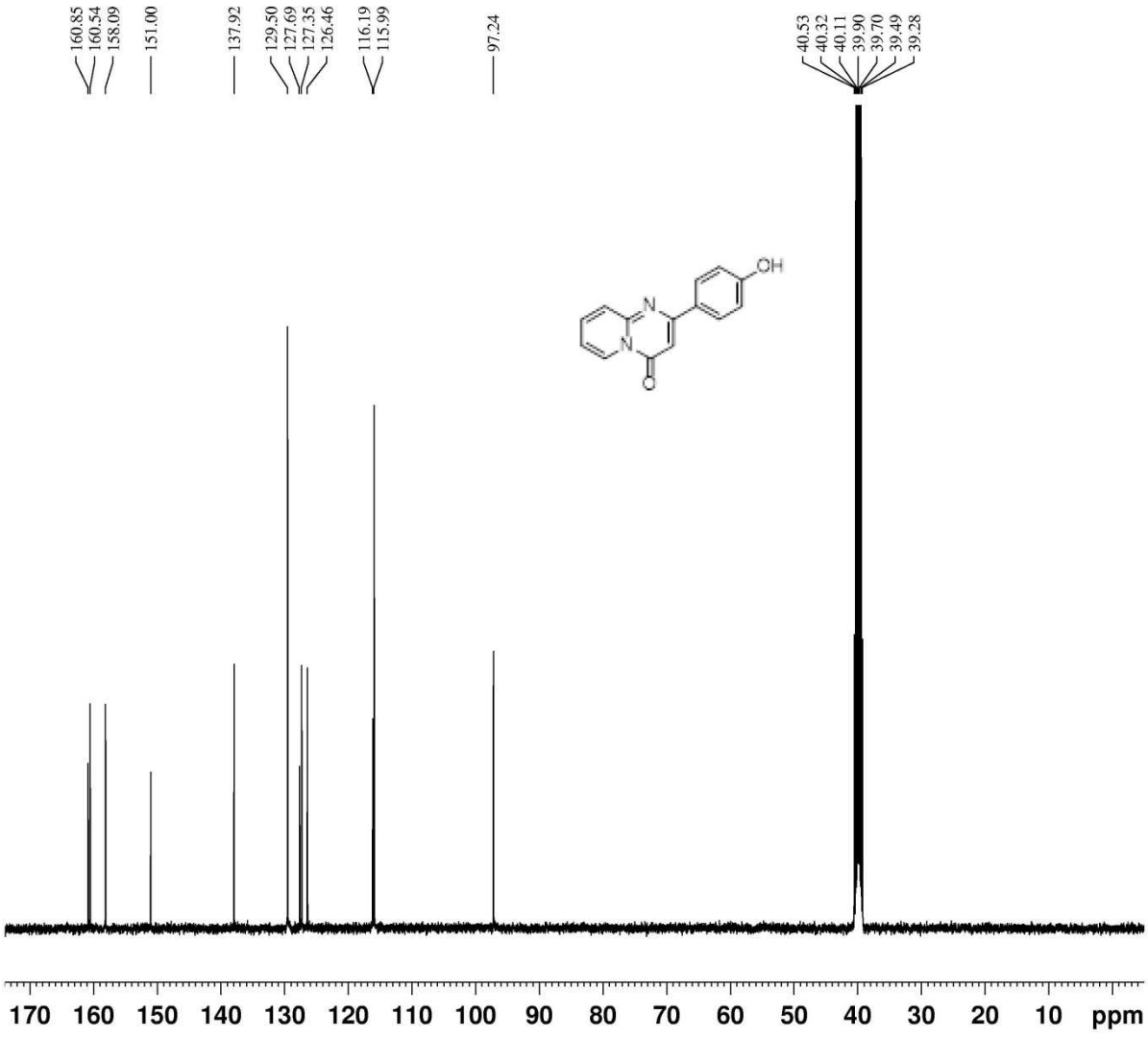

3s: ^{1}H NMR

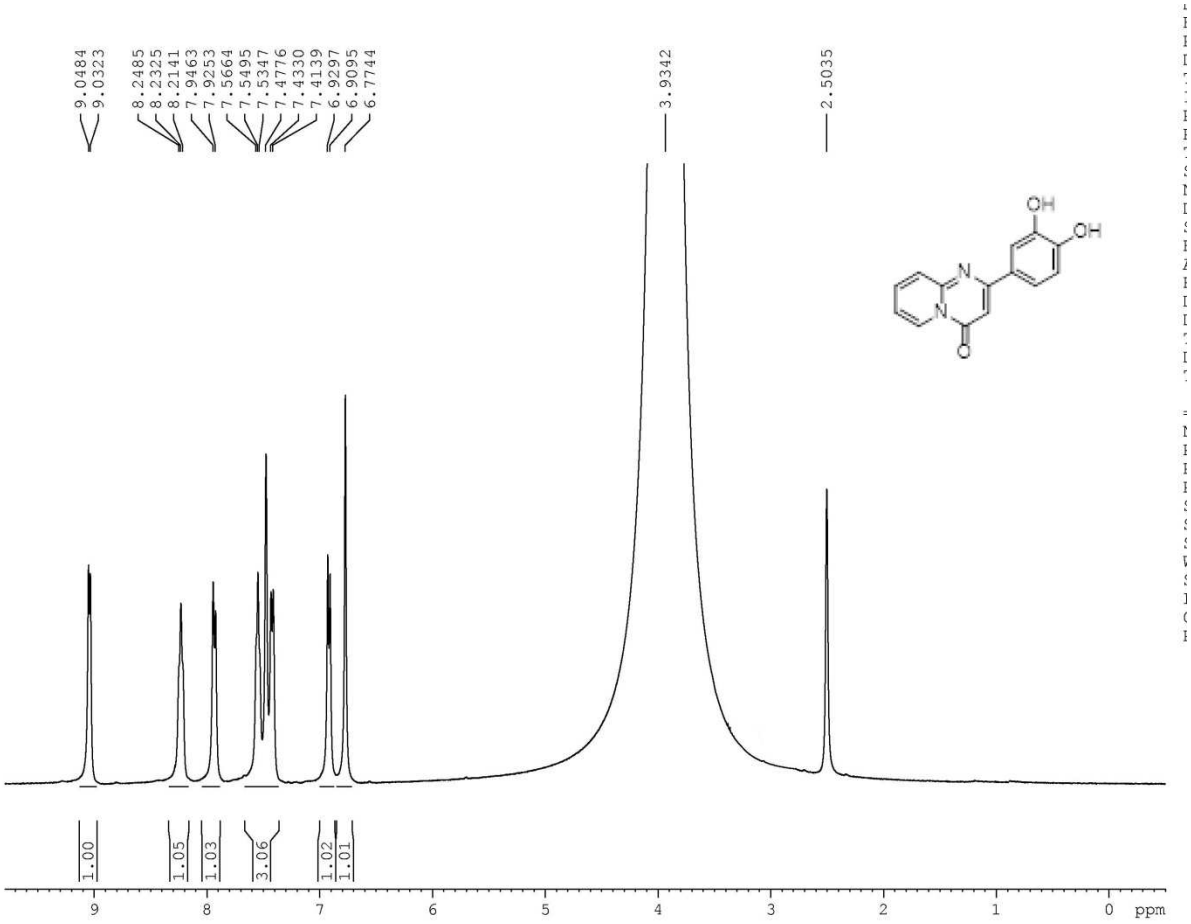

3s: ^{13}C NMR

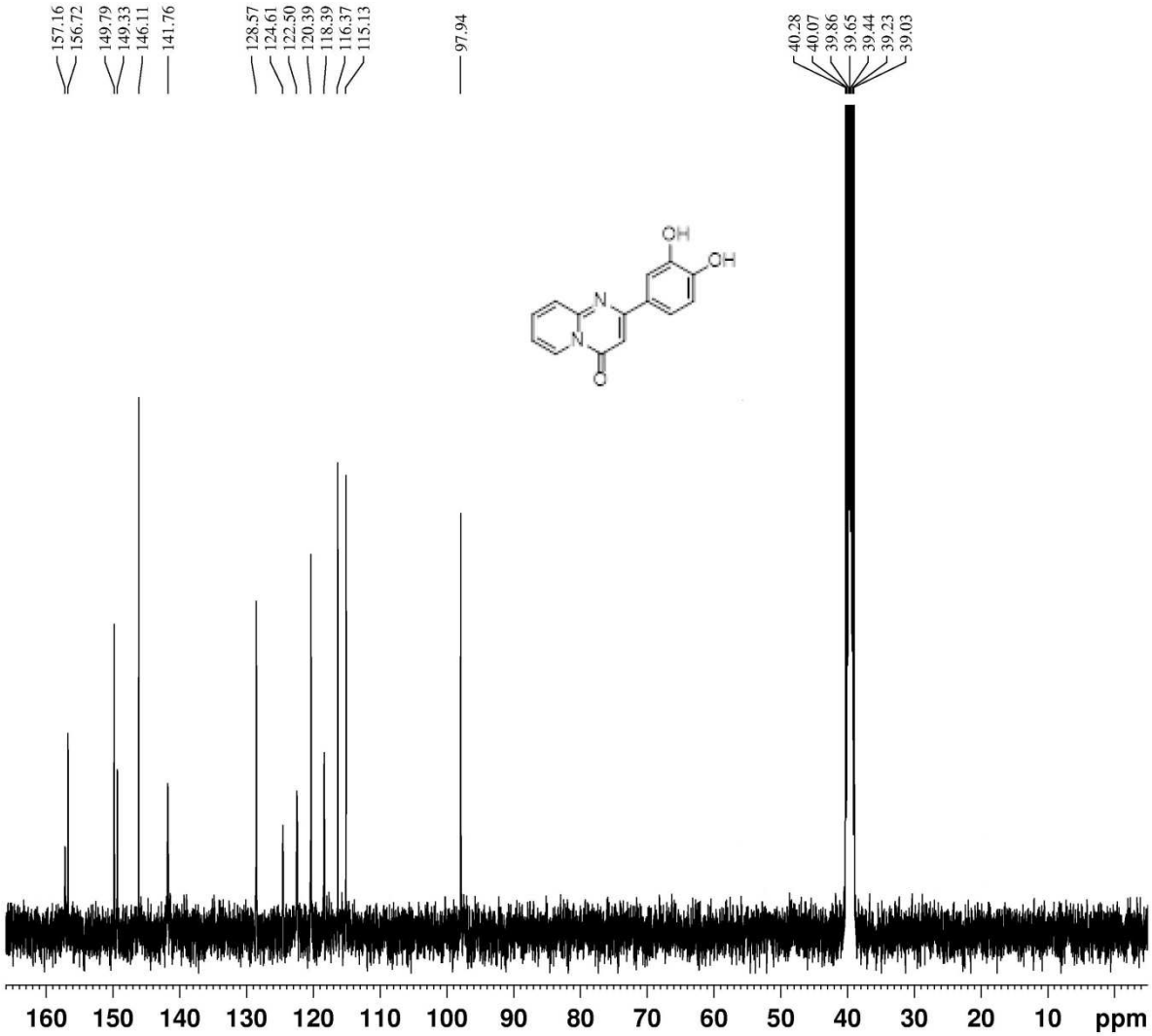

3t: ^{1}H NMR

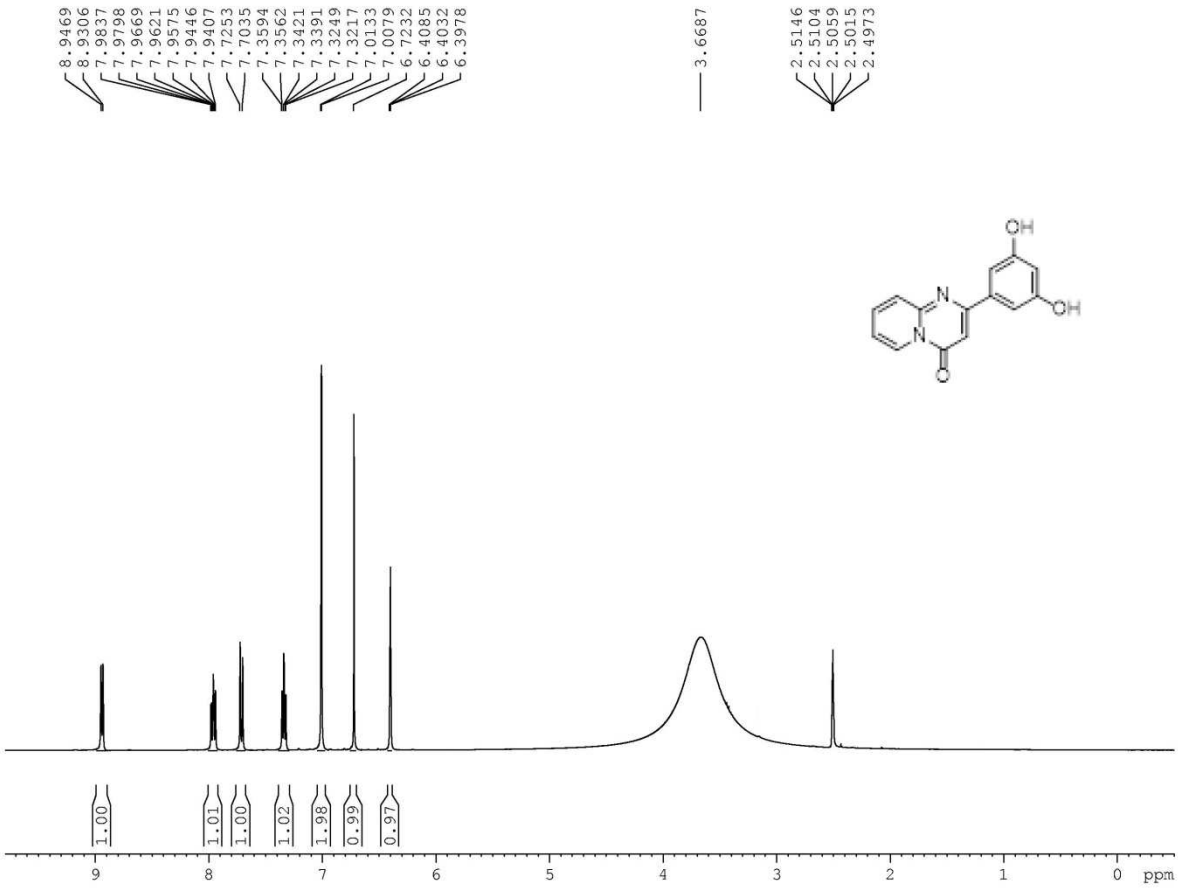

3t: ^{13}C NMR

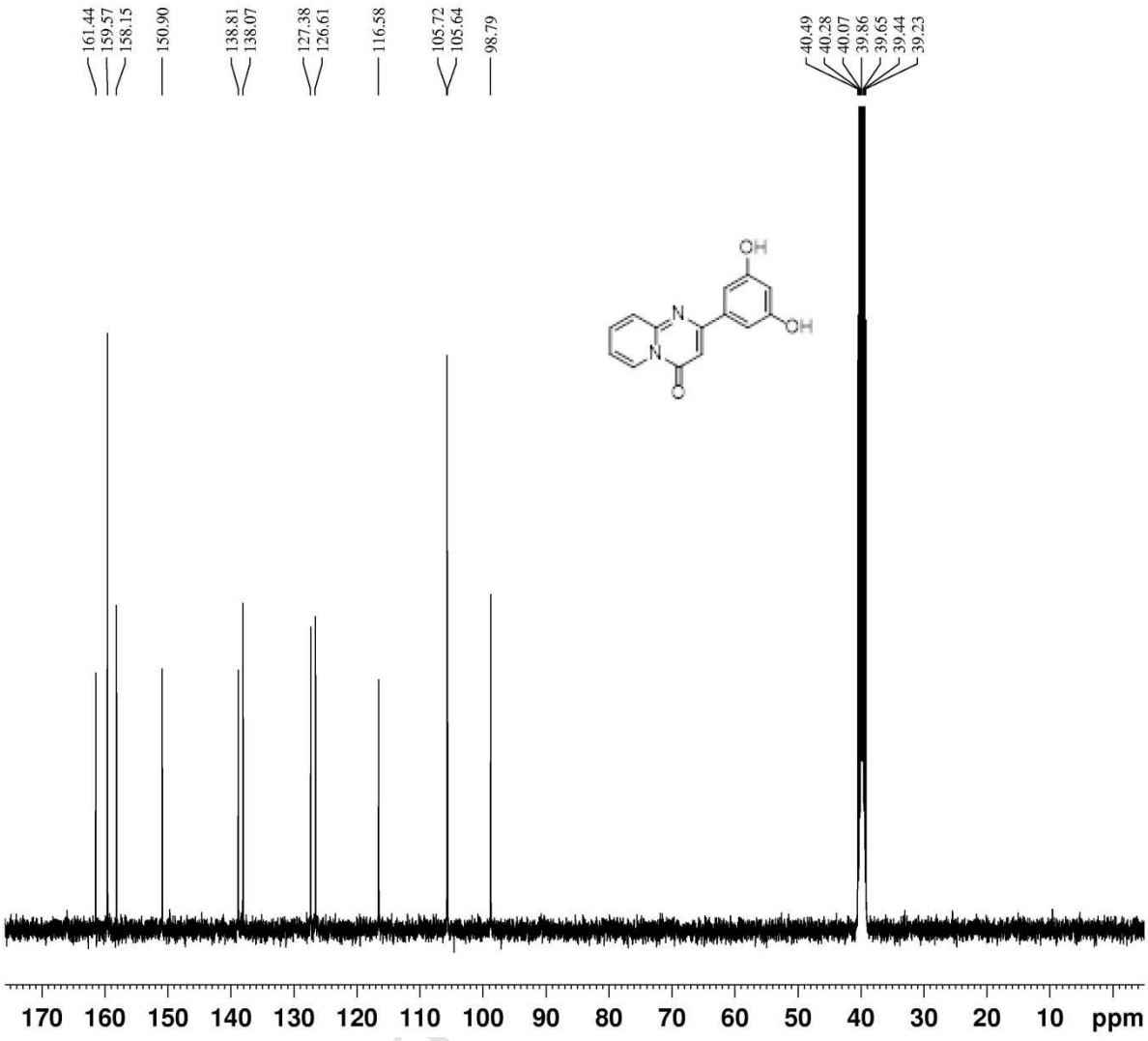

6t: ^{1}H NMR

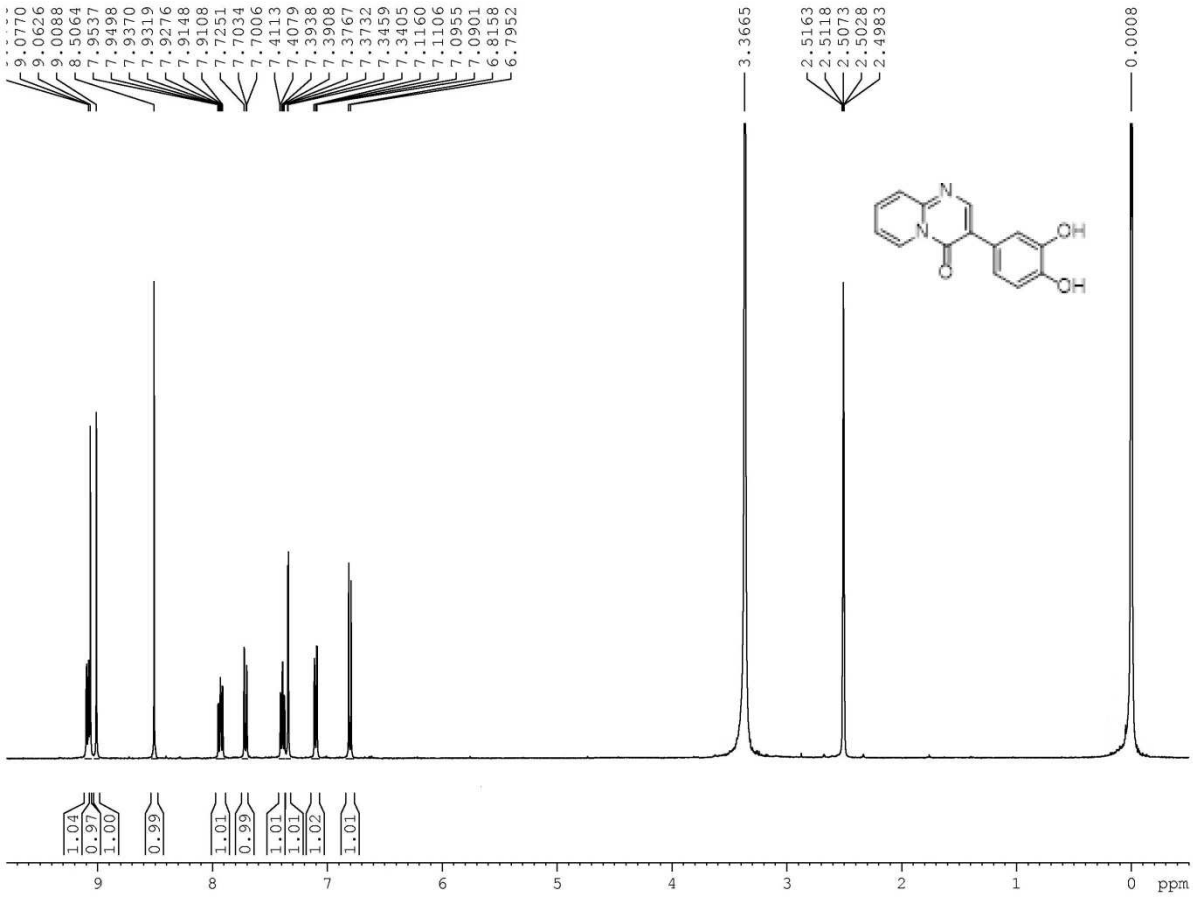

6t: ^{13}C NMR

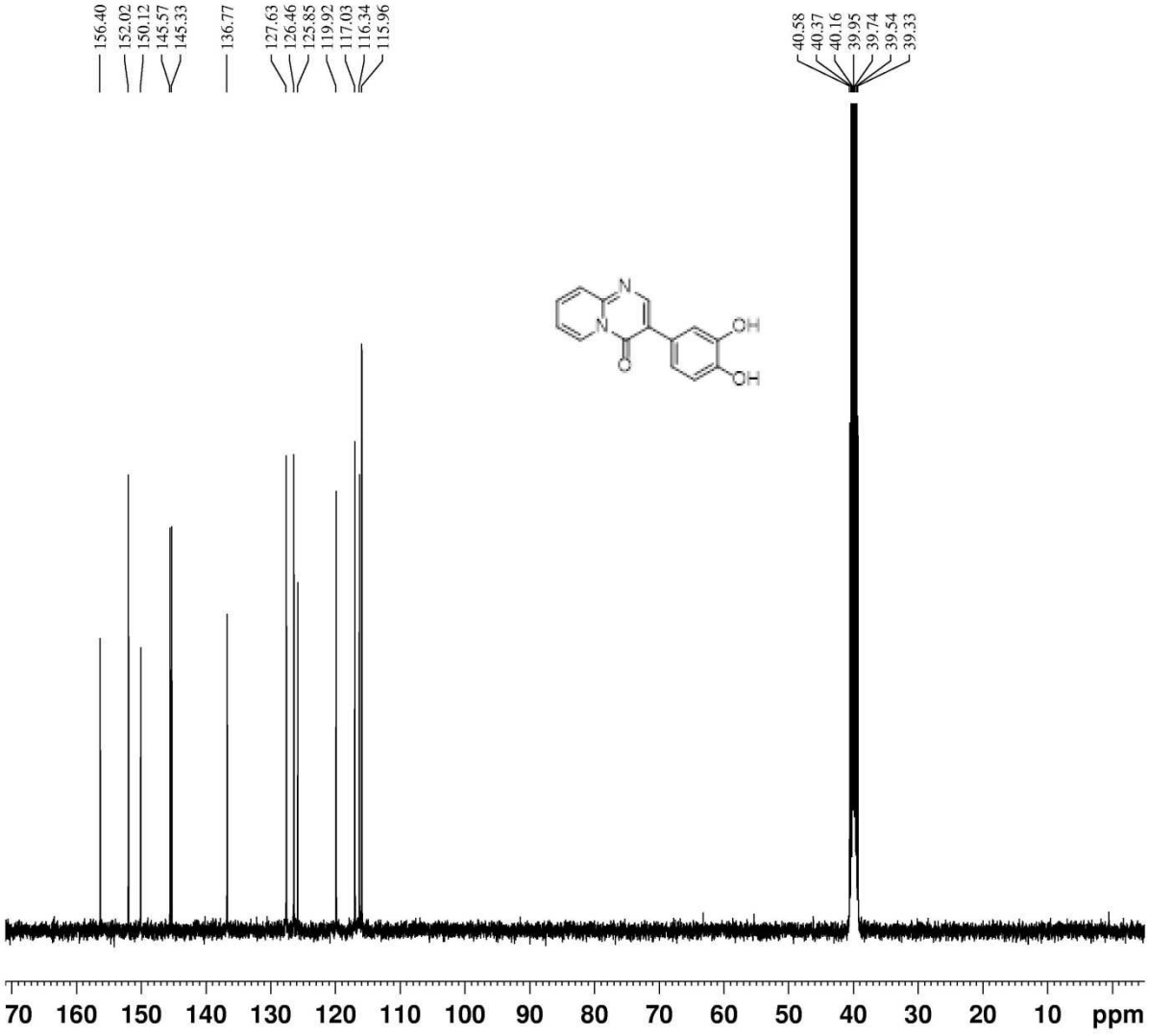

6u: ^{1}H NMR

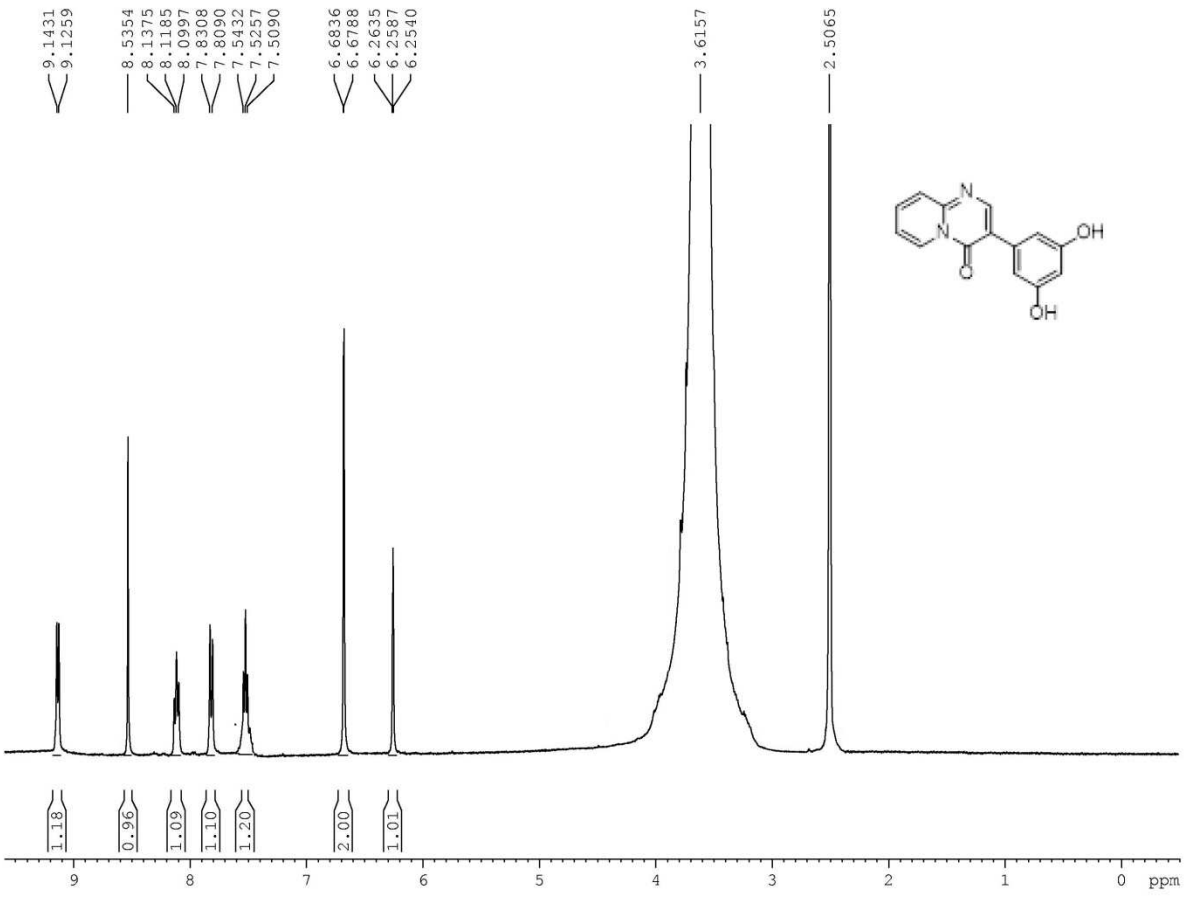

6u: ^{13}C NMR

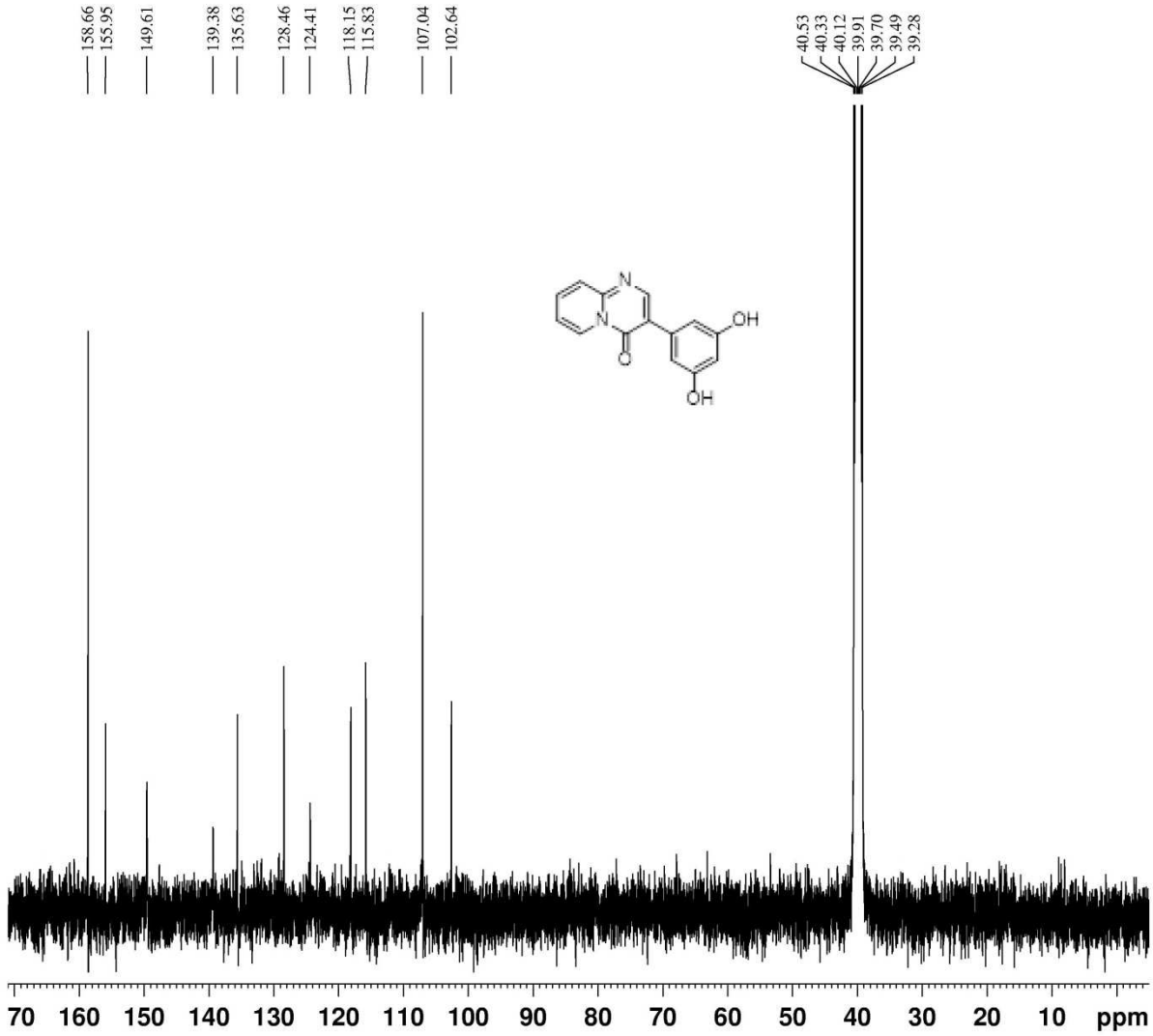

6v: ^{1}H NMR

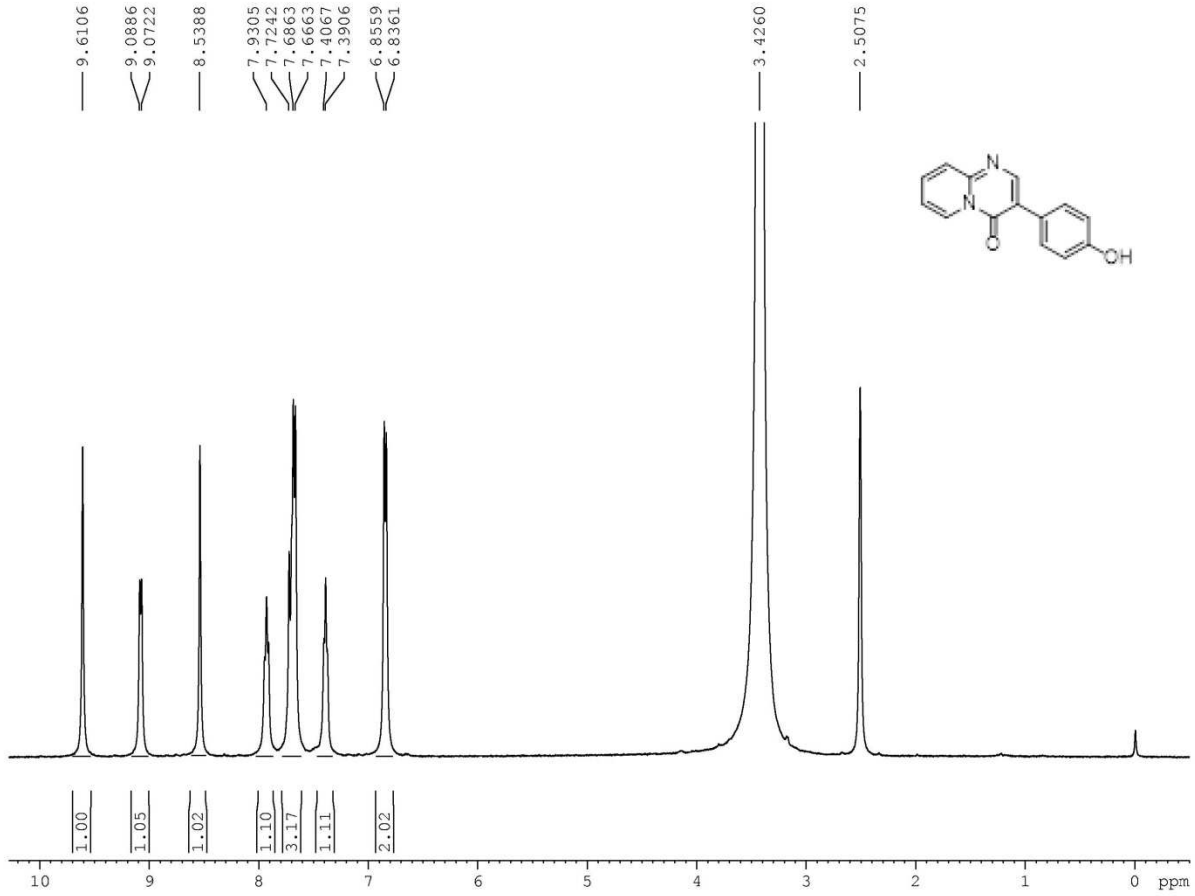

6v: ^{13}C NMR

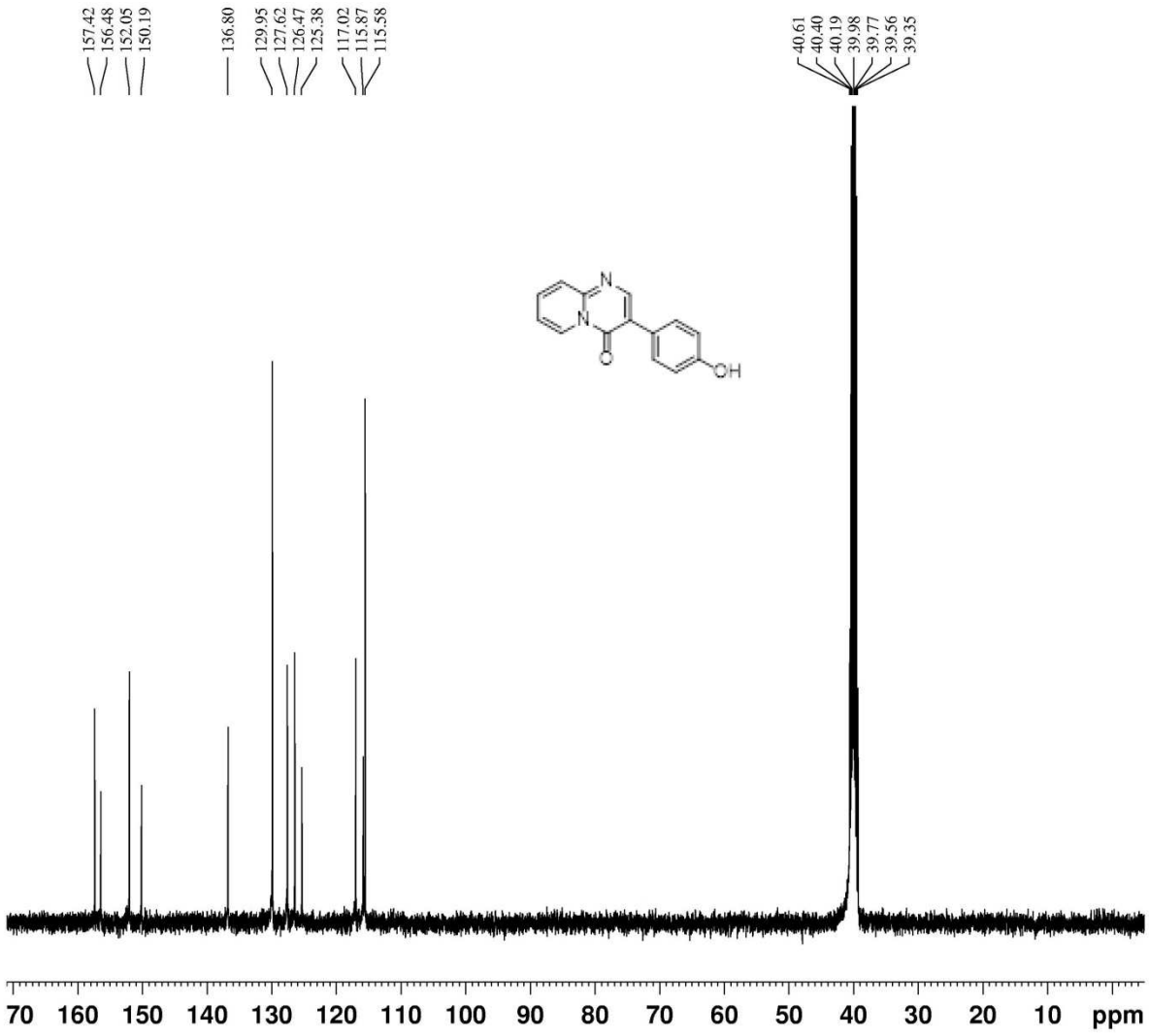

6w: ^{1}H NMR

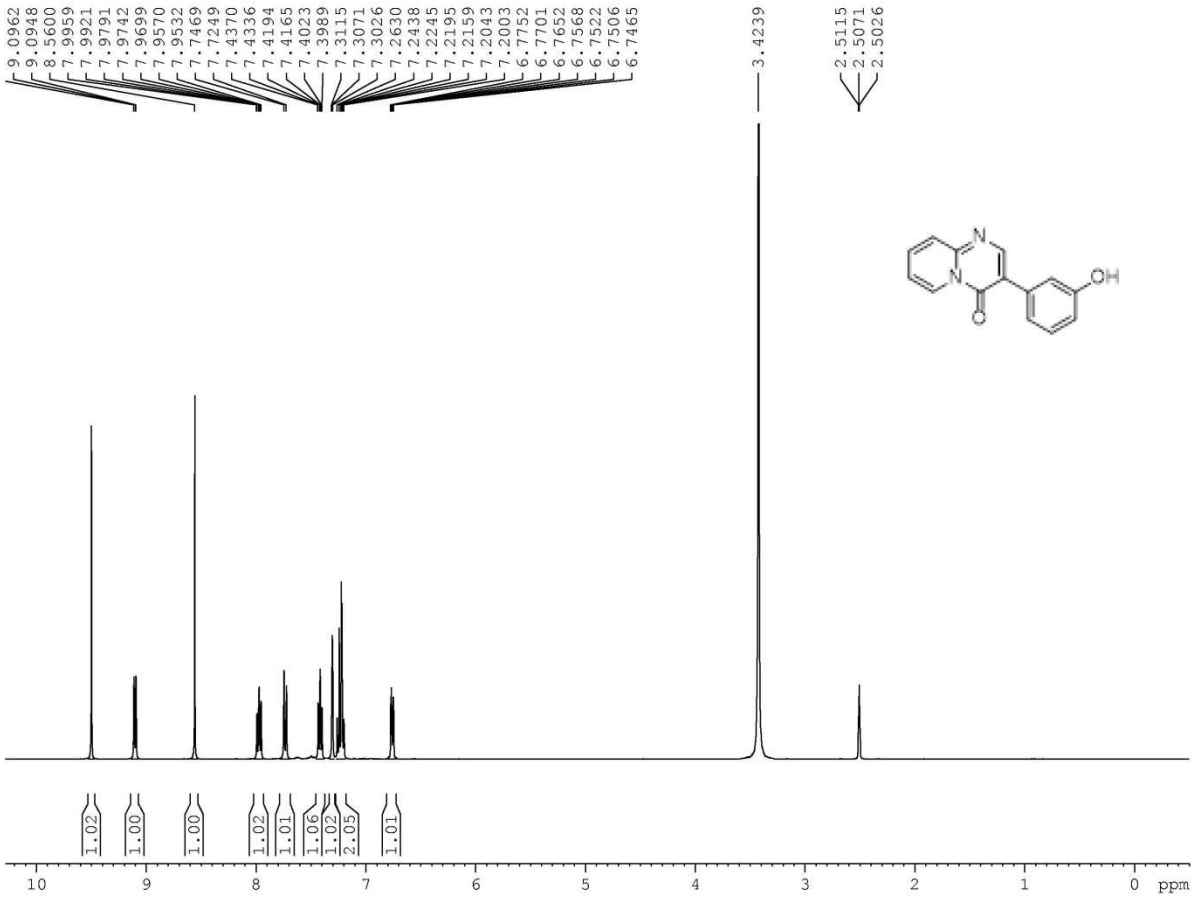

6w: ^{13}C NMR

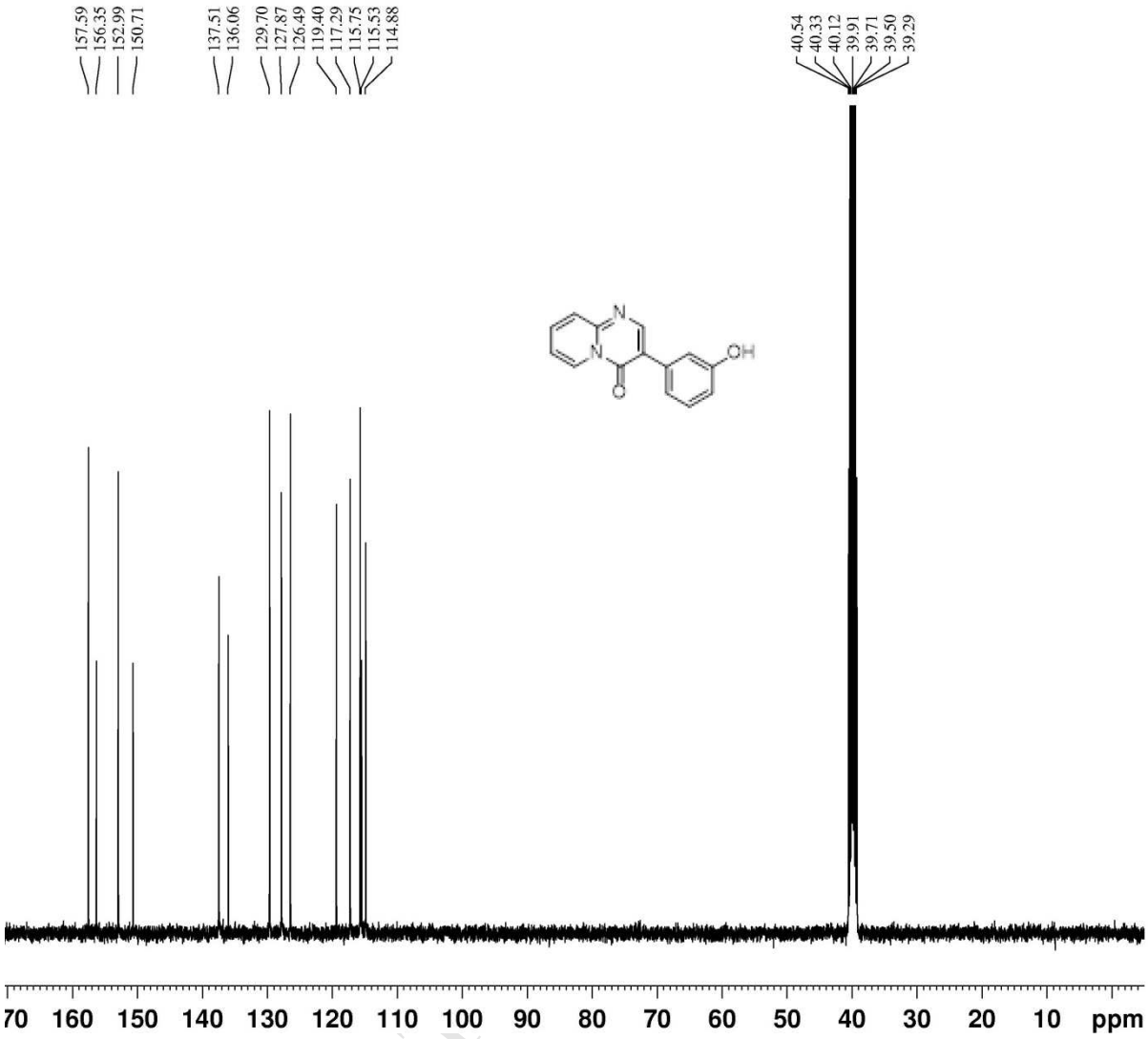

C1: ^{1}H NMR

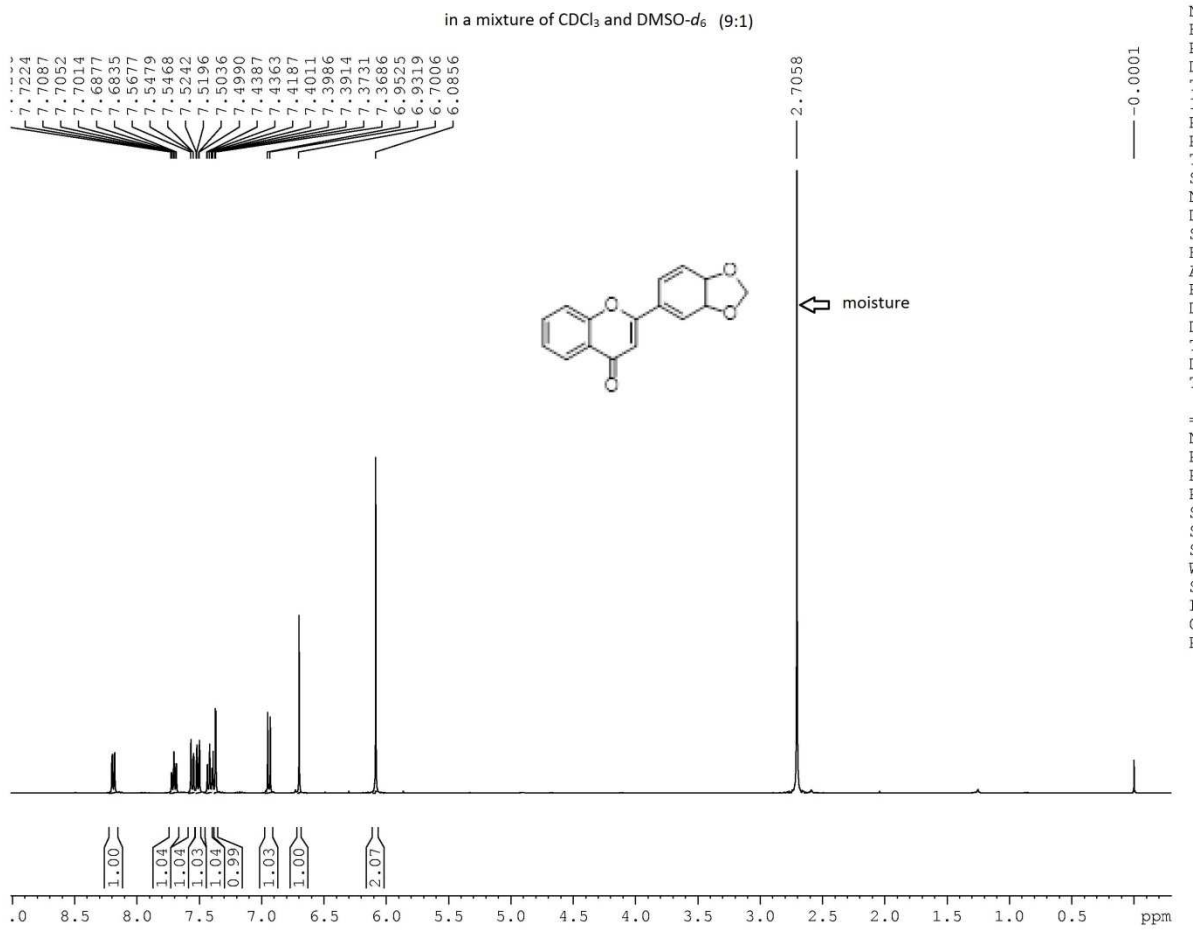

C1: ^{13}C NMR

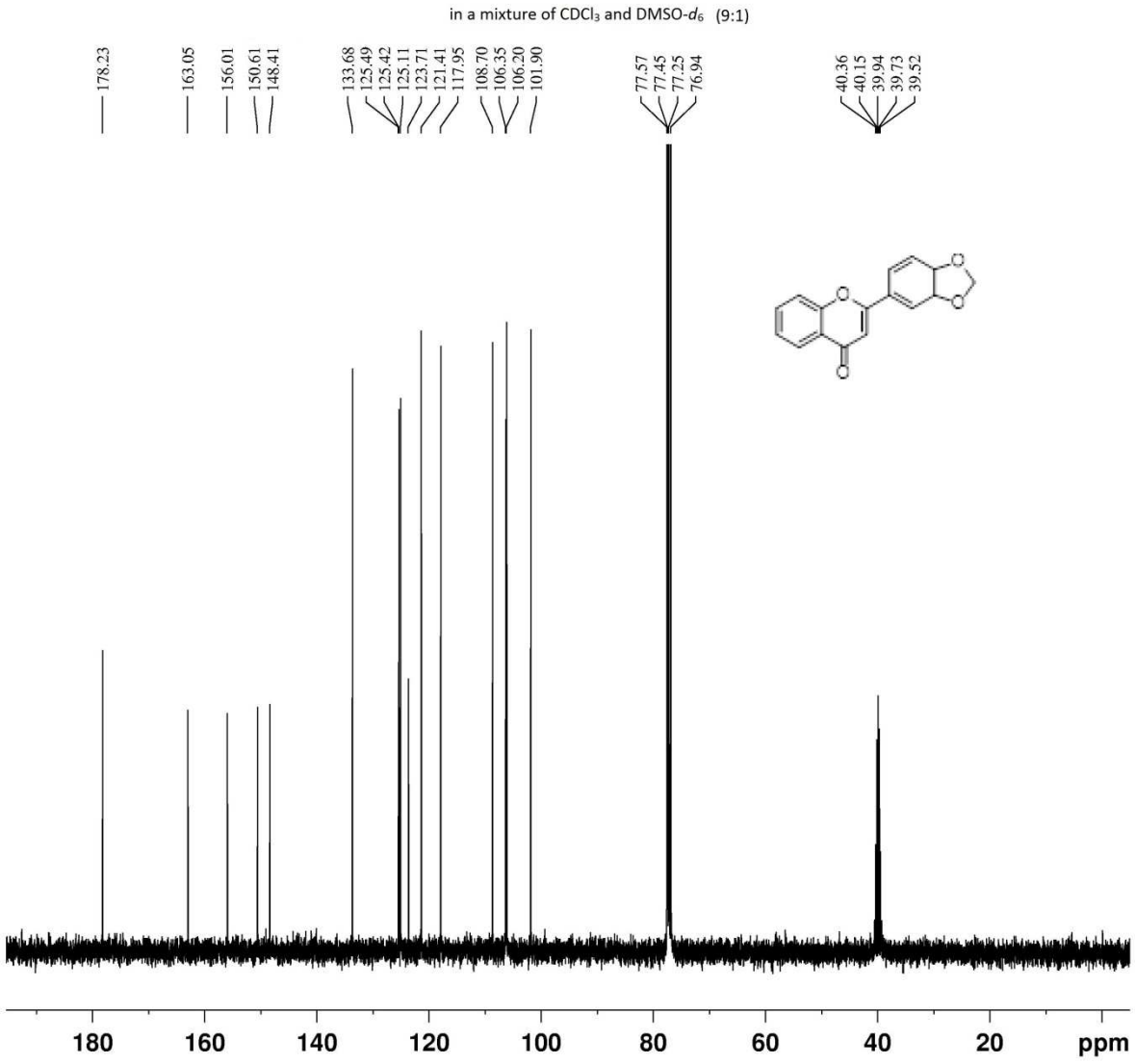

C2: ^{1}H NMR

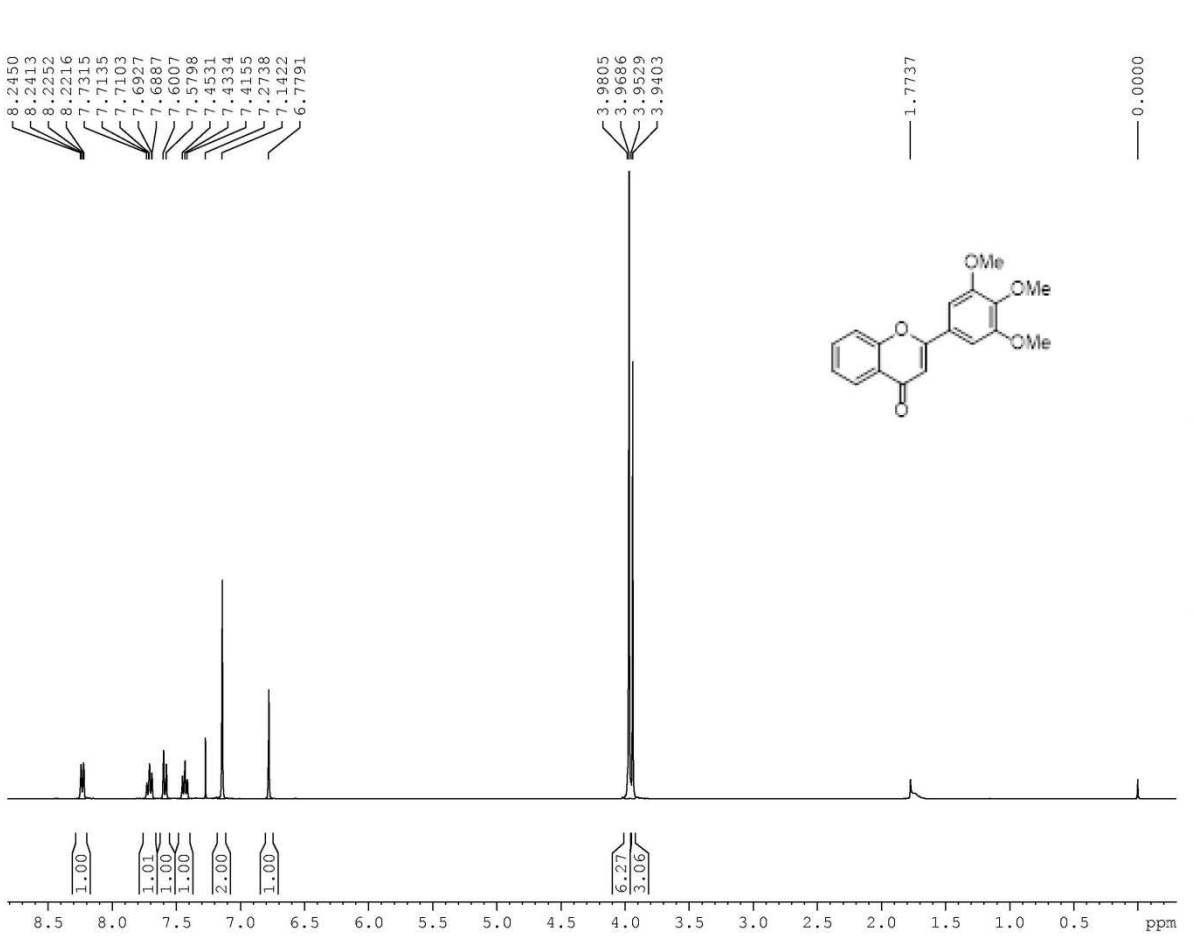

C2: ^{13}C NMR

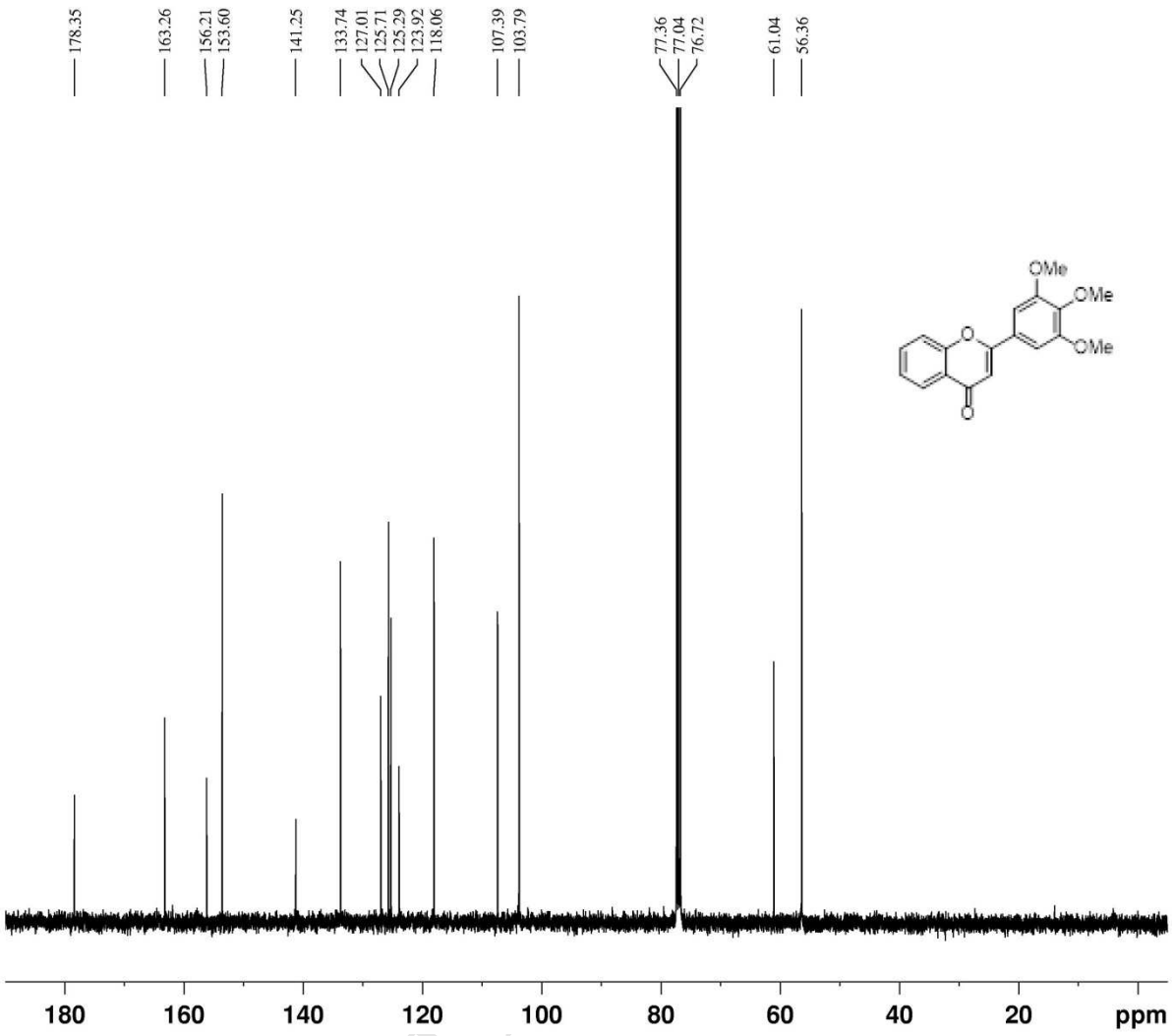

C3: ^{1}H NMR

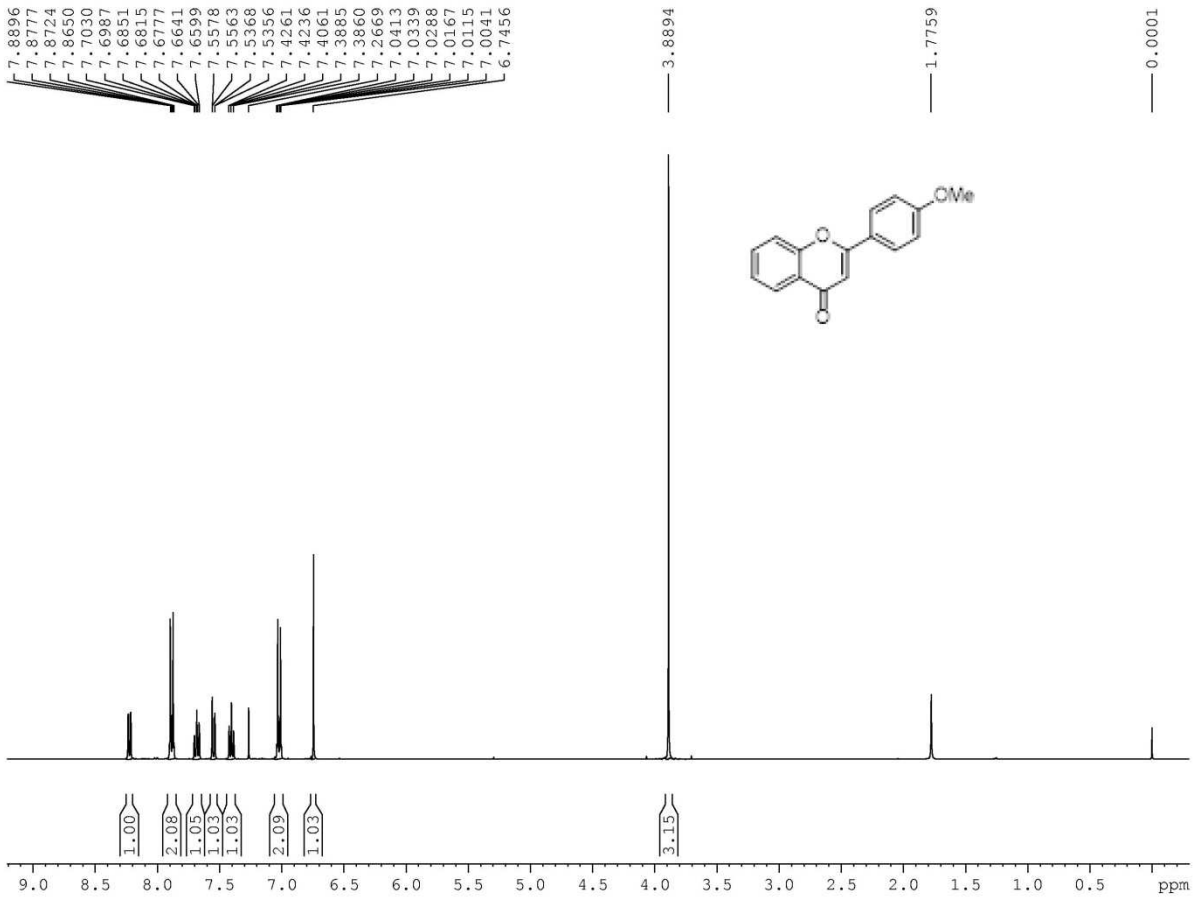

C3: ^{13}C NMR

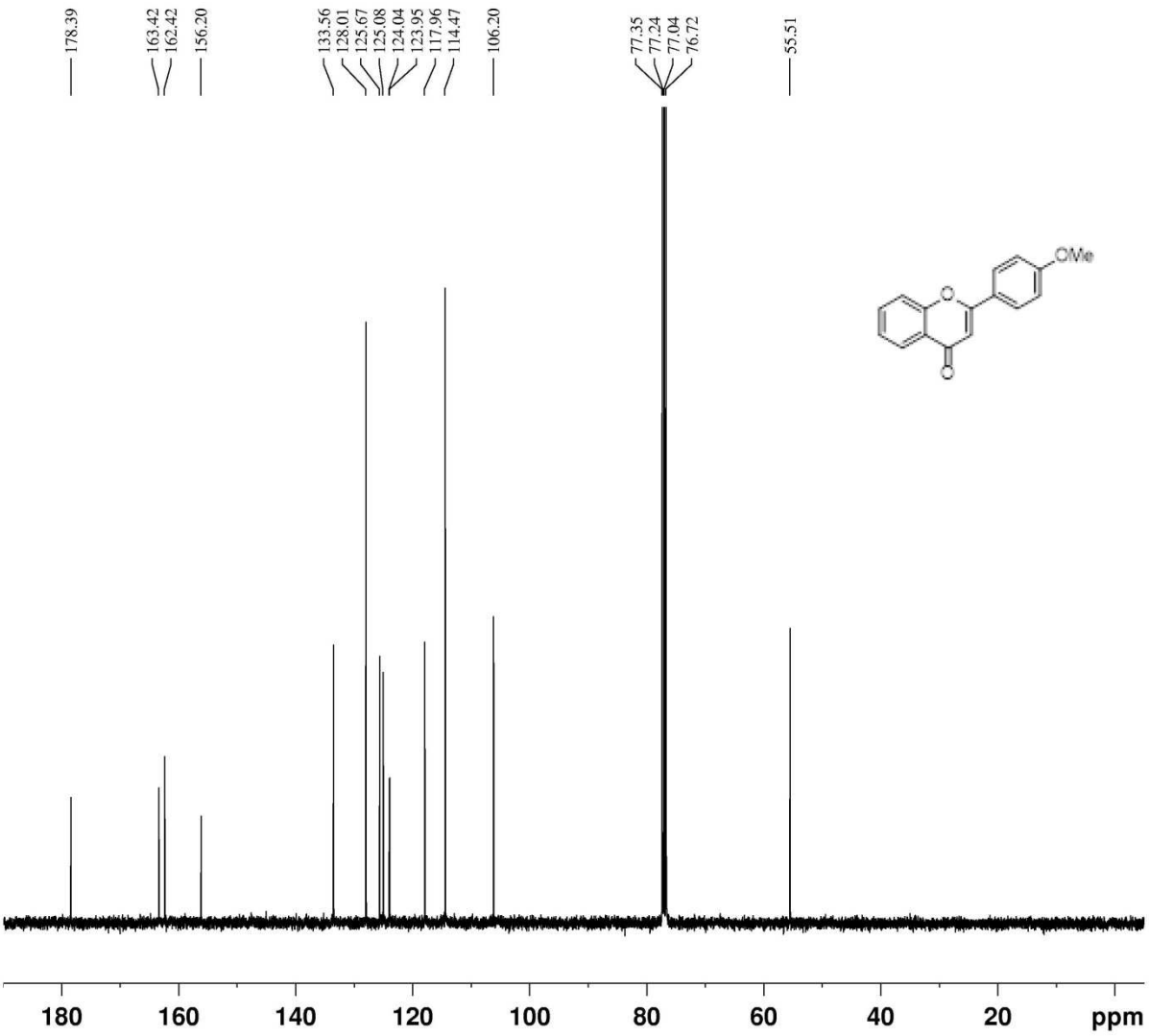

C4: ^{1}H NMR

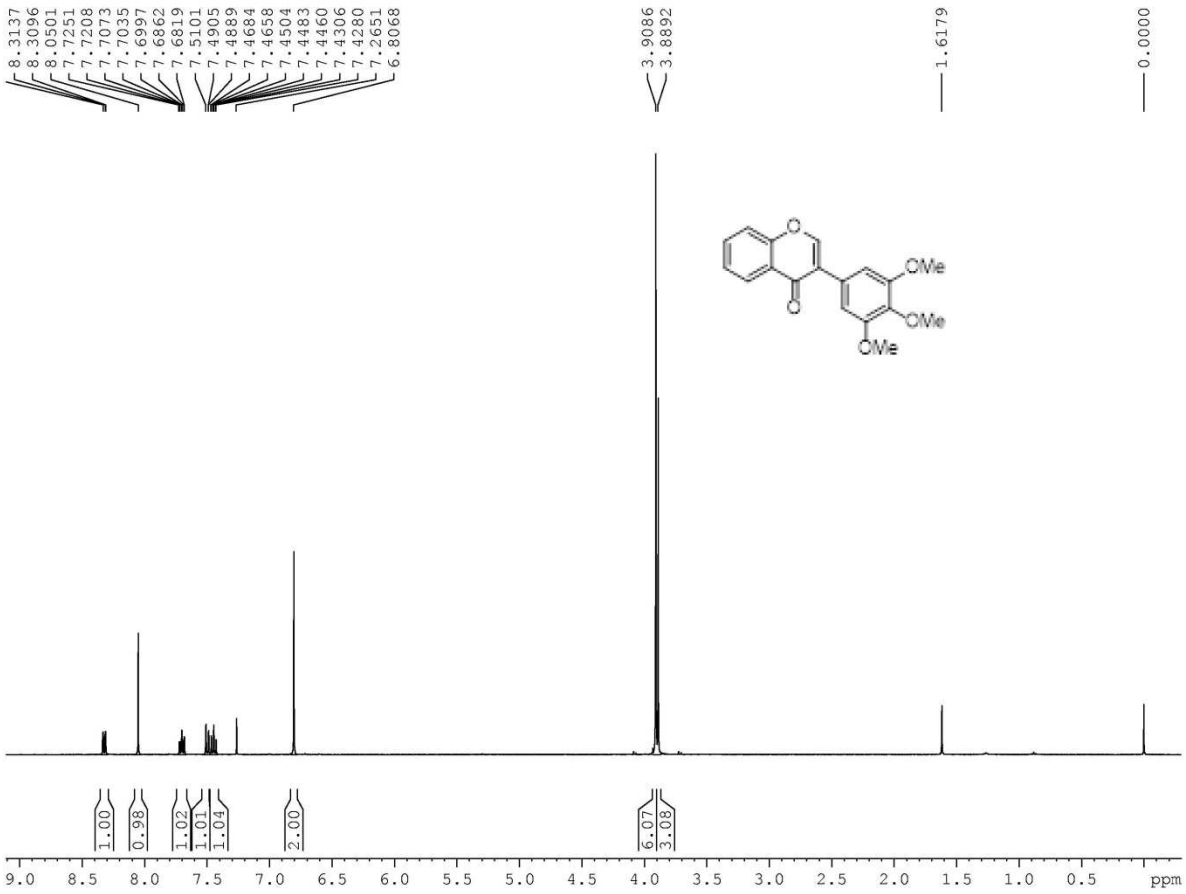

C4: ^{13}C NMR

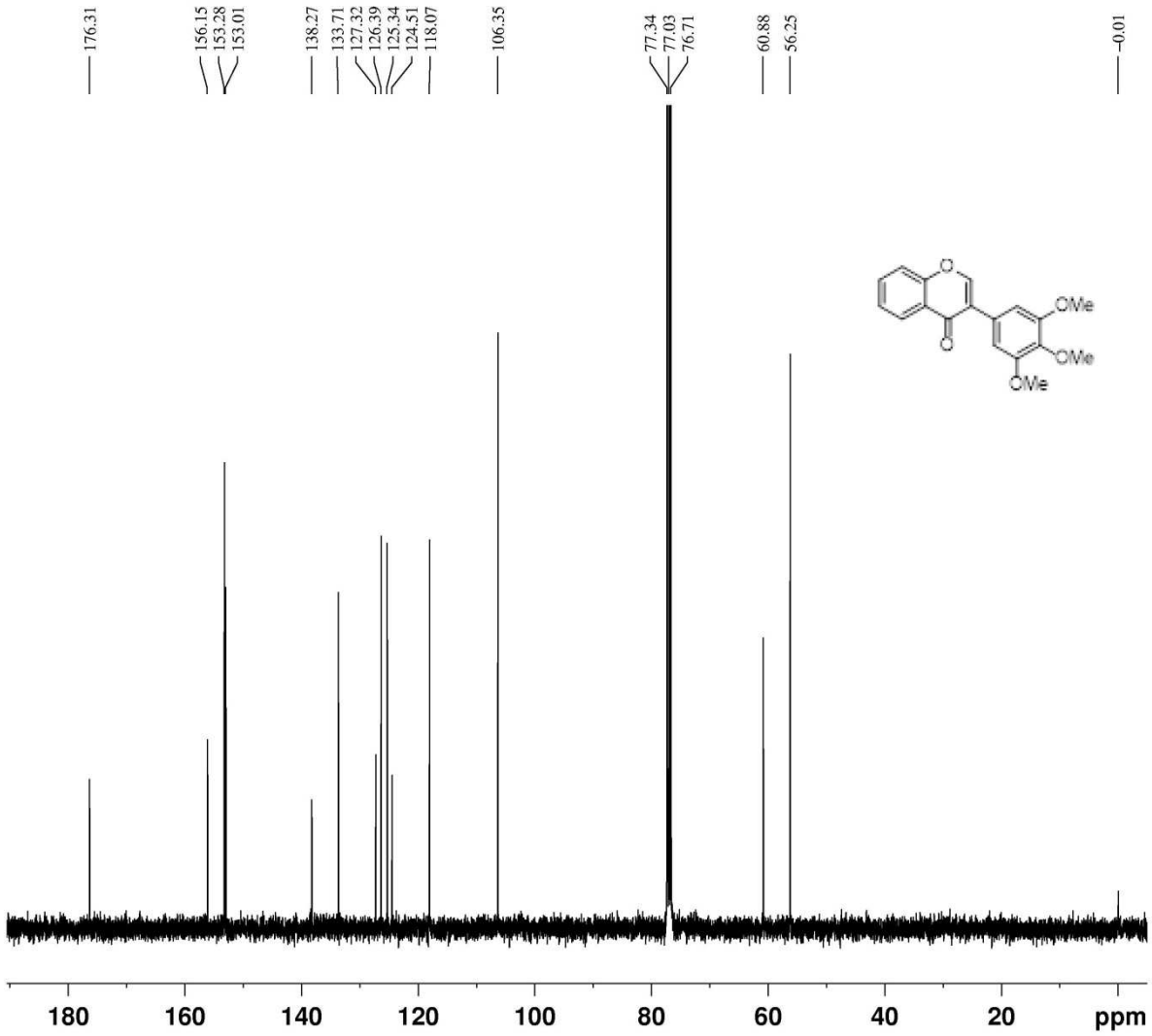

C5: ^{1}H NMR

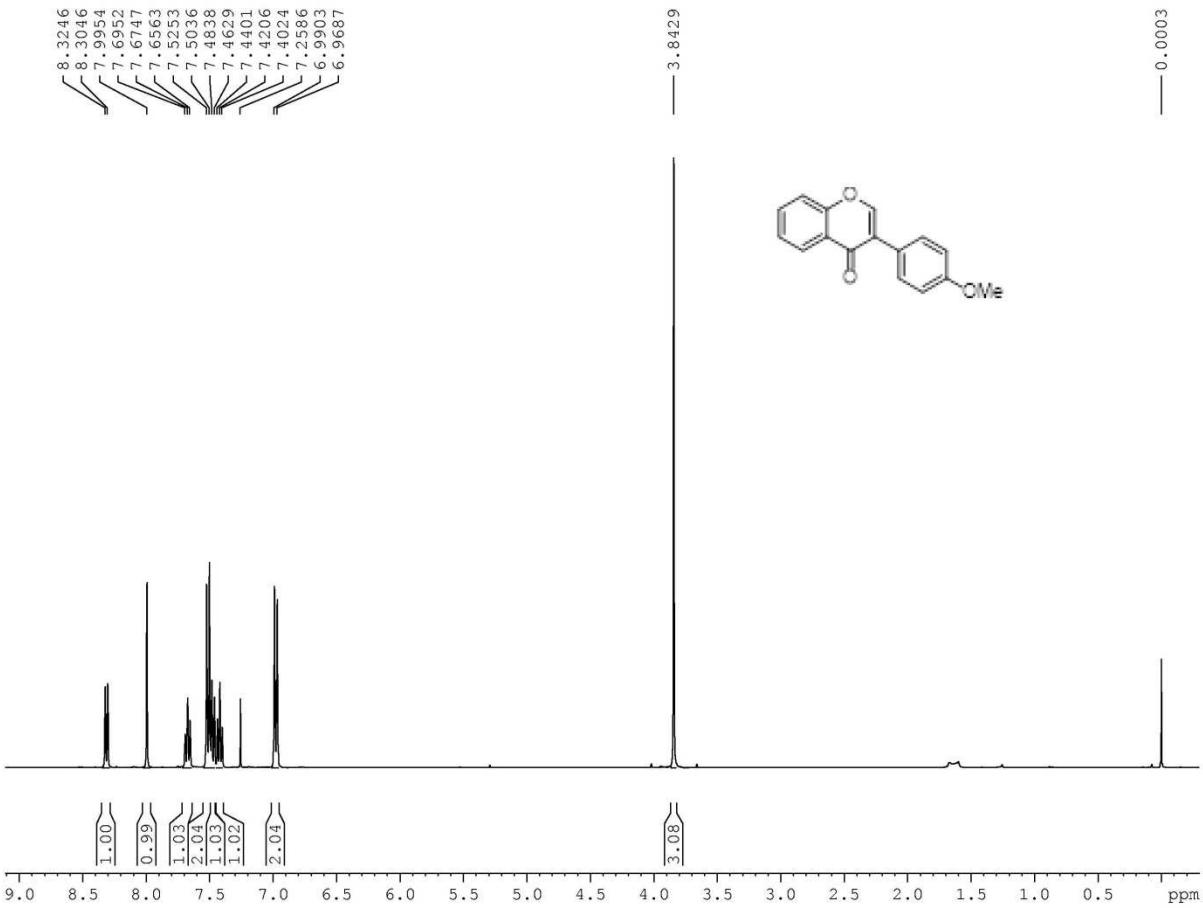

C5: ^{13}C NMR

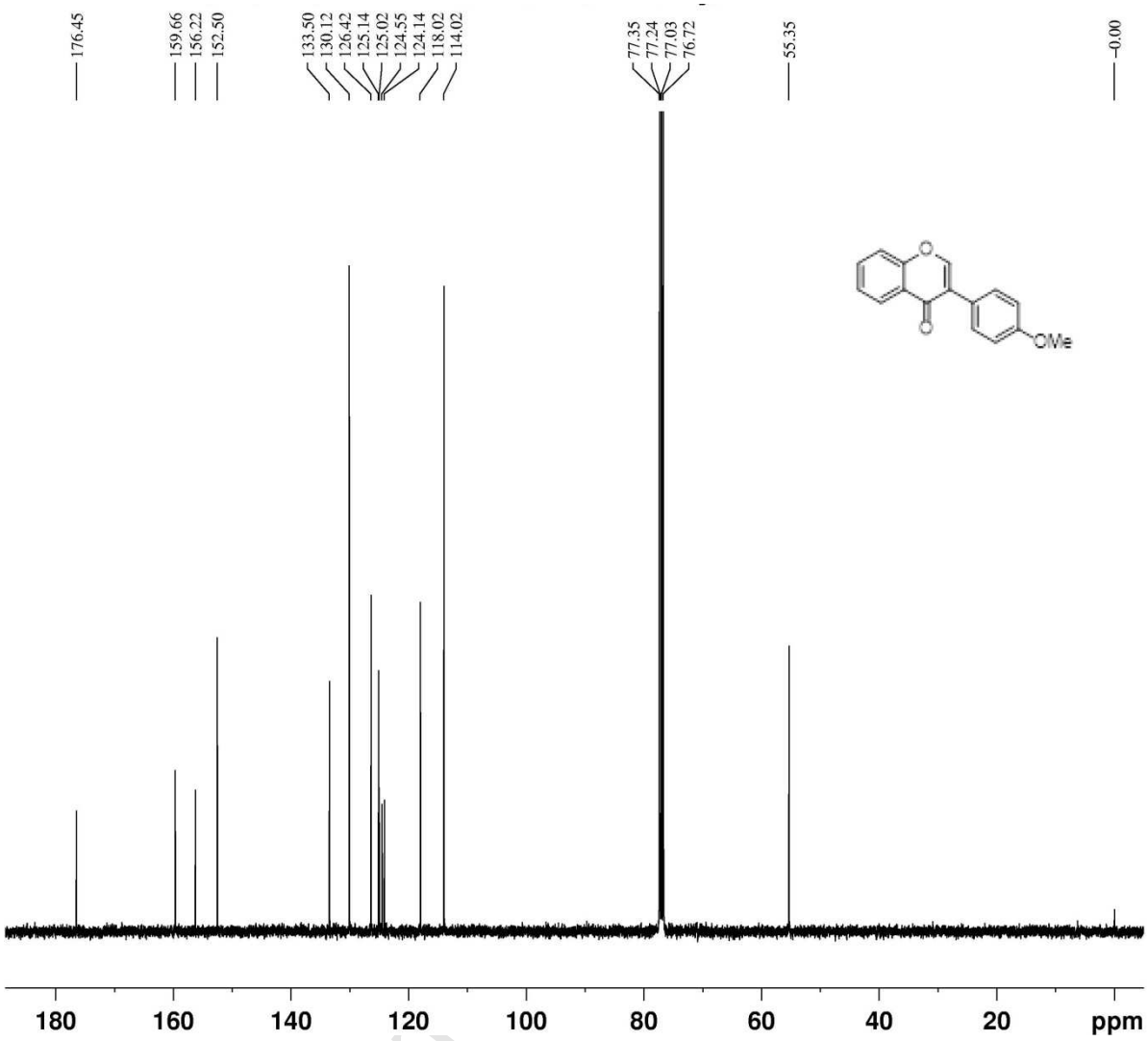

C6: ^{1}H NMR

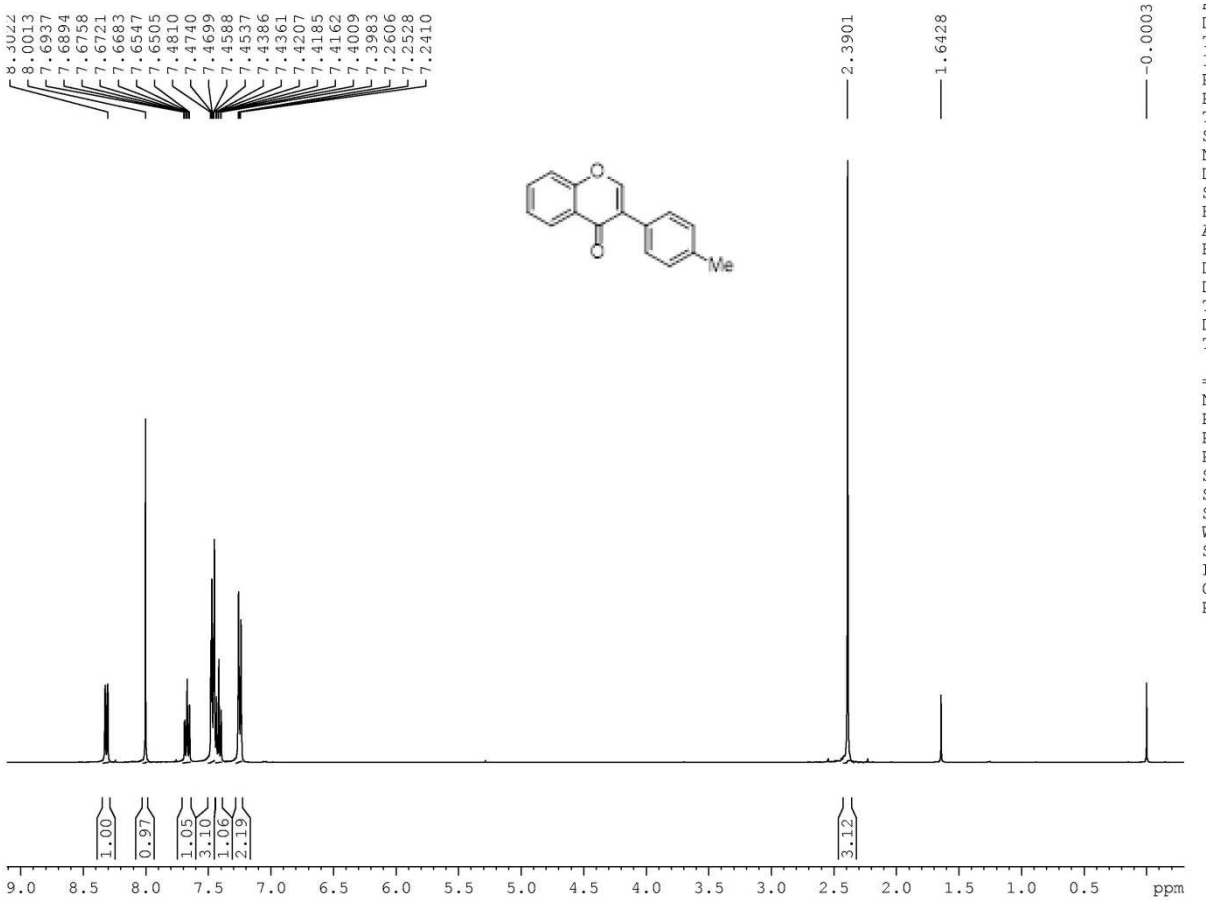

C6: ^{13}C NMR

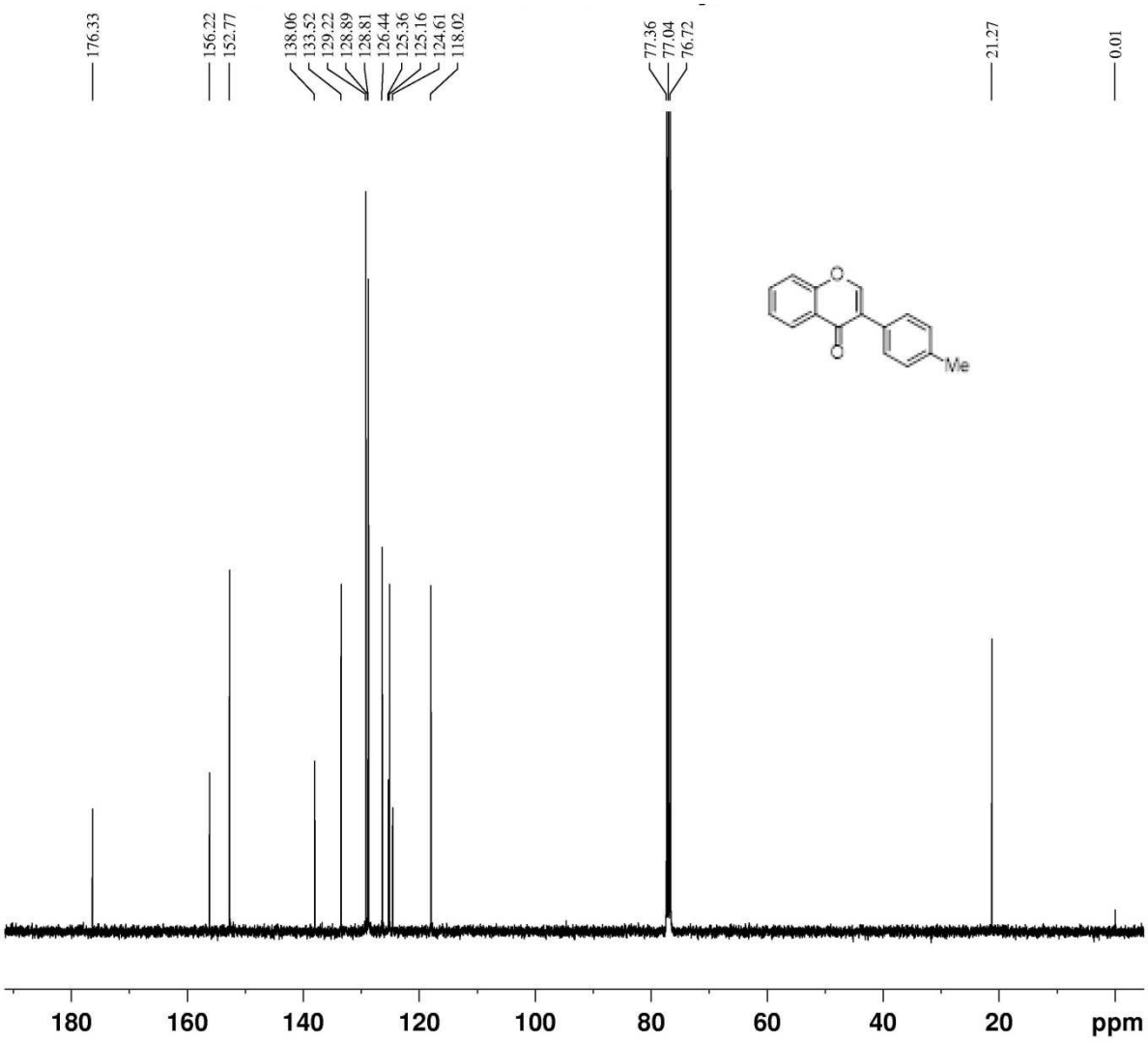

C7: ^{1}H NMR

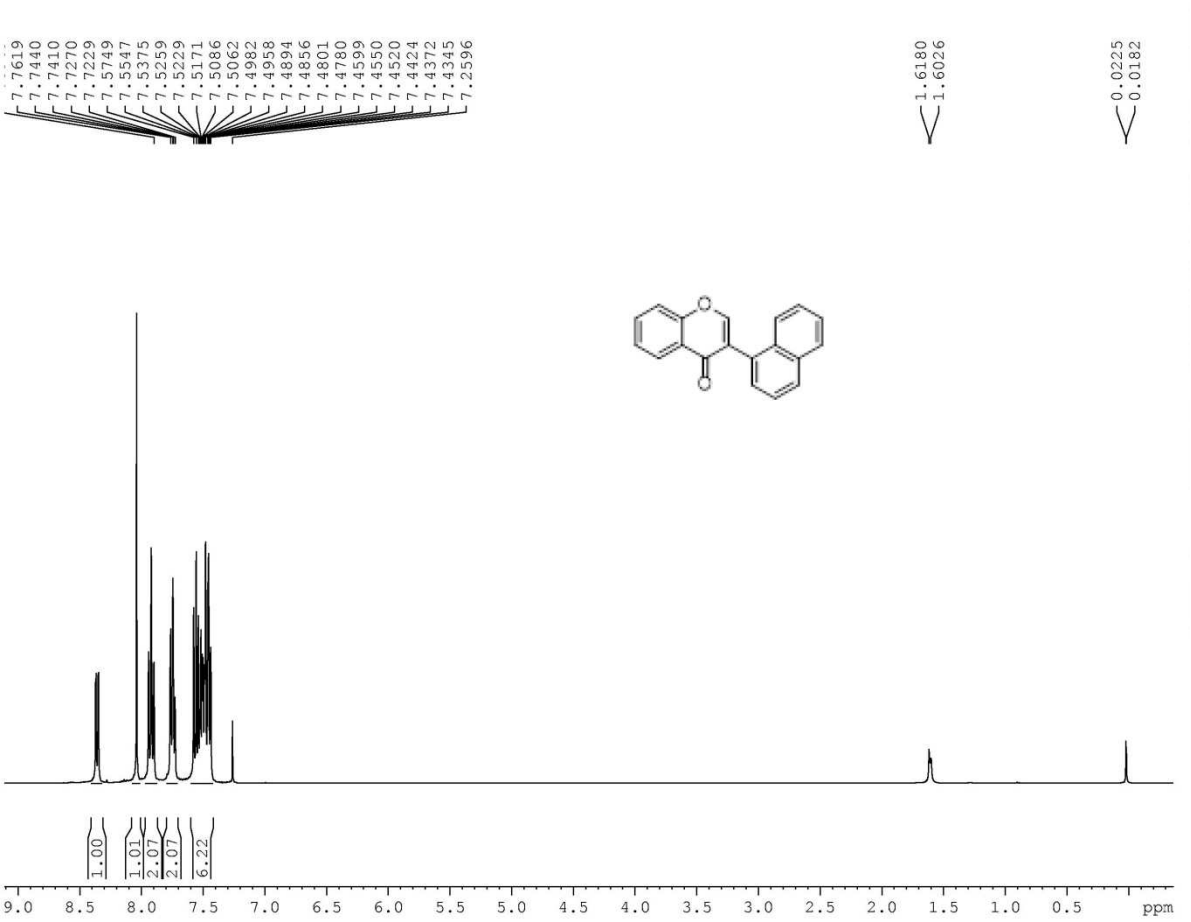

C7: ^{13}C NMR

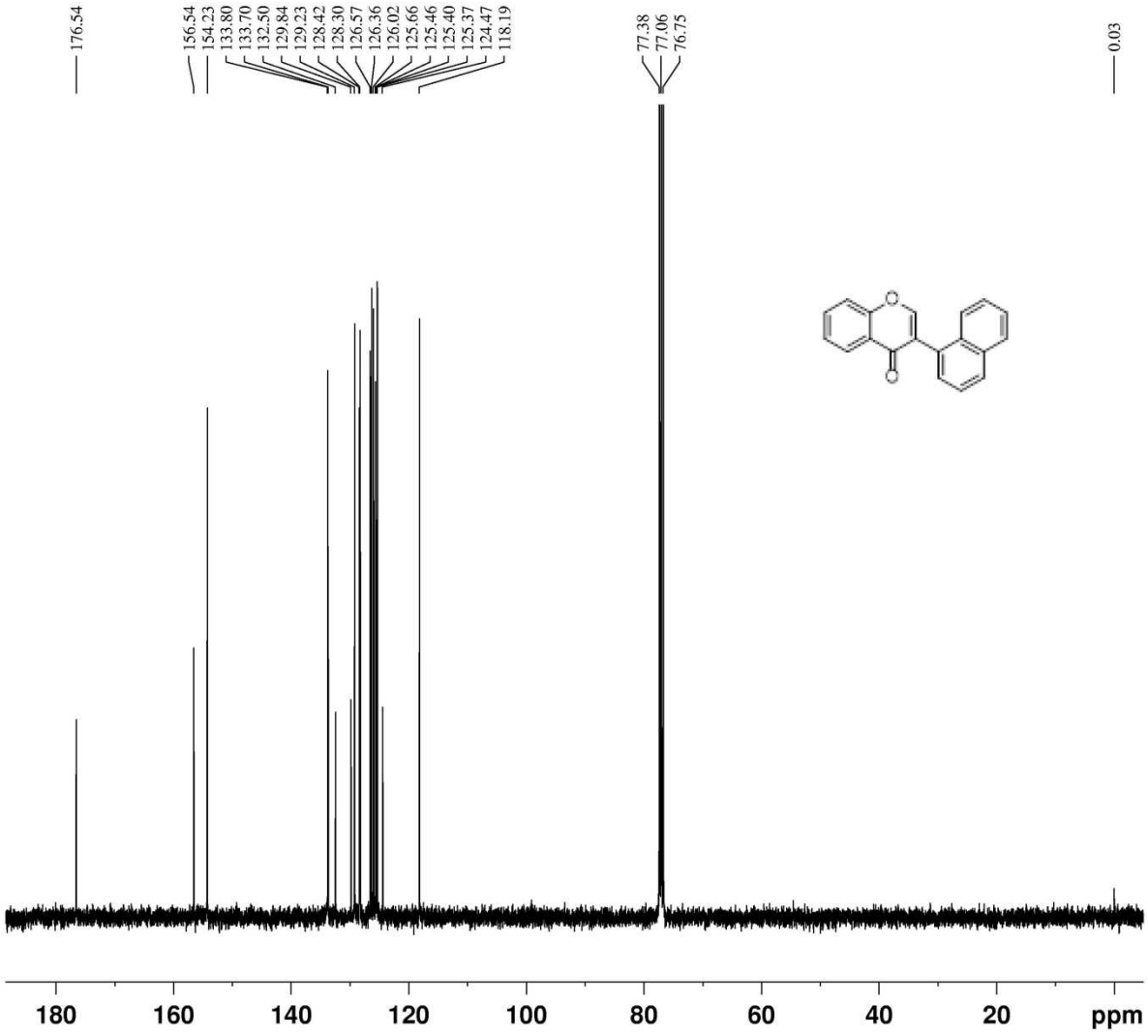

Scanned HPLC chromatogram of representative compounds:

1. 3c

==== Shimadzu LCsolution Analysis Report ====

C:\LabSolutions\Data\NEHA H\garima\LC data file\skg 25 3.lcd

Acquired by	: Admin
Sample Name	: skg 25 3
Sample ID	: skg 25 3
Vail #	: 3
Injection Volume	: 5 uL
Data File Name	: skg 25 3.lcd
Method File Name	: 50 AcN50 water20min1ml.lcm
Batch File Name	:
Report File Name	: Default.lcr
Data Acquired	: 12/22/2015 6:50:54 PM
Data Processed	: 12/22/2015 7:10:57 PM

<Chromatogram>

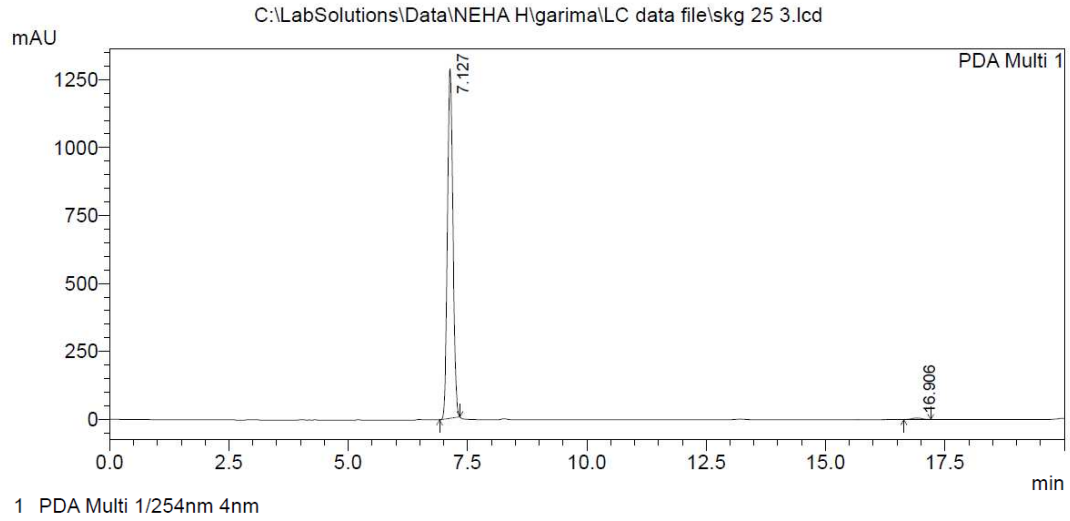

1 PDA Multi 1/254nm 4nm

PeakTable

PDA Ch1 254nm 4nm

Peak#	Ret. Time	Area	Height	Area %	Height %
1	7.127	10303482	1286641	99.125	99.561
2	16.906	90968	5672	0.875	0.439
Total		10394450	1292313	100.000	100.000

2. 3d

==== Shimadzu LCsolution Analysis Report ====

C:\LabSolutions\Data\NEHA H\garima\LC data file\skg 25 4 3.lcd

Acquired by	: Admin
Sample Name	: sur 709
Sample ID	: sur 709
Vail #	: 1
Injection Volume	: 5 uL
Data File Name	: skg 25 4 3.lcd
Method File Name	: 50 AcN50 water20min1ml.lcm
Batch File Name	:
Report File Name	: Default.lcr
Data Acquired	: 12/22/2015 3:56:43 PM
Data Processed	: 12/22/2015 4:11:51 PM

<Chromatogram>

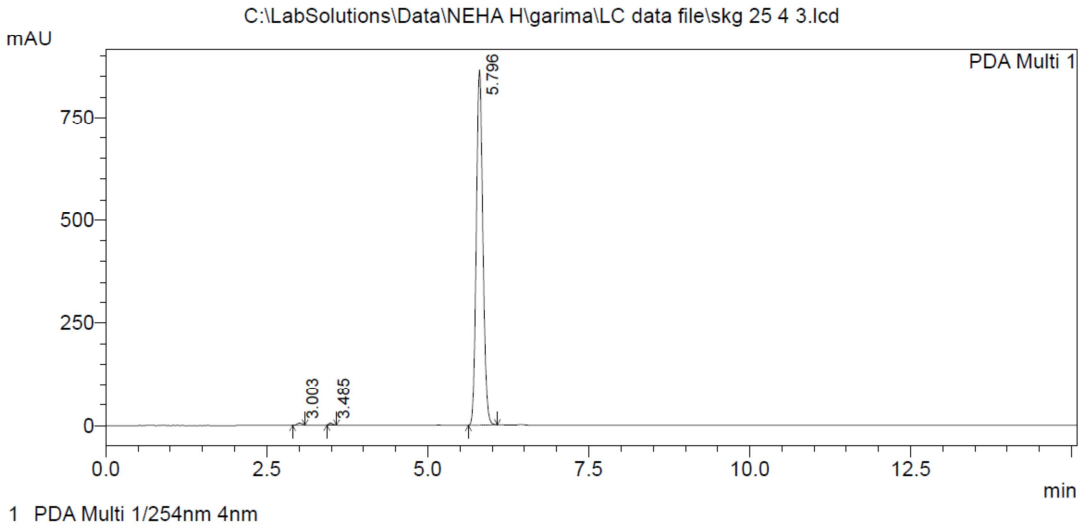

1 PDA Multi 1/254nm 4nm

PeakTable

PDA Ch1 254nm 4nm

Peak#	Ret. Time	Area	Height	Area %	Height %
1	3.003	27507	5377	0.441	0.614
2	3.485	21219	4798	0.340	0.548
3	5.796	6192269	865730	99.219	98.838
Total		6240996	875905	100.000	100.000

3. 3e

==== Shimadzu LCsolution Analysis Report ====

C:\LabSolutions\Data\NEHA H\garima\LC data file\skg 26\skg 26 2.lcd

Acquired by	: Admin
Sample Name	: skg 26 2
Sample ID	: skg 26 2
Vail #	: 2
Injection Volume	: 5 uL
Data File Name	: skg 26 2.lcd
Method File Name	: 50 AcN50 water20min1ml.lcm
Batch File Name	:
Report File Name	: Default.lcr
Data Acquired	: 12/23/2015 4:32:39 PM
Data Processed	: 12/23/2015 4:52:41 PM

<Chromatogram>

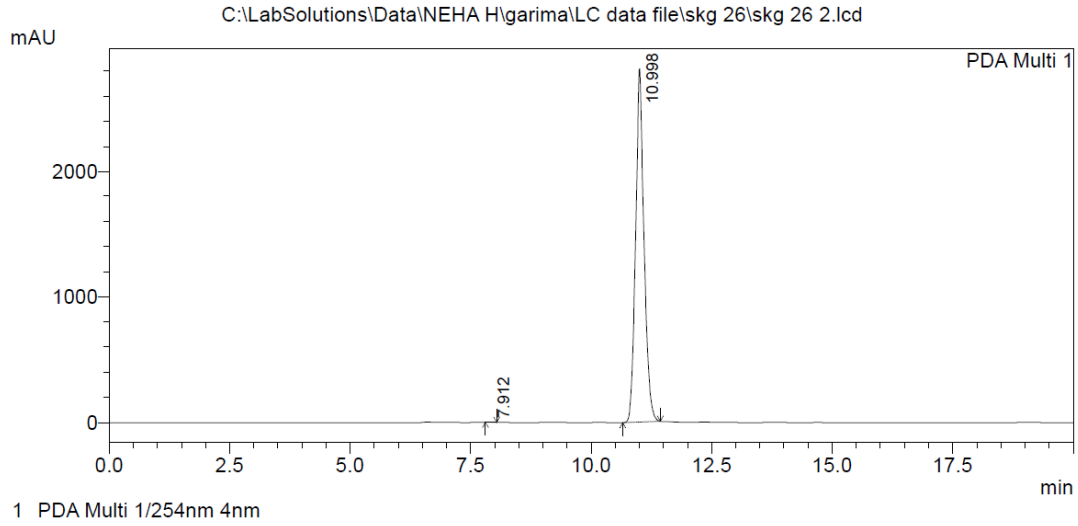

1 PDA Multi 1/254nm 4nm

PeakTable

PDA Ch1 254nm 4nm

Peak#	Ret. Time	Area	Height	Area %	Height %
1	7.912	18210	2211	0.054	0.079
2	10.998	34002148	2814571	99.946	99.921
Total		34020358	2816782	100.000	100.000

4. 3o

==== Shimadzu LCsolution Analysis Report ====

C:\LabSolutions\Data\NEHA H\garima\LC data file\skg 25 7 1.lcd

Acquired by	: Admin
Sample Name	: skg 25 7 1
Sample ID	: skg 25 7 1
Vail #	: 4
Injection Volume	: 5 uL
Data File Name	: skg 25 7 1.lcd
Method File Name	: 60 AcN40 water20min1ml.lcm
Batch File Name	:
Report File Name	: Default.lcr
Data Acquired	: 12/23/2015 12:03:55 PM
Data Processed	: 12/23/2015 12:23:57 PM

<Chromatogram>

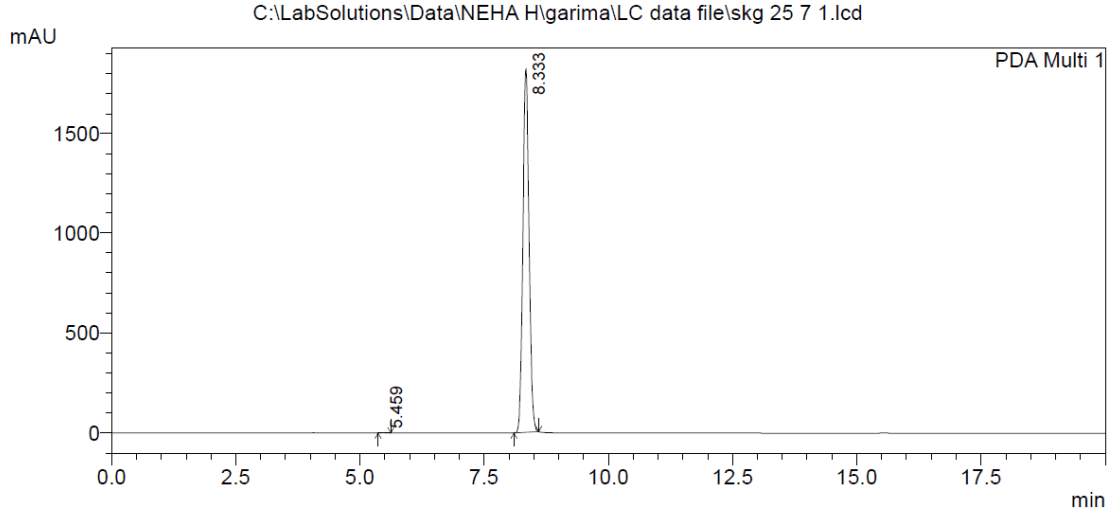

1 PDA Multi 1/254nm 4nm

PeakTable

PDA Ch1 254nm 4nm

Peak#	Ret. Time	Area	Height	Area %	Height %
1	5.459	8110	1447	0.051	0.079
2	8.333	15769761	1822470	99.949	99.921
Total		15777871	1823917	100.000	100.000

5. 6d

==== Shimadzu LCsolution Analysis Report ====

C:\LabSolutions\Data\NEHA H\garima\LC data file\skg 26\skg 26 4 3.lcd

Acquired by	: Admin
Sample Name	: skg 26 4 3
Sample ID	: skg 26 4 3
Vail #	: 1
Injection Volume	: 5 uL
Data File Name	: skg 26 4 3.lcd
Method File Name	: 50 AcN50 water20min1ml.lcm
Batch File Name	:
Report File Name	: Default.lcr
Data Acquired	: 12/23/2015 4:57:29 PM
Data Processed	: 12/23/2015 5:17:31 PM

<Chromatogram>

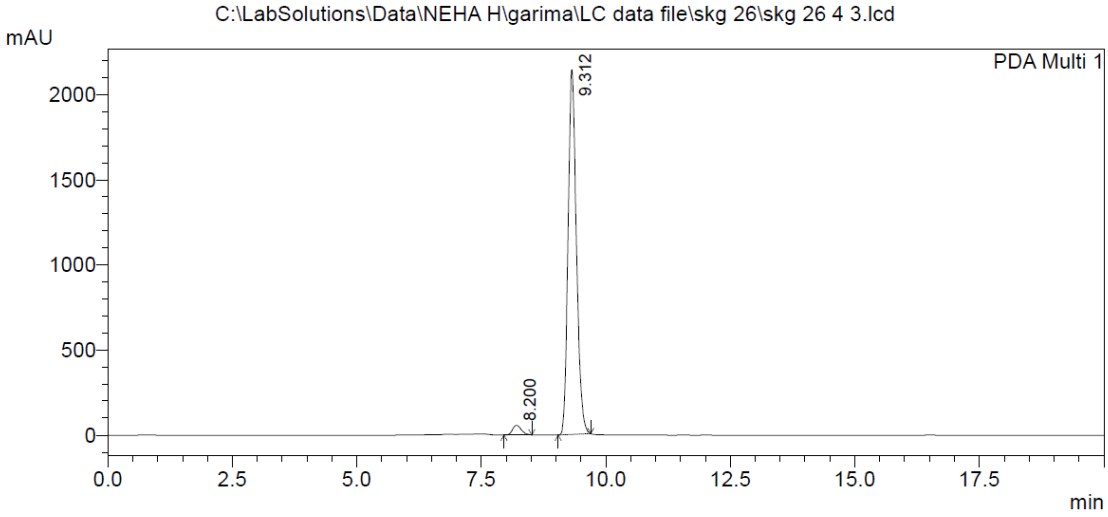

1 PDA Multi 1/254nm 4nm

PeakTable

PDA Ch1 254nm 4nm

Peak#	Ret. Time	Area	Height	Area %	Height %
1	8.200	703341	57358	2.749	2.609
2	9.312	24886233	2141139	97.251	97.391
Total		25589574	2198497	100.000	100.000

6. 6n

==== Shimadzu LCsolution Analysis Report ====

C:\LabSolutions\Data\NEHA H\garima\LC data file\skg 26\skg 26 20 2.lcd

Acquired by	: Admin
Sample Name	: skg 26 20 1
Sample ID	: skg 26 20 1
Vail #	: 3
Injection Volume	: 5 uL
Data File Name	: skg 26 20 2.lcd
Method File Name	: 50 AcN50 water20min1ml.lcm
Batch File Name	:
Report File Name	: Default.lcr
Data Acquired	: 12/23/2015 4:06:56 PM
Data Processed	: 12/23/2015 4:26:59 PM

<Chromatogram>

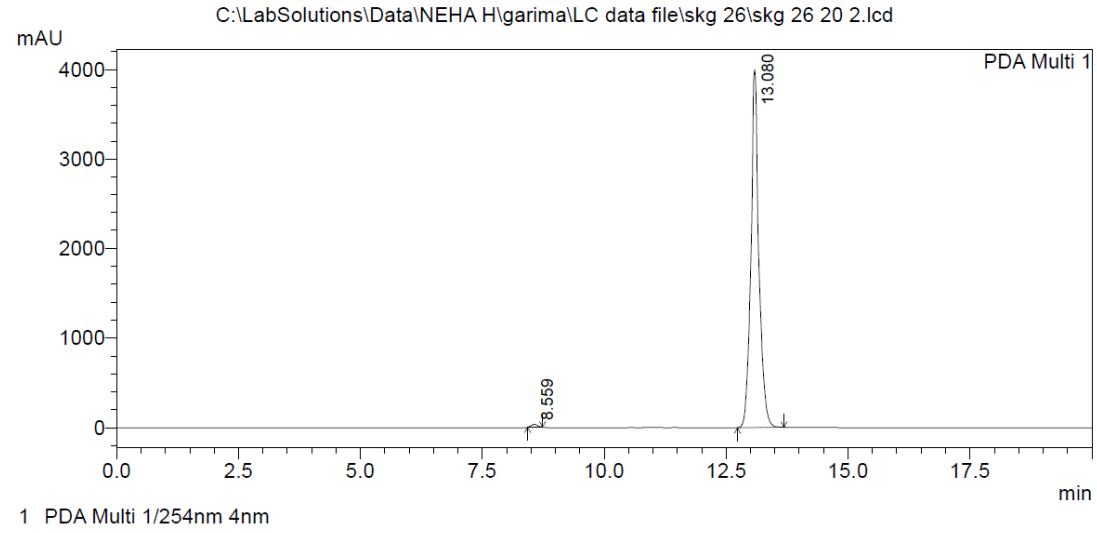

1 PDA Multi 1/254nm 4nm

PeakTable

PDA Ch1 254nm 4nm

Peak#	Ret. Time	Area	Height	Area %	Height %
1	8.559	300454	31251	0.657	0.776
2	13.080	45465495	3996431	99.343	99.224
Total		45765949	4027682	100.000	100.000

7. 6o

==== Shimadzu LCsolution Analysis Report ====

C:\LabSolutions\Data\NEHA H\garima\LC data file\skg 26\skg 26 21.lcd

Acquired by	: Admin
Sample Name	: skg 26 21
Sample ID	: skg 26 21
Vail #	: 4
Injection Volume	: 5 uL
Data File Name	: skg 26 21.lcd
Method File Name	: 50 AcN50 water20min1ml.lcm
Batch File Name	:
Report File Name	: Default.lcr
Data Acquired	: 12/23/2015 6:56:31 PM
Data Processed	: 12/23/2015 7:21:34 PM

<Chromatogram>

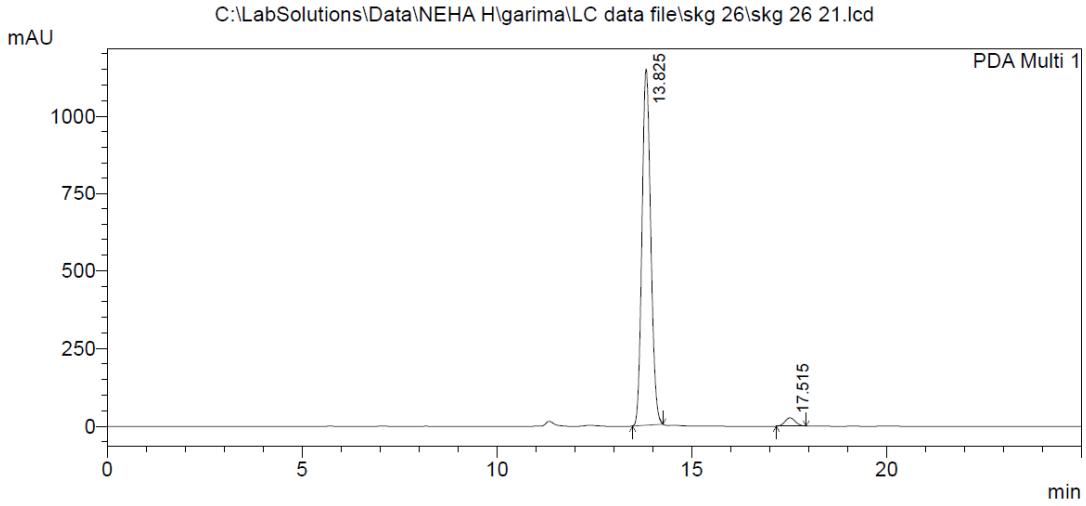

1 PDA Multi 1/254nm 4nm

PeakTable

PDA Ch1 254nm 4nm

Peak#	Ret. Time	Area	Height	Area %	Height %
1	13.825	17904229	1147471	97.304	97.726
2	17.515	496056	26705	2.696	2.274
Total		18400286	1174175	100.000	100.000

8. C2

==== Shimadzu LCsolution Analysis Report ====

C:\LabSolutions\Data\NEHA H\garima\LC data file\control 25 n 26\skg 25 c3 1.lcd

Acquired by	: Admin
Sample Name	: skg 25 c3
Sample ID	: skg 25 c3
Vail #	: 2
Injection Volume	: 5 uL
Data File Name	: skg 25 c3 1.lcd
Method File Name	: 50 AcN50 water20min1ml.lcm
Batch File Name	:
Report File Name	: Default.lcr
Data Acquired	: 12/23/2015 7:57:58 PM
Data Processed	: 12/23/2015 8:18:02 PM

<Chromatogram>

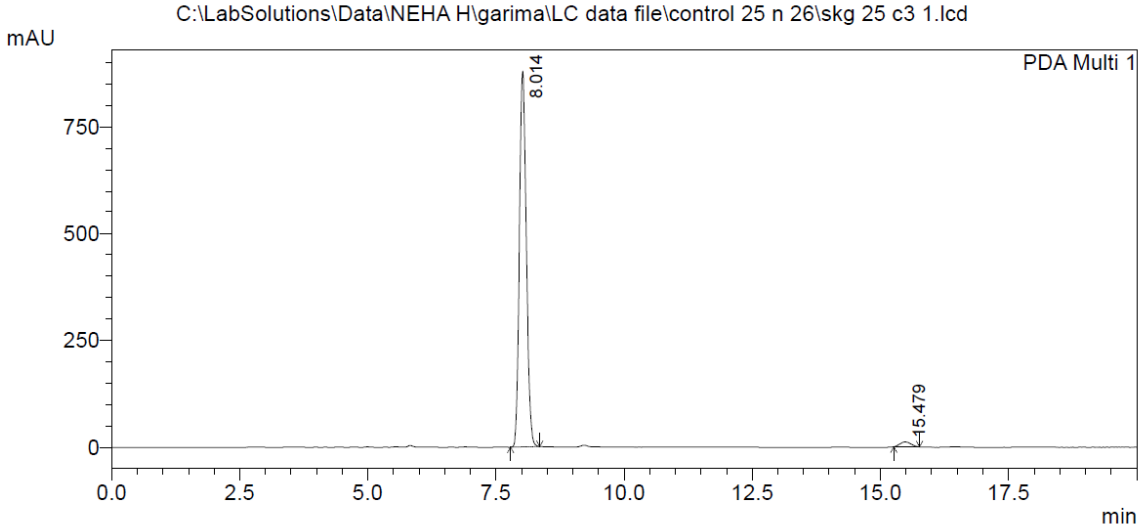

1 PDA Multi 1/254nm 4nm

PeakTable

PDA Ch1 254nm 4nm

Peak#	Ret. Time	Area	Height	Area %	Height %
1	8.014	8231024	879205	97.965	98.713
2	15.479	170987	11459	2.035	1.287
Total		8402011	890664	100.000	100.000

9. C3

==== Shimadzu LCsolution Analysis Report ====

C:\LabSolutions\Data\NEHA H\garima\LC data file\control 25 n 26\skg 25 c1 1.lcd

Acquired by	: Admin
Sample Name	: skg 25 c1
Sample ID	: skg 25 c1
Vail #	: 1
Injection Volume	: 5 uL
Data File Name	: skg 25 c1 1.lcd
Method File Name	: 50 AcN50 water20min1ml.lcm
Batch File Name	:
Report File Name	: Default.lcr
Data Acquired	: 12/23/2015 7:34:06 PM
Data Processed	: 12/23/2015 7:54:09 PM

<Chromatogram>

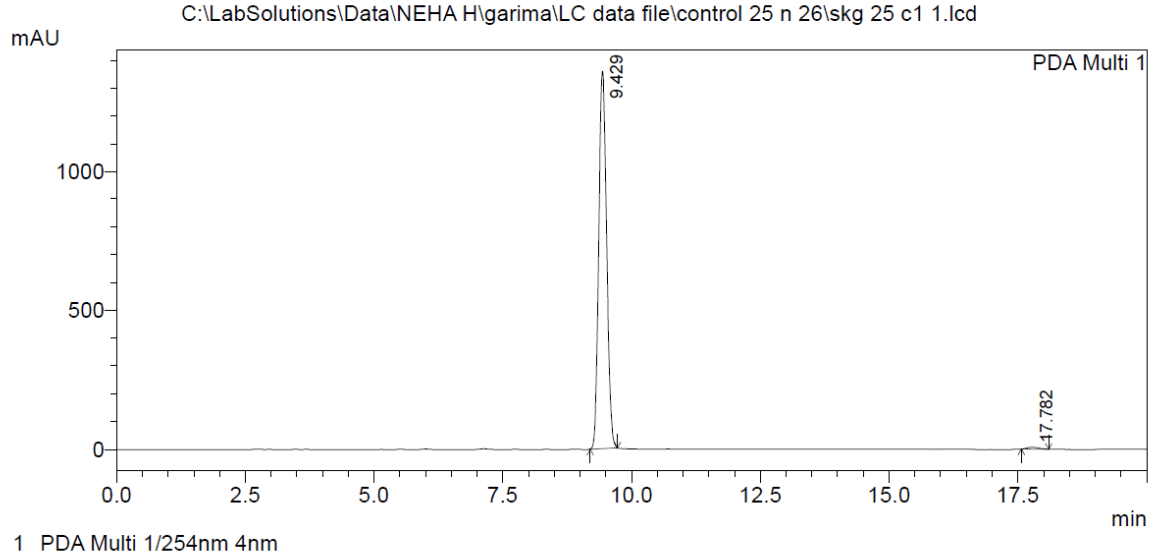

PeakTable

PDA Ch1 254nm 4nm

Peak#	Ret. Time	Area	Height	Area %	Height %
1	9.429	14483448	1357158	99.243	99.499
2	17.782	110419	6837	0.757	0.501
Total		14593867	1363995	100.000	100.000

10. C4

==== Shimadzu LCsolution Analysis Report ====

C:\LabSolutions\Data\NEHA H\garima\LC data file\control 25 n 26\skg 26 c3 1.lcd

Acquired by	: Admin
Sample Name	: skg 26 c3
Sample ID	: skg 26 c3
Vail #	: 3
Injection Volume	: 5 uL
Data File Name	: skg 26 c3 1.lcd
Method File Name	: 50 AcN50 water20min1ml.lcm
Batch File Name	:
Report File Name	: Default.lcr
Data Acquired	: 12/23/2015 9:09:51 PM
Data Processed	: 12/23/2015 9:29:55 PM

<Chromatogram>

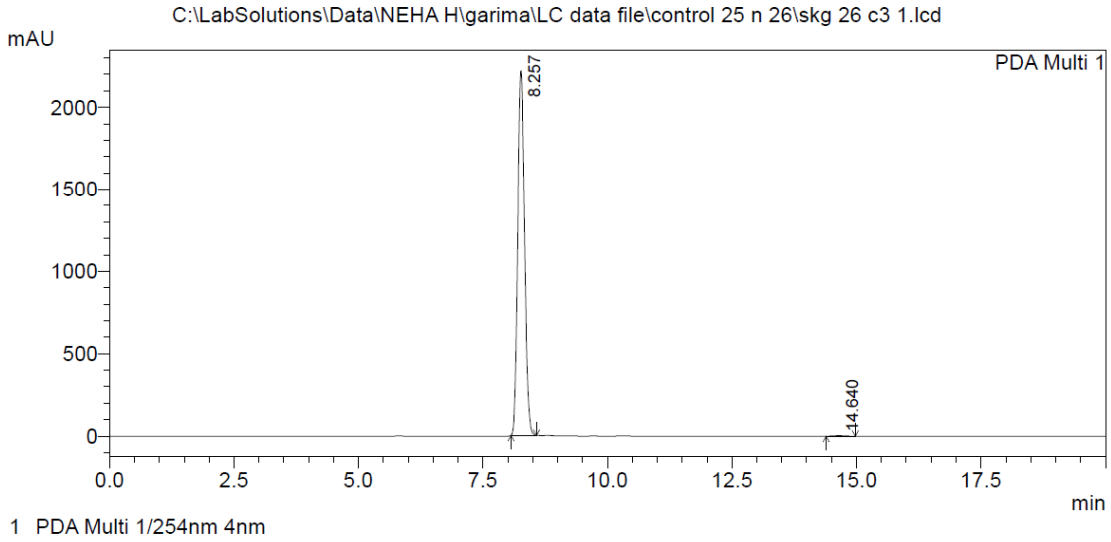

PeakTable

PDA Ch1 254nm 4nm

Peak#	Ret. Time	Area	Height	Area %	Height %
1	8.257	21035367	2215978	99.832	99.893
2	14.640	35456	2370	0.168	0.107
Total		21070824	2218348	100.000	100.000

11. C7

==== Shimadzu LCsolution Analysis Report ====

C:\LabSolutions\Data\NEHA H\garima\LC data file\control 25 n 26\skg 26 c4 1.lcd

Acquired by	: Admin
Sample Name	: skg 26 c4
Sample ID	: skg 26 c4
Vail #	: 4
Injection Volume	: 5 uL
Data File Name	: skg 26 c4 1.lcd
Method File Name	: 50 AcN50 water20min1ml.lcm
Batch File Name	:
Report File Name	: Default.lcr
Data Acquired	: 12/23/2015 9:57:08 PM
Data Processed	: 12/23/2015 10:27:12 PM

<Chromatogram>

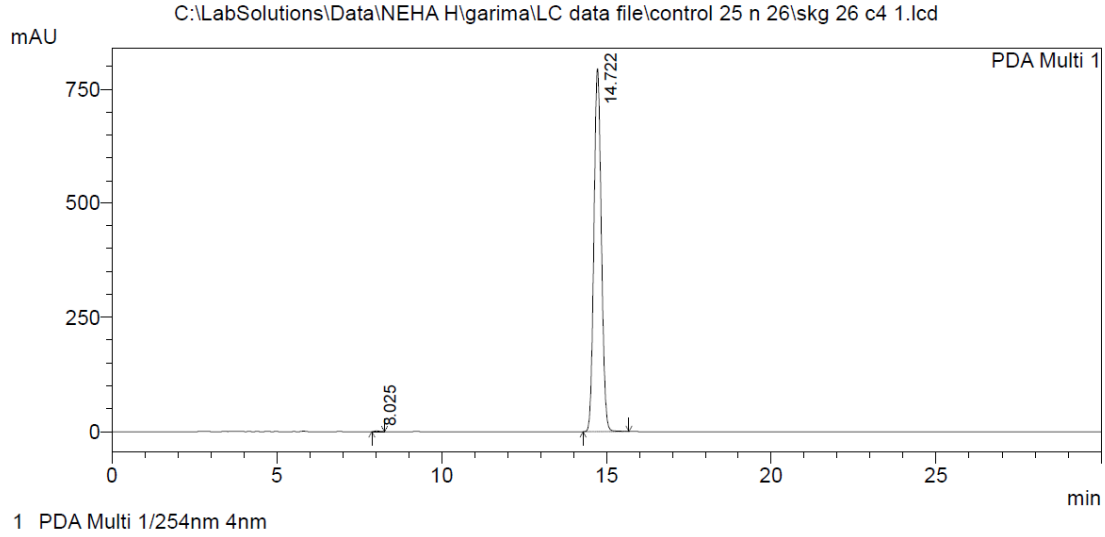

1 PDA Multi 1/254nm 4nm

PeakTable

PDA Ch1 254nm 4nm

Peak#	Ret. Time	Area	Height	Area %	Height %
1	8.025	12933	1412	0.104	0.177
2	14.722	12451661	794653	99.896	99.823
Total		12464594	796065	100.000	100.000

Research Highlights

- Represents an unprecedented target-based scaffold-hopping of NPs, flavonoids.
- 2/3-Arylpyridopyrimidinones were synthesized *via* Pd-catalyzed activation–arylation.
- Compounds were potent hTopoIIα-selective catalytic inhibitors.
- Interaction with DNA in groove domain was identified
- Afforded significant/higher activities than etoposide, flavones and isoflavones.